Studies on the Development and Consequences of Neuroinflammation in Obesity

By

Laura Beth Buckman

Dissertation

Submitted to the Faculty of the

Graduate School of Vanderbilt University

in partial fulfillment of the requirements

for the degree of

DOCTOR of PHILOSOPHY

in

Molecular Physiology and Biophysics

August, 2014

Nashville, Tennessee

Approved:

Alyssa Hasty, Ph.D.

Roger Colbran, Ph.D.

Richard O'Brien, Ph.D.

John Stafford, M.D., Ph.D.

Amy Major, Ph.D.

Miki Aschner, Ph.D.

Kate L.J. Ellacott, Ph.D.

TABLE OF CONTENTS

LIST OF FIGURES

LIST OF TABLES

LIST OF ABBREVIATIONS

AA	arachidonic acid
AgRP	agouti-related peptide
AH	anterior hypothalamus
Aldh1L1	aldehyde dehydrogenase 1 family, member L1
AMPAR	AMPA receptors
α-MSH	α-melanocyte-stimulating hormone
ANG1	angiopoetin 1
APOE	apolipoprotein E
AQPs	aquaporins
ARC	arcuate nucleus
AT	adipose tissue
ATM	adipose tissue macrophage
BBB	blood brain barrier
bFGF	basic fibroblast growth factor
BMDC	bone-marrow-derived cells
BMT	bone marrow transplant
CART	cocaine- and amphetamine-regulated transcript
CCR2	C-C chemokine receptor type 2
CNS	central nervous system
CSF	cerebrospinal fluid

CVD	cardiovascular disease
CVO	circumventricular organ
DIO	diet-induced obese
DMN	dorsomedial nuclei
ER	endoplasmic reticulum
FKN	fractalkine
GDNF	glial-derived neurotrophic factor
GFAP	glial-fibrillary acidic protein
GFP	green fluorescent protein
GLAST	glutamate-aspartate transporter
GLT-1	glial glutamate transporter 1
GLUT-1	glucose transporter type 1
GS	glutamine synthase
HF	high-fat
IFN-γ	interferon-gamma
IKK-β	inhibitor of κB kinase
IL	interleukin
iNOS	inducible nitric oxide synthase
IRS	insulin receptor substrate
JNK	c-jun N-terminal kinase
KO	knockout
LF	low-fat
LH	lateral hypothalamus

LPS	lipopolysaccharide
MBH	medial basal hypothalamus
MC3R	melanocortin-3 receptor
MC4R	melanocortin-4 receptor
ME	median eminence
MHC	major histocompatibility complex
MPO	medial preoptic area
MS	multiple sclerosis
NO	nitric oxide
NPY	neuropeptide Y
NTS	nucleus of the tractus solitaries
Pa	Paraventricular
PGE	prostaglandin
PGE2	prostaglandin E2
POMC	pro-opiomelaocortin
RAGE	receptor for advanced glycation end-products
ROS	reactive oxygen species
S100B	S100 calcium binding protein β
SOCS	suppressor of cytokine signaling
SVF	stromal vascular fraction
T2D	type 2 diabetes
TGF-β	transforming growth factor-β
TLR	toll-like receptor

TLR4	toll-like receptor 4
TNF-α	tumor necrosis factor-α
VMH	ventromedial hypothalamic nucleus
WT	wild-type

CHAPTER 1

Introduction

Obesity Epidemic

Obesity, defined as a body mass index of greater than 30 kg/m^2, represents an increasingly important cause of human morbidity and mortality throughout the world. In the United States alone obesity effects more than one-third of adults (33.8%) [1] and approximately 17% of children aged 2-19 years [2]. The rise in obesity rates has been paralleled by increases in obesity-related health problems, such as type-2 diabetes (T2D) and cardiovascular disease (CVD), with estimated healthcare costs in the United States ranging from $147 billion to nearly $210 per year [3]. Caloric restriction and weight-loss surgery are currently the most effective treatments for obesity; however, caloric restriction alone has limited long term success and nearly two-thirds of people regain the weight lost within 1 to 5 years [4-6]. Therefore, there is a critical need for novel therapeutic options for obesity and its associated co-morbidities. An improved understanding of the pathology and pathophysiology of obesity will guide the development of successful treatments that target molecular mechanisms underlying the disease.

Central Nervous System Regulation of Energy Homeostasis

Obesity reflects a sustained state of positive energy balance that develops when energy intake exceeds energy expenditure. The central nervous system (CNS) plays a vital role in regulating food intake and energy expenditure to effectively maintain energy balance and, in turn, a healthy body weight [7-9]. This process is known as energy homeostasis. Information from the

periphery relating to energy status is relayed to the brain via nutritional, nervous and humoral signals and integrated by two key brain areas - the hypothalamus and caudal brainstem. Within the medial basal hypothalamus the arcuate nucleus (ARC) contains two neuronal subtypes that directly respond to energy peripheral cues; neurons that produce the orexigenic (appetite stimulating) neuropeptides, agouti-related peptide (AgRP) and neuropeptide Y (NPY), and neurons that produce anorexigenic (appetite suppressing) neuropeptides, pro-opiomelaocortin (POMC) and cocaine- and amphetamine-regulated transcript (CART) [10, 11]. Activation of NPY/AGRP neurons stimulates food intake and decreases energy expenditure by antagonizing the melanocortin-3 and -4 receptors (MC3R and MC4R) [11]. In contrast, neurons that release POMC/CART exert a tonic inhibitory effect on feeding and increase energy expenditure *via* the production and release of the melanocortin agonist α-melanocyte-stimulating hormone (α-MSH) [11]. Both sets of neurons (NPY/AgRP and POMC/CART) send axonal projections to second-order neurons in adjacent hypothalamic nuclei, including the paraventricular nucleus (PVN) and the lateral hypothalamic area (LHA), as well as autonomic centers in the hindbrain that receive afferent input from key peripheral tissues such as the gastrointestinal tract, liver, pancreas and adipose tissue (described below) [10-12].

Several hormones are instrumental in regulating energy balance. Among the best-researched examples are the pancreatic beta-cell derived hormone insulin and the adipocyte-derived hormone leptin. Insulin and leptin circulate in proportion to body fat, which in turn, constitute a negative feedback signal to reduce food intake and body weight by acting on neuronal systems that regulate energy balance [10]. Importantly, both NPY/AgRP and POMC/CART neurons express receptors for leptin and insulin [13]. Binding of leptin and insulin to hypothalamic receptors increases feedback inhibition of hypothalamic orexigenic pathways, as indicated by

decreased hypothalamic *Npy* and *Agrp* gene expression [10, 14]. At the same time, leptin and insulin promote increased POMC/CART anorexigenic neuronal activity as suggested by increased mRNA expression of POMC and CART, which bind melanocortin receptors to decrease food intake [10]. Thus, high levels of insulin and leptin signal the brain to decrease energy intake through activation of POMC neurons, and simultaneous inhibition of NPY/AgRP neurons.

Other factors contributing to the regulation of food intake and body weight include crosstalk between the hypothalamus and brainstem. For example, vagal and sympathetic afferents from the liver and gastrointestinal tract convey information to the CNS through fibers that project to the nucleus of the tractus solitaries (NTS) of the caudal brainstem, contributing to a bidirectional communication between the brain and the gut known as the gut-brain axis [10, 15, 16]. Moreover, a population of hypothalamic PVN neurons that express MC4R mRNA have direct projections to the NTS [15], and intra-NTS injection of either MC4R agonists or leptin decrease food intake and body weight in rodents [17, 18]. Combined, these data suggest that neurons in the NTS integrate with hypothalamic input to influence energy balance.

Obesity-related Inflammation

Inflammation and inflammatory immune cells are critical factors underlying the development of obesity-associated co-morbidities such as T2D and CVD [19]. In obesity, macrophage infiltration and activation in adipose tissue mediates a localized inflammatory response [19], which is an integral component of the chronic low-grade systemic inflammation associated with the disease [20]. In addition to adipose tissue inflammation, intense research efforts have also focused on the potential contribution of obesity-associated inflammation in other organs such as liver, pancreas, and muscle to disease pathology in obesity [20].

Crosstalk between insulin signaling and inflammatory pathways

In rodents and humans, obesity is accompanied by activation of inflammatory pathways, including increased expression of pro-inflammatory cytokines tumor necrosis factor α (TNFα) and interleukin-6 (IL-6) [21, 22], which are known to directly inhibit insulin signaling and therefore reduce insulin sensitivity [23, 24]. This can eventually lead to insulin resistance, a state defined by the inability of insulin to stimulate glucose uptake. These cytokines activate several serine kinases, including c-jun N-terminal kinase (JNK) and inhibitor of κB kinase (IKK-β), that phosphorylate serine residues of the insulin receptor and insulin receptor substrate (IRS) proteins, such as IRS-1 that are critical for activation of the insulin signaling cascade [23, 24]. Conversely, normal glucose homeostasis depends on insulin-induced tyrosine phosphorylation of IRS proteins, resulting in glucose uptake into muscle, adipose and several other tissues [25, 26]. It is now widely appreciated that a number of conditions associated with increased inflammation, such as injury, infection or disease, are linked with the development of insulin resistance. These include hepatitis C, HIV, rheumatoid arthritis, and sepsis [20]. Importantly, the expression of pro-inflammatory cytokines is upregulated in the brain during injury and disease where they modulate characteristics of sickness behavior, including fever, activation of the hypothalamic-pituitary-adrenal axis, hyperalgesia, lethargy as well as changes in whole-body energy homeostasis [27, 28]. Injection of IL-1 induces taste aversion [29] and suppresses food intake [30] by rats. This anorectic effect is mediated, at least in part, by central melanocortin signaling following the activation of anorexigenic hypothalamic POMC neurons that release the appetite suppressing hormone α-MSH [31].

Hypothalamic inflammation and obesity

Intriguingly, recent experimental evidence suggests that the brain, and specifically the hypothalamus, also shows activation of inflammatory pathways in response to obesity and high-fat feeding [32-34].

A role for neuroinflammation in obesity was first demonstrated by Zhang and colleagues in the form of nuclear factor-kappa B (NF-κB) activation, increased levels of prostaglandin E2 (PGE2), and oxidative stress due to reactive oxygen species (ROS) production induced by 20 weeks exposure to a high-fat diet (HFD)[35]. Moreover, in a later study, the same group showed that increased activation of IKKβ (NF-κB canonical signaling) in hypothalamic neurons is associated with impaired insulin and leptin signaling in the hypothalamus as well as weight gain and increased food intake; whereas suppression of IKKβ/NF-κB signaling in orexigenic (appetite-stimulating) hypothalamic neurons expressing agouti-related peptide (AgRP) protects against obesity and preserves both insulin and leptin signaling [36]. NF-κB plays a key role in neuroinflammation and the development of reactive gliosis [37, 38], which is mediated, in part, by the signal-induced degradation of the inhibitory protein IκBα, thus allowing NF-κB to enter the nucleus and initiate pro-inflammatory gene expression (**Figure 1-1**) [39]. Building on these observations, De Souza et al. [32] demonstrated increased expression of pro-inflammatory cytokines (including interleukin-1β (IL-1β), TNF-α, and interleukin-6 (IL-6)) and induction of endoplasmic reticulum (ER) stress in the rat hypothalamus in response to chronic high-fat feeding. More recently, studies indicate that obesity and chronic consumption of a HFD also activate central nervous system (CNS) glial cells [34, 40-42], which are thought to be the principal source of pro-inflammatory mediators in the brain. Consistent with data from rodents, evidence of gliosis, a condition associated with increased numbers of activated astrocytes and

microglial cells, has been discovered in humans using neuroimaging techniques [34, 40]. These findings demonstrate that obesity triggers inflammatory pathways in both the human and rodent CNS.

Neuroinflammation and Relevance to CNS Disease

Inflammation in the CNS, also known as neuroinflammation, is a complex integrative response that is usually associated with trauma, infection and neurodengerative disease. Microglia and astrocytes make up the resident innate immune cells within the CNS that serve as the first line of defense, which can be modulated by adaptive immune responses composed of invading immune cells from the periphery [44]. This two-way communication between innate and adaptive immunity drives the brain's inflammatory response, which can serve supportive roles, under physiological conditions, or defend the CNS during pathological insults by transiently upregulating inflammatory processes. Consequently, activation of endogenous glial cells and recruitment of peripheral leukocytes are characteristic features of inflammation and pathology in the CNS.

The CNS was historically considered an immune privileged site where immune responses were highly attenuated or fully excluded to preserve brain tissue. Medawar [45] introduced the concept of "immune privilege" in the mid 1900s by demonstrating that foreign tissue grafts show prolonged survival when placed in the brain as compared with other, non-privileged sites, such as skin. Highly specialized barrier structures including the blood brain barrier (BBB) and blood-cerebrospinal-fluid barrier, isolate nervous tissue from physiological fluctuations in the periphery and limit entry of immune cells and immune mediators into the brain parenchyma [46]. Other factors that contribute to immune privilege include: 1) lack of lymphatic drainage; 2)

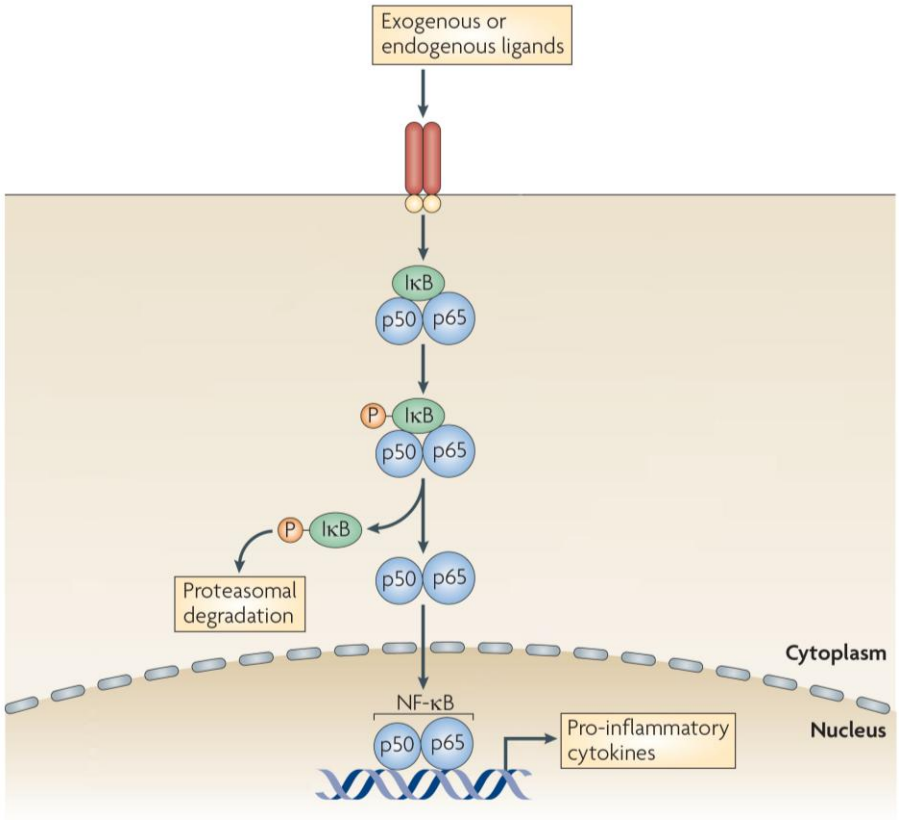

Figure 1-1. Canonical NF-κB Signaling Pathway. In the classical (or canonical) pathway, NF-κB is restrained in the cytoplasm, where it is bound and inhibited by a group of proteins called Iκβ (inhibitors of κβ). Upon stimulation by pro-inflammatory cytokines or activation of immune receptors, such as Toll-like receptors (TLRs), Iκβ is phosphorylated, leading to its ubiquitylation and proteasome-mediated degradation. Subsequently, the NF-κB heterodimer, consisting of p65 (RelA) and p50 (NFKB1) subunits, dissociates from Iκβ, thereby allowing nuclear NF-κB translocation NF-κB and induction of transcription of target genes; NF-κB, nuclear factor κB. Adapted from [43].

low expression of major histocompatibility complex (MHC) molecules; and 3) an immunosuppressive CNS microenvironment [47, 48]. Traditionally, these features were thought to divide the immune system and the CNS into two separate entities; however, it is now widely accepted that the CNS is under constant surveillance by the peripheral immune system (for reviews, see [49-51]). Furthermore, systemic inflammatory and infectious stimuli, such as bacterial endotoxin lipopolysaccharide (LPS), trigger brain inflammatory responses suggesting continuous crosstalk between the immune system and CNS [52-54].

Interactions between the CNS and immune system involve two major routes: the first is the humoral pathway consisting of cytokines, chemokines, adhesion molecules and immunoreceptors; the second is the neurochemical pathway mediated by stimulation of vagal afferents [43, 55]. Circulating cytokines enter the intact CNS by selective, saturable transport systems at the BBB or by passive diffusion through the fenestrated capillaries of the choroid plexus and circumventricular organs (CVOs), which have a less restrictive BBB [56]. There are also membrane transporter routes, such as IL-1 receptors on perivascular macrophages surrounding the endothelium of the BBB, as well as dendritic cells and macrophages residing in the meninges and choroid plexus, which express molecules required to act as antigen-presenting cells (APCs) and thus intercept incoming immune signals [48, 56]. In a pathological context, such as after ischemia, BBB breakdown can lead to increased permeability of brain endothelial cells, allowing entry of plasma components and immune cells into brain tissue [46]. In addition, increased production of pro-inflammatory cytokines during intestinal inflammation may stimulate autonomic nerve fibers, which induces rapid activation of immune signaling to the brain [57]. Thus, despite the immune-privileged environment, the CNS is capable of initiating and perpetuating inflammatory immune responses, and bidirectional interactions with the

peripheral immune system playing a role in health and disease.

Neuroinflammation is linked to virtually all forms of CNS insults, ranging from blunt trauma and infection to long-term neurodegenerative disease [58]. Thus, it is frequently used as a marker of damage and disease activity in the brain. Neuroinflammation can be classified as acute or chronic. Acute inflammation is the initial defense against harmful stimuli, characterized by rapid activation of microglial cells and astrocytes (collectively referred to as gliosis). However, prolonged exposure to harmful stimuli can lead to excessive and inappropriate activation of glial cells, contributing to pathological changes [59, 60]. In general, acute inflammation is thought to have beneficial effects that are important for restoring CNS homeostasis, whereas chronic inflammation is a key pathologic feature of numerous CNS diseases [61]. Since neuroinflammation can be both beneficial and detrimental, a delicate balance must be maintained between the pro- and anti-inflammatory signals that modulate inflammatory reactions. As will be discussed in further detail below, these processes are usually kept in check by endogenous glial cells, namely microglia and astrocytes.

Microglia: Biology and Functions

Origin and historical view of microglia

Microglia are among the first responders during an inflammatory response in the CNS. Microglial cells, which constitute 5-12% of the cellular population in the brain, are specialized macrophages in the CNS, belonging to the mononuclear phagocyte system [62]. Unlike neurons, astrocytes and oligodendrocytes, which develop from neuroepithelial cells, microglia are derived from primitive myeloid progenitors that originate from the extra-embryonic yolk sac [63]. Shortly after entering the brain, microglial precursors mature and take on a characteristic

branching morphology. While microglia are distributed throughout the CNS, including the spinal cord, they are predominant in grey matter and are particularly abundant in some brain regions, including the hippocampus, substantia nigra, basal ganglia and olfactory cortex [62]. Under normal physiological conditions, microglia are extremely long-lived and are maintained by division of local progenitor cells [64]. This is in contrast to peripheral macrophages that are continuously replenished by circulating blood monocytes, especially during inflammation [65]. The replicative capacity of microglia can be influenced by CNS pathology, which often results in a higher turnover rate of microglial cells, primarily through rapid proliferation and to a lesser extent by renewal from circulating blood-borne monocytes [66, 67]. It is now well established that peripheral leukocyte invasion into the CNS is involved in immune surveillance of healthy tissue and participates in the complex inflammatory reaction that characterizes the innate immune response of the brain [44].

Morphologic and molecular characteristics of microglia

In the healthy nervous system, microglia have a ramified morphology characterized by long, thin branching extensions that is generally referred to as the “resting” state [68]. However, “resting” microglia actively survey the brain parenchyma and respond rapidly to any disturbance [69-71]. In contrast to macrophages, resting microglia exhibit low expression of the leukocyte common antigen (CD45) and CD11b/CD18 (Mac-1), and low/undetectable levels of membrane-bound signaling molecules needed for antigen presentation and phagocytosis, such as the major histocompatibility complex class I (MHCI) and MHCII antigens [72]. The resting state of microglia is heavily influenced by the neuronal microenvironment, which exerts numerous inhibitory mechanisms. These include production of cell surface mediators with anti-inflammatory

properties, such as IL-10 and transforming growth factor (TGF)-β, and induction of proteins, such as suppressor of cytokine signaling (SOCS) proteins, and transcriptional repressors, Nurr1 and ATF3, that inhibit production of neurotoxic/pro-inflammatory factors in microglia [73-75]. Physical interactions between microglia and neurons through ligand-receptor pairs, including CX3CL1-CX3CR1 and CD200-CD200R, also attenuate microglial activation [76, 77].

Microglia activation: neurotoxicity and neuroprotection

Microglial activation, a change from a resting to a pro-inflammatory phenotype, can be triggered by foreign material or disturbances in CNS homeostasis. Microglial responses upon activation include proliferation and upregulation of inflammatory markers CD45 and CD11b, as well as co-stimulatory molecules (CD40, CD80, and CD86) [72]. Importantly, expression of these molecules gradually increases upon microglial activation. Once activated, microglia undergo a dramatic morphological transformation, with the processes retracting resulting in an amoeboid morphology similar to that of immature microglia (**Figure 1-2**) [68]. This phenomenon is termed reactive microgliosis. Activated microglia express many markers of macrophage differentiation: Fc receptors (Fcγ RI, RII, RIII), pattern recognition receptors (CD14, TLR4), complement receptors (CR3, CR4) and cytokine and chemokine receptors [55, 72]. The neurotoxic consequences of microglial activation are commonly associated with production of pro-inflammatory cytokines, such as TNF-α, reactive oxygen species and inducible nitric oxide synthase (iNOS), which increase neuronal damage following brain injury [71, 75]. Despite these negative consequences, activated microglia have also been shown to perform many essential beneficial functions such as clearing apoptotic cellular debris and pruning neuronal synapses [75]. Further, they can produce neurotrophic factors and anti-inflammatory cytokines, such as IL-10 and TGF-β, which promote

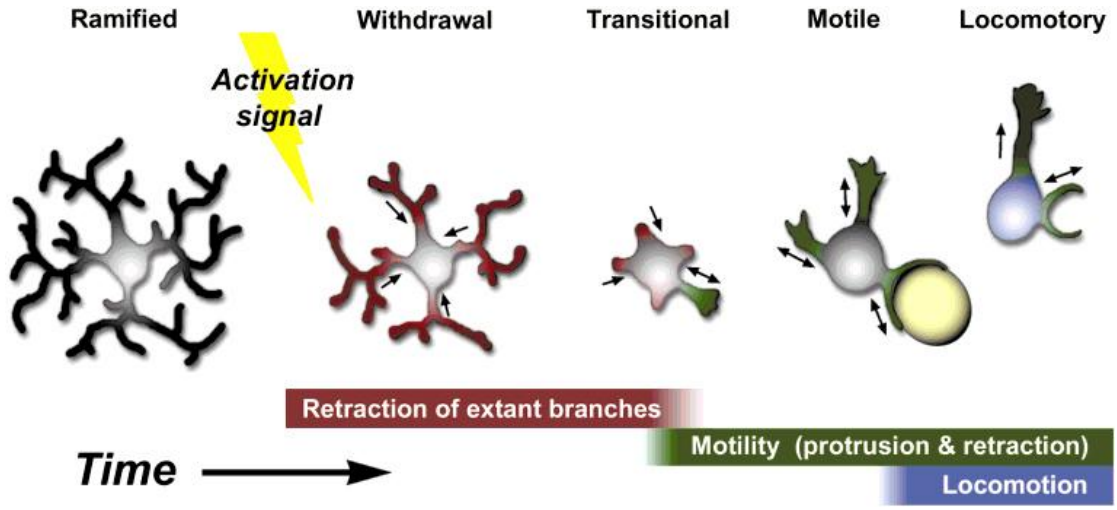

Figure 1-2. Structural dynamics of reactive microgliosis. This diagram shows that microglia undergo substantial morphological changes in response to tissue injury or inflammatory stimuli, which involves rapid alterations in the cell body and number of processes. Microglia evolve from a ramified (or resting) state, characterized by small cell bodies with thin, spider-like projections, into roundish amoeboid cells with enlarged cell bodies. Conversion into the activated state occurs in a stepwise progression in which existing ramified branches retract into the cell body so that they are partially or completely resorbed, classified as the locomotory stage whereby microglia can rapidly migrate throughout tissue. Taken from [68].

neurogenesis and suppress further microglial activation [75]. Clearly there is an important balance between beneficial and detrimental effects of microglial activation. Consequently, failure of these homeostatic mechanisms or unrestrained microglial activation can contribute to neuronal damage and degeneration.

Under inflammatory conditions, microglia can be functionally classified into pro-inflammatory or anti-inflammatory subsets according to the M1/M2 nomenclature, in a similar manner as peripheral macrophages. This classification system distinguishes microglia by their cytokine profile and expression of cell surface markers into two major types, pro-inflammatory M1 and anti-inflammatory M2. M1 is defined as the classical activation state, characterized by expression of cytokines such as TNFα, IL-6, IL- 1β, interferon-γ (IFNγ) and NO as well as surface molecules CD86 and CD68 [78-81]. Hence they are geared towards antigen presentation and show neurotoxic effects in the brain. In contrast, the “alternatively activated” M2 microglia are known to express arginase 1, the mannose receptor CD206 and anti-inflammatory cytokines such as IL-4 and IL-10 [78-81]. This second class exerts neuroprotective and anti-inflammatory actions such as wound healing and phagocytosing cellular debris to restore homeostasis. Indeed, mice lacking M2-polarizing signals such as IL-4 and IL-10 show worsened neurological function and increased brain infarction following focal cerebral ischemia [82, 83], whereas M1 microglial markers increase during disease progression, as with spinal cord injury [84, 85].

In addition to microglia, the brain contains macrophage populations that are distinguished by location, morphology and constitutive expression of standard macrophage markers such as class I and class II MHC antigens [48]. These include macrophages in the choroid plexus, the meninges and the perivascular spaces. Perivascular macrophages are localized between the parenchyma and vascular system and have an elongated cell body and branching processes, which encase

the blood vessel membrane [72, 86]. They have a critical influence on blood vessel function owing to their close association with the BBB, which separates the circulating blood from the brain. Interestingly, many studies indicate that perivascular and meningeal macrophages are the primary antigen-presenting cells in the CNS. Furthermore, unlike parenchymal microglia, these cells are short-lived and frequently replaced by blood-borne precursors [72, 87].

In summary, microglia are the principal immune cells in the brain, which can be distinguished from other CNS cell types, such as neurons and astrocytes, by their unique myeloid origin. They are remarkably plastic cells, capable of exerting cytotoxic or protective functions depending upon microenvironment signals. Microglia play essential roles in neuroinflammation and tissue homeostasis due to their ability to express cytokines and immune receptors, which are a crucial part of immune effector functions such as antigen presentation and phagocytosis.

Astrocytes: Biology and Functions

Origin and historical view of astrocytes

Astrocytes are specialized glial cells of ectodermal origin. In 1893, Michael von Lenhossek coined the term astrocyte to describe their star-shaped morphology [88]. In the human brain, astrocytes constitute nearly half of the cells in the CNS [89]. While they are present in all regions of the CNS, the term astrocyte usually refers to protoplasmic astrocytes, which densely populate gray matter tissue. There is also a second class of astrocytes called fibrous astrocytes that exist in white matter regions [90].

Morphologic and molecular characteristics of astrocytes

Traditionally, the morphological features and spatial relationship with neurons are often used to

distinguish between astrocyte subclasses (i.e. protoplasmic vs. fibrous) [90]. Protoplasmic astrocytes, the most common, have a complex morphology with numerous fine processes that can contact synapses, dendrites and cell bodies of neurons. In contrast, fibrous astrocytes have less branching and exist around bundles of axons in white matter tracts. This broad classification system does not address other forms of astrocyte heterogeneity, such as molecular and physiological properties (for review see [91]). Astrocytes differ in their physiological properties such as membrane potential, potassium conductance, glutamate transporter and receptor expression, and/or the expression of proteins such as glial fibrillary acidic protein (GFAP). Other defining characteristics of astrocytes include calcium-mediated intracellular communication [92, 93], the presence of intercellular connections (gap junctions) [94, 95], and the close apposition of astrocytic processes to both neurons and blood vessels, *via* end-feet [46].

Astrocytes are often identified using immunohistochemical markers for astrocyte specific proteins. The most well characterized and extensively studied marker is GFAP, an intermediate filament protein, which is enriched in the cell body and major processes of astrocytes [96]. GFAP has been used as the primary marker for astrocytes since its discovery in 1971 when it was isolated from the CNS of multiple sclerosis patients [97]. Other molecular markers used for the identification of astrocytes include: S100 calcium binding protein β (S100B) [98], glutamine synthase (GS), excitatory amino acid (EAA) transporters GLAST (glutamate-aspartate transporter) or GLT-1 (glial glutamate transporter 1), and most recently the aldehyde dehydrogenase 1 family, member L1 (Aldh1L1) [99]. However, no molecular marker, including GFAP, is universal to all astrocytes [60].

Functions of astrocytes in the CNS

Astrocytes have elaborate processes that extend between the synaptic connections of neurons and also separate neurons from blood vessels [46]. It has been estimated that each human astrocyte can contact more than one million cortical synapses [100]. This close association with neurons makes astrocytes key participants in modulating neuronal activity. Astrocytes synthesize biochemicals and receptors also expressed by neurons. These features enable astrocytes to regulate the release and uptake of neurotransmitters such as glutamate and ATP, and in turn control synaptic transmission and neuronal excitability [93, 101]. In particular astrocytes are critical for modulation of glutamatergic neurotransmission as they express high levels of glutamate transporters (in particular GLAST and GLT-1) that tightly regulate glutamate concentrations in the synaptic cleft [102].

In conjunction with endothelial cells and neurons, astrocytes are intimately involved in BBB formation, integrity and maintenance, limiting entry of leukocytes and antigens into the CNS [46]. Astrocytic processes terminate in end-feet on blood vessels where they tightly ensheath endothelial cells and secrete factors including TGF-β, glial-derived neurotrophic factor (GDNF), angiopoetin 1 (ANG1) and basic fibroblast growth factor (bFGF) that support the formation of tight junctions between endothelial cells [46]; consequently, reducing permeability of the BBB. Astrocytes that envelope endothelial cells are ideally positioned to control the volume of the extracellular space via modulation of blood flow and brain water content. Astrocytic end-feet actively participate in the regulation of blood flow by producing and releasing molecular mediators that dilate and constrict blood vessels, such as nitric oxide (NO), prostaglandins (PGE), and arachidonic acid (AA) [60, 103]. They also express transmembrane channels called aquaporins (AQPs) that drive water transport across the BBB and thus play a critical role in

cerebral edema, which significantly contributes to pathology in many neurological disorders [60, 102].

Another critical function of astrocytes is the supply of energy to neurons in the form of lactate [104, 105]. Glucose enters the brain parenchyma where is taken up by astrocytes *via* glucose transporter type 1 (GLUT 1) and is subsequently converted to lactate to be transferred to nearby neurons or alternatively is stored in astrocytes in the form of glycogen [104, 105]. Astrocytic glycogen makes up the largest energy reserve in the brain [60]. Astrocytes also supply lipids to neurons, and in the absence of glucose can oxidize fatty acids to produce ketone bodies as an alternative energy source [106, 107]. Synaptic formation strictly depends on cholesterol and other brain lipids, which pass from the blood stream to neurons *via* apolipoprotein E (ApoE), a major lipid transport protein in the CNS that is predominantly localized in astrocytes [108, 109]. The energetic coupling between astrocytes and neurons is essential to sustain the high-energy demands during brain activity, and thus is critical for normal brain function. This is exemplified by recent evidence demonstrating that lactate transport between neurons and astrocytes plays an essential role in long-term memory formation [110].

Astrocyte activation: reactive astrogliosis

In part due to their intimate relationship with neurons and the BBB, astrocytes also have fundamental roles in the innate immune response of the CNS and undergo key morphological changes in response to CNS pathologies [59]. In the context of neuroinflammation, astrocytes respond by a process referred to as reactive astrogliosis, characterized by cellular hypertrophy, proliferation, and increased expression of the intermediate filaments GFAP, vimentin, and nestin [59, 111]. In general, upregulation of GFAP expression underlies the transition of quiescent

astrocytes to the activated (reactive) phenotype. Reactive astrogliosis is a graded phenomenon, ranging from mild alterations in gene expression and cellular morphology to severe (sometimes permanent) tissue reorganization in which astrocyte processes overlap extensively with adjacent cells to form glial scars [59]. Astrocytes, like microglia, produce either pro- or anti-inflammatory cytokines and have immunoregulatory receptors in their membranes including MHC antigens, costimulatory molecules (B7-1, B7-2) and adhesion molecules (ICAM-1, VCAM-1) [112]. Traditionally, reactive astrogliosis is a marker of neuropathology; however, it is well established that like microglia, reactive astrocytes can have either beneficial or detrimental effects depending on the disease or specific molecular signaling pathways involved. Astrocyte mediated neuronal injury is caused predominantly by overproduction of reactive oxygen species (ROS) or proinflammatory cytokines and chemokines, including interferon (IFN)-γ, IL-1, IL-6, and MCP-1 [113]. Other studies, however, show protective and reparative roles for reactive astrocytes. Rothstein et al. [114] demonstrated that loss of astrocyte glutamate transporters GLAST or GLT-1 leads to elevated extracellular glutamate levels, resulting in excitotoxcity, neural degeneration and paralysis in rats. Further, ablation of GFAP-positive reactive astrocytes has been shown to substantially increase CNS leukocyte invasion and inhibit protective glial scar formation that restricts inflammation and tissue damage after injury [115]. These observations clearly illustrate the importance of astrocyte function in maintaining multiple aspects of CNS homeostasis.

In summary, astrocytes are key glial cells responsible for the structural support and proper functioning of neurons and cerebral vascular endothelial cells of the BBB. Astrocytes not only have a significant role in the regulation of neuronal synaptic activity, but are also an important source of inflammatory mediators and regulate BBB permeability. They help maintain the CNS microenvironment and are consequently highly reactive to disturbances in CNS homeostasis,

undergoing morphological and functional changes referred to as reactive astrogliosis.

Functional interactions between neurons, microglia and astrocytes

Astrocytes, neurons and microglia are continuously interacting. The mediators of these interactions consist of surface receptors and associated signaling molecules, which include neurotransmitters, cytokines, and neuropeptides. One candidate signal is the membrane-bound chemokine CX3CL1, also known as fractalkine (FKN), and its receptor CX3CR1 [116]. Fractalkine is constitutively expressed by neurons throughout the CNS. Neuronal excitation induces the release of fractalkine, which then binds and activates CX3CR1 receptors on microglia [117, 118] whose function is to inhibit microglial inflammatory activity. In this way, it has been proposed that microglia are able to sense and respond to neuronal activity. In turn, FKN/CX3CR1 signaling exerts regulatory control over neuronal activity related to synapse development and plasticity. Mice deficient in CX3CR1 exhibit deficits in developmental synaptic pruning [119], a process that involves the elimination or strengthening of connections between neurons, known as synapses. Consequently, these mice have reduced functional connectivity between the hippocampus and prefrontal cortex, resulting in social behavioral abnormalities [119]. Additionally, neurons can also act on microglia in a paracrine manner *via* secreted factors such as cytokines. For example, the anti-inflammatory cytokines IL-10 and TGFβ have been shown to down-regulate the microglial activation state in the presence of LPS, as indicated by decreased expression of activation molecules such as MHCII, and inflammatory mediators including pro-inflammatory cytokines TNFα and IL-1β, as well as nitric oxide [120-122]. These cytokines and their receptors are expressed throughout the CNS in both glial cells and neurons [123]. Additionally, TNFα released from astrocytes can affect neuronal excitability. Recent discoveries show that

astrocyte-released TNFα modulates basal synaptic transmission in the hippocampal dentate gyrus [124], and actively participates in mechanisms of homeostatic synaptic plasticity, such as synaptic scaling, that provide neurons with an activity-dependent mechanism to modify individual synapses [125, 126]. Specifically, TNFα has been reported to increase cell surface expression of AMPA receptors (AMPAR) leading to an increase in synaptic strength [127].

In addition to glial modulation of neuronal activity, an essential aspect of normal brain function is the bidirectional interaction between astrocytes and microglia. For example, co-culture experiments show that crosstalk between astrocytes and microglia, following activation, can amplify CNS inflammatory responses. Saijo et al. [73] found that LPS-induced neurotoxicity of dopaminergic neurons *in vitro* was significantly enhanced by the combination of activated astrocytes and microglia, as compared to either cell type alone. It has also been shown that pathological activation of microglia following LPS stimulation induces ATP release, recruiting nearby astrocytes that in turn, trigger the release of glutamate and additional ATP on hippocampal synapses to enhance the frequency of excitatory neuronal activity [128]. Alternatively, astrocytes have the ability to suppress pro-inflammatory responses in microglia. Min et al. [129] showed that treatment with astrocyte-conditioned culture media markedly attenuated hydrogen peroxide-induced production of ROS in primary cultures of microglial cells by stimulating antioxidant gene expression. This study indicates that astrocytes can activate a negative feedback loop down-regulating production of neurotoxic compounds by microglia, such as ROS. Taken together, these examples show that neurons and glial cells functionally interact in healthy conditions, and may also advance the development of a number of pathological states, such as inflammation of the brain.

Goals of Thesis

The effects of obesity and high-fat feeding on neuroinflammation remain poorly understood. Thus, the primary goal of this dissertation is to advance our understanding of inflammatory changes in the brain in response to obesity and high-fat feeding, and to begin to address their potential physiologic significance. In other disease pathologies, neuroinflammation is commonly attributed to the activation of microglial cells and astrocytes, as well as infiltration of non-CNS immune cells. To date, no studies have directly tested for recruitment of peripheral innate immune cells to the CNS during obesity, and only a few studies have investigated the contribution of resident glial cells to neuropathology during obesity. Critically, no studies have addressed the physiologic significance of glial cell activation in response to obesity and high-fat feeding.

This dissertation aims to address several key outstanding questions relating to the involvement of neuroinflammation in the physiologic response to obesity and high-fat feeding:

Chapter 3: In this chapter we test the hypothesis that chronic exposure to high-fat diet results in accumulation of peripheral immune cells in the CNS of diet-induced obese (DIO) mice.

Chapter 4: In this chapter we characterize the anatomical distribution of reactive astrocytes (as determined by increased GFAP-immunoreactivity), based on the hypothesis that reactive astrogliosis is present throughout several nuclei of the hypothalamus involved in food intake and body weight regulation.

Chapter 5: Chapter 5 focuses on circulating concentrations of a glial-derived neurotrophic factor S100B as a putative biomarker for obesity-associated inflammation. In this chapter we test the

hypothesis that elevated serum S100B contributes to obesity-associated inflammation in a DIO mouse model, consistent with previous observations in obese patients.

Chapter 6: Based on the findings from our anatomic characterization studies (**Chapter 4**), we hypothesized that astrocytes play a critical role in the physiologic response to high-fat diet. **Chapter 6** describes the development of a tetracycline-inducible mouse model allowing inactivation of the canonical NF-κB signaling pathway to determine whether inhibiting astrocyte activation (reactive astrogliosis) modulates food intake and protects against high-fat diet induced weight gain.

Overall, the studies performed in this dissertation have advanced our understanding of how neuroinflammation contributes to disease pathology in obesity that may aid in the development of novel therapeutics aimed at limiting or modulating neuroinflammation, which may eventually help improve obesity-associated co-morbidities and enhance successful long-term weight loss.

CHAPTER 2

Materials and Methods

Ethics Statement

All experiments were conducted in accordance with the National Institutes of Health (NIH) Guide for the Care and Use of Laboratory Animals and approved by the Animal Care and Use Committee of Vanderbilt University.

Mice

Unless otherwise indicated, animals were given ad libitum access to a 13% kcal standard laboratory chow (Std Chow; Picolab rodent diet 20, PMI Nutrition International, St. Louis, MO) and water. Animals were housed under constant temperature (21±2^{o}C) and light conditions (12 h light: 12 h dark) at 5 animals per cage, except where noted.

Mice used in Chapter 3: Mice for bone marrow transplant studies: Global green fluorescent protein (GFP)-transgenic mice (Stock #006567) of the C57BL/6 background were bred at Vanderbilt University from a founder purchased at Jackson laboratories (Bar Harbor, ME). In this transgenic model, GFP is expressed under the control of a chicken β-actin promoter and human cytomegalovirus enhancer. GFP transgenic mice were used as bone marrow donors at 10 weeks of age. Wild-type (WT) C57BL6/J mice (stock number: 000664) were purchased from Jackson Laboratories at 7-weeks of age and were allowed to acclimatize for 3 weeks. At 10 weeks of age, recipient (WT) mice were placed on antibiotic-containing (100 mg/l neomycin) water for one week prior to bone marrow transplant (BMT) and continued for one week after

the procedure. Recipient animals were initially placed on a 13% kcal Std Chow for 4 weeks post-BMT and then switched to a 60% kcal high-fat diet (HFD; Cat. no. D12532, Research Diets, New Brunswick, NJ) for an additional 15 or 30 weeks.

Mice used in Chapter 4: For the DIO studies: at 12–17 weeks of age, female C57BL6/J mice (*n* = 3–5 per diet) were placed on high-fat chow (60% kcal from fat; Cat. no. D12532, Research Diets, New Brunswick, NJ) or maintained on standard laboratory chow and body weights monitored weekly. After 20 weeks of high-fat feeding mice were deeply anesthetized and underwent tissue fixation via transcardial perfusion with 0.9% saline followed by ice-cold fixative (4% paraformaldehyde in 0.01 M phosphate-buffered saline pH 7.4 [PBS]). For the $MC4R^{-/-}$ versus $MC4R^{+/+}$ studies: Female MC4R-deficient mice (abbreviated $MC4R^{-/-}$) on the C57BL6/J background were generously provided by Dr. Roger Cone of Vanderbilt University, and have been described [130]. $MC4R^{-/-}$ mice (*n* = 5/genotype) were maintained on standard laboratory chow and were 24–28 weeks at the time of tissue collection after transcardial perfusion, as described for the DIO animals. $MC4R^{-/-}$ mice were backcrossed to the C57BL6/J background greater than 10 generations.

Mice used in Chapter 5: For the diet-induced obesity study: Male WT mice were purchased from Jackson Laboratories at 7-weeks of age. After one week of acclimatization, mice were weighed and divided into 2 groups (n=12/13 mice/diet) on Std Chow or HFD for a total of 15 weeks. For the weight-loss study: Eight-week old male WT mice, purchased from Jackson Laboratories at 7-weeks of age, were weighed and divided into one of three feeding treatments: 1) Lean – mice maintained on Std Chow diet for 20 weeks, 2) DIO - mice maintained on HFD diet for 20 weeks, or 3) Weight-loss group – mice fed HFD diet for 15 weeks then switched back to Std Chow for 5 weeks resulting in weight loss.

Mice used in Chapter 6: For conditional and specific suppression of NF-κB activity in astrocytes, GFAP-rtTA*M2 (abbreviated GFAP-rtTA) mice, purchased from Jackson laboratories (stock number 014098), were crossed with Tet-O Ikβα-DN (abbreviated IκBdN) mice containing the NFkB inhibiting construct. In this transgenic model (called IκB-DN in this Dissertation), the tetracycline responsive rtTA transactivator, under transcriptional control of the astrocyte GFAP promoter, undergoes conformational change and binds the tetracycline operator (TetO) to inhibit expression of NF-κB after administration of doxycycline (Dox). IκBdN mice were generously provided by Dr. Fiona Yull at Vanderbilt University, and have been described previously (Cheng et al., 2007; Connelly et al., 2011). Mice were of mixed background consisting of GFAP-rtTA on a C57BL6/J background and IκBdN on an FVB strain background. Transgene-negative (IκB-DN$^-$) littermates were used as control animals. Mice were individually housed and were acclimatized to Dox-treated drinking water (as described below) for a period of 1 week before beginning high-fat diet studies. Water and food intake were measured daily for a period of two weeks and every 2-3 days thereafter. Body weight of mice was measured once a week.

Body Weight and Composition

Body weights of mice were recorded weekly unless otherwise stated. Prior to sacrifice, fat and lean body mass were measured by nuclear magnetic resonance in unanesthetized mice using the Bruker Minispec Analyzer (Bruker Optics, TX) in the Vanderbilt Mouse Metabolic Phenotyping Center.

Reagents

All reagents used in electrophoretic separations were obtained from Bio-Rad Laboratories

(Hercules, CA). All other reagents were purchased from Sigma-Aldrich (St. Louis, MO), unless stated otherwise.

Doxycycline Preparation and Administration (Chapter 6)

Doxycycline (Sigma, St Louis, MO) was dissolved in drinking water containing 1% Splenda (zero-calorie sucralose as a sweetener) for a final concentration of 2mg/ml doxycycline. Dox-treated water was freshly prepared and administered twice weekly in light-protected bottles until study termination.

Western Blot Analysis

Samples of frozen tissue (i.e. brain and liver) were homogenized in RIPA buffer (Sigma-Aldrich, St. Louis, MO) containing protease inhibitors (Complete Protease Inhibitor Cocktail Tablets; Roche Applied Science, Indianapolis, IN), centrifuged at 13,000*g* for 10 minutes at 4^0C, and the protein content of the supernatant assessed by the Bradford method according to the manufacturer's instructions (Bio-Rad, Hercules, CA). Proteins were resolved by loading 10 µg tissue homogenate alongside a protein standard (Kaleidoscope ladder; Bio-Rad) on a 4–15% stacking sodium dodecyl sulfate-polyacrylamide gel electrophoresis (SDS-PAGE) gel (mini-protean TGX gel; Bio-Rad) and electrotransferred using a semidry transfer system (Bio-Rad) onto a nitrocellulose membrane (Perkin-Elmer, Boston, MA). The membranes were blocked using 5% skim milk in Tris-buffered saline (TBS) or LI-COR Odyssey blocking buffer (Li-Cor Biosciences, Lincoln, NE) and then incubated overnight at 4^0C with different combinations of primary and secondary antibodies as follows**:**

Chapter 4: The anti-glial fibrillary acidic protein (GFAP) antibody was diluted 1:1,000 in Odyssey blocking buffer containing 0.1% Tween 20 and then incubated with 1:20,000 anti-mouse IRDye 800 (Li-Cor Biosciences) for 1 hour at room temperature. The immunoreactivity was detected using the Odyssey Infrared Imaging Scanner (Li-Cor Biosciences).

ELISA

For measuring S100B in mouse plasma **(Chapter 5)**, immediately before sacrifice ~0.7 ml of blood was drawn by cardiac puncture into 3.2% sodium citrate–containing tubes (volume citrate solution: blood = 1:9) on ice, centrifuged 13,000*g* for 15 minutes at 4^0C and frozen at -70^0C prior to use**.** For measuring protein content in brain homogenates **(Chapter 5 & 6)**, frozen tissue was homogenized in RIPA buffer containing protease inhibitors, centrifuged at 13,000*g* for 10 minutes at 4^0C, and the supernatant immunoassayed for TNFα (eBioscience, France), GFAP and S100B (Millipore, Billerica, MA), according to manufacturer's instructions. ELISA sensitivity: 2.7pg/mL for S100B, 1.5ng/mL for GFAP, 8pg/mL for TNFα.

Quantitative Real Time RT-PCR (qPCR)

Total RNA was extracted using Trizol reagent (Life Technologies Corp., NY) and complementary DNA (cDNA) synthesized using iScript cDNA synthesis kits (Bio-Rad Laboratories, CA), according to manufacturer's instructions. Real-time RT-PCR (qPCR) reactions were performed using a CFX96 thermal cycler (Bio-Rad Laboratories, CA) and FAM-conjugated primer/probe sets (TaqMan Gene Expression Assays; all from Life Technologies Corp, NY) normalized to β-actin (catalogue no 4352341E) or *gapdh* (Mm99999915_g1). Quantification of target mRNA was calculated using the comparative Ct method (ΔΔCt). The assays used were *CD68*

(Mm00839636_g1) and *Ccl2* (Mm00441242_m1) for **Chapter 3**; and *Ccl2*, *s100b* (Mm00485897_m1), *rage* (Mm01134790_g1), *tnf* (Mm00443258_m1), *adipoq* (Mm00456425_m1) and *emr1* (Mm00802529_m1) for **Chapter 5**.

Immunohistochemistry

Confocal Imaging of Adipose Tissue: Fresh epididymal adipose tissue was harvested from 0.9%-saline-perfused mice and a portion post-fixed in 1% paraformaldehyde followed by 5% goat serum in PBS to block non-specific antibody binding. For **Chapter 3**, donor-derived cells were identified in adipose tissue sections by their endogenous expression of GFP. DAPI staining was used in all studies to visualize cell nuclei. Images were obtained with a Zeiss LSM 710 confocal microscope (Carl Zeiss International, Germany) in the Cell Imaging Shared Resource at Vanderbilt Medical Center. Immunohistochemistry of adipose tissue **(Chapter 5)** was performed with the following primary-secondary antibody combinations: 1:200 rabbit monoclonal anti-S100B (Cat # 52642; Abcam, Cambridge, MA) followed by 1:500 donkey anti-rabbit Alexa 488 (Life Technologies Corp., Carlsbad, NY) and 1:250 rat monoclonal anti-F4/80 (Cat # ab109497; Abcam, Cambridge, MA) followed by 1:500 donkey anti-rat Alexa 594 (Life Technologies Corp., Carlsbad, NY). Imaging with laser confocal microscopy (Zeiss LSM 710, Carl Zeiss International, Germany) was performed in the Cell Imaging Shared Resource at Vanderbilt Medical Center.

Immunohistochemistry of brain sections: Immunohistochemical analysis was performed on free-floating coronal brain sections, cut at a thickness of 30µm per slice from mice perfused with 0.9% saline followed by 4% paraformaldehyde. After initial blocking in 5% normal donkey serum in PBS containing 0.3% Triton X-100, sections were incubated with primary antibodies for 24 hours at 4^0C followed by secondary detection for 1 hour at room temperature, diluted 1:500

in blocking buffer. For brightfield images in **Chapter 3**, a primary antibody against GFP (dilution 1:5000; A-11122, Life Technologies, NY) was used followed by secondary detection with a horse radish peroxidase conjugated anti-rabbit IgG (W4018, Promega, WI) and visualized using Immpact DAB (Vector Laboratories, CA) on a wide-field microscope, Axioimager Z1 (Zeiss, NY). For quantification of GFP^+ recruited cells, the number of GFP-positive cells were counted in five sections per animal from five brain regions in Std Chow and HFD mice: cortex, septum and striatum (coordinates: 1.10-0.38mm from the bregma); thalamus and hypothalamus (coordinates: -0.70-2.54mm from the bregma). For confocal microscopy in **Chapter 3**, a primary antibody against Iba1 was used as a marker for microglia (dilution 1:1000; 019-19741, Wako, Germany) followed by secondary detection with donkey anti-rabbit Alexa 594 (dilution 1:500; Life Technologies Corp., NY) and images obtained using a Zeiss confocal microscope (see above *Confocal imaging of AT*). Guidance on nomenclature and anatomic boundaries was taken from [131]. Immunohistochemistry of brain sections in **Chapter 4** were stained and quantified as follows: Primary antibodies against GFAP (Cat # MAB360, Millipore, MA) and GFP (Cat # A-11122, Life Technologies, CA) were diluted 1:7,500 and 1:5,000, respectively, followed by secondary detection with donkey anti-mouse HRP (Cat # W4021; Promega, WI) and visualized using Immpact DAB. For fluorescent, double-labeling studies, secondary antibodies donkey anti-rabbit Alexa 488 (Cat # A-21206; Life Technologies, CA) and donkey anti-mouse Alexa 594 (Cat # A-21203; Life Technologies, CA) were used. Relative density of GFAP staining was qualitatively assessed and scored as follows: +/-, sparse staining; + light staining; ++ moderate staining; +++ extensive staining; ++++ very extensive staining. A minimum of two sections per animal per brain region were included for smaller nuclei and fives sections per animal examined for the larger more extensive nuclei.

Adipose Tissue Fractionation (Chapter 5)

Epididymal adipose tissue was dissected from lean and DIO mice and finely minced in PBS containing 0.5% bovine serum albumin (PBS-B) and then digested with 0.1 mg/mL collagenase (Cat# C6885; Sigma-Aldrich, MO). After incubating for 30 min at 37°C under constant agitation, cell suspensions were filtered through a 100µm mesh dissociation sieve and centrifuged to collect the stromal vascular fraction (SVF) cell pellets. The supernatant was subsequently centrifuged at 16,00rpm and collected as the total adipocyte fraction. After removal of the adipocyte layer, the stromal vascular fraction (SVF) cell pellets were gently resuspended in ACK lysing buffer (KD Medical Inc., MD) to remove red blood cells and washed in PBS-B. The final pellets were resuspended in Trizol (Life Technologies Corp., NY) for RNA extraction.

Flow Cytometry (Chapter 3)

Blood was taken at euthanasia by cardiac puncture, followed by brief erythrolysis with water to isolate peripheral blood leukocytes. Whole brain was removed from saline-perfused mice, the cerebellum and hindbrain removed, and the right cerebral hemisphere minced in phosphate buffered saline (PBS) and processed to obtain a single-cell suspension using a papain dissociation system (Worthington Biochemical Corp., NJ) according to the manufacturers' instructions. Samples were incubated with rat anti-mouse CD16/CD32 in FACS buffer (1XPBS plus 2% fetal calf serum, filter sterilized) for blockade of Fc receptors and immunostained as appropriate with fluorophore-conjugated antibodies: Rat anti-CD11b (clone M1/70; PE-conjugated), and Rat anti-CD45 (clone 30-F11; APC-conjugated; all from BD Biosciences, CA). Data from 20,000 live, single-cell events was acquired using FACSDiva software (BD Biosciences, CA). Cells were processed using a 5 Laser BD LSR Fortessa machine (BD Biosciences, CA) in the

Vanderbilt Flow Cytometry Core. For data analysis and collection, cells were initially gated on forward-scatter and side-scatter to exclude cell doublets. Dead cells were excluded based on DAPI labeling. Fluorescent compensations were performed using cells isolated from normal non-chimeric WT control animals and stained with each fluorochrome separately.

Name	Manufacturer	Description
CD11 antigen like family member B antibody (CD11b)	Cat. # 561688, BD Biosciences, CA	Cd11b is an integrin family member that is predominantly expressed on the surface of monocytes, which mediates leukocyte adhesion and migration to mediate the inflammatory response.
CD45 (**Leukocyte Common Antigen, L-CA) antibody**	Cat. # 55081, BD Biosciences, CA	CD45 is a receptor-like protein tyrosine phosphatase (RPTP) family member that is highly expressed on all nucleated haematopoietic cells and plays an essential role in antigen receptor-mediated signal transduction pathways.

Statistics

Statistics were performed with Graphad Prism version 5.04 software (GraphPad Software, San Diego, CA), and a significance level of 0.05 was used for statistical inference. Data are presented as mean ± standard error of the mean (S.E.M.). Unpaired t-tests were used to assess differences between two groups (animals on standard chow vs. high-fat diet). In **Chapter 3**, two-way ANOVA was used to determine the relationship between morphology and diet in the immunohistochemical analyses. Spearman's correlation analysis was used to quantify relationships between %GFP^+ brain-infiltrating immune cells and variables of interest (i.e. fat mass). For the weight-loss study in **Chapter 5**, one-way ANOVA was used to assess differences

between lean, obese and weight-loss groups. Two-way ANOVA was used to assess differences in gene expression between adipose tissue fractions of lean and DIO mice. In **Chapter 6**, two-way ANOVA was used to assess differences between groups of animals of different genotypes on different diets as well as assess the effects of diet, genotype, and their interaction.

CHAPTER 3

Obesity induced by a high-fat diet is associated with increased immune cell entry into the central nervous system

Laura B. Buckman[1], Alyssa H. Hasty[1], David K. Flaherty[2], Christopher T. Buckman[3], Misty M. Thompson[1], Brittany K. Matlock[2], Kevin Weller[2] and Kate L.J. Ellacott[1]

[1]Department of Molecular Physiology & Biophysics, and [2]Vanderbilt Flow Cytometry Shared Resource, and [3]Department of Cell and Developmental Biology, Vanderbilt University Medical Center, Nashville, TN 37232

The contents of this chapter have been published in Brain, Behavior, and Immunity, vol 35, pp. 33-42; January 2014.

Introduction

Leukocyte infiltration into the CNS is a key pathological feature in various inflammatory neurological disorders. These include neurodegenerative CNS disorders, like multiple sclerosis (MS) or Alzheimer's disease [132]. Infiltration of peripheral immune cells into the CNS is not significant under normal physiological conditions; however, massive CNS infiltration of bone-marrow-derived cells (BMDC) is a feature of the inflammatory state in mouse models of stroke and neuronal injury [132-134].

In common with what is seen in peripheral tissues, obesity causes inflammation in the CNS. For example, increased production of pro-inflammatory cytokines and reactive oxygen species occurs in the hypothalamus in response to both acute and chronic high-fat feeding in mice [32, 34]. Further, it has been demonstrated that high-fat feeding and obesity are associated with increased iba1-immunoreactivity [34, 42]; however, it is not known whether this is a result of increased activation of resident microglia or recruitment of peripheral immune cells, such as monocytes/macrophages that also express iba1 when present in the CNS. The presence of infiltrating macrophages in the CNS of rodent models of obesity has been inferred by increased expression the expression of CD45 (a pan leukocyte marker) immunoreactivity [40]. However, this methodology is limited and cannot be used to definitively demonstrate the recruitment of peripheral immune cells into the CNS during obesity due to the fact that high-levels of CD45 may be found on both activated microglia as well as infiltrating monocytes/macrophages [66]. We hypothesize that monocytes, which are amongst the earliest immune cells to infiltrate adipose tissue, are recruited into CNS parenchyma during obesity, thereby contributing to the neuropathological features associated with the disease. To study the migration of leukocytes into the CNS during obesity we employed a bone marrow chimeric mouse model generated by

transplanting green fluorescent protein (GFP)-expressing bone marrow into irradiated hosts, which distinguishes CNS microglia (radio-resistant cells) from peripheral monocytes solely by the expression of GFP. Previous studies using these mice demonstrated the ability of BMDCs to enter the CNS where they differentiate into microglial-like cells [135].

Results

Bone marrow chimeric animals show significant weight gain and adipose tissue inflammation in response to high-fat feeding

To confirm that the chimeric mice showed the "normal" physiologic response to diet-induced obesity we measured body weight, fat mass and peripheral inflammation in epididymal white adipose tissue. There was a statistically significant increase in weight gain (**Figure 3-1B**; 15 weeks, $t(14) = 5.15$, $P = 0.0001$; 30 weeks, $t(9) = 6.64$, $P < 0.0001$) within groups fed HFD due primarily to increased fat mass (**Table 3-1**). Assessment of adipose tissue whole mount preparations revealed adipocyte hypertrophy, and the accumulation of donor-derived GFP^+ cells, which often formed crown-like structures in obese adipose tissues (**Figure 3-1D**). In contrast, adipocyte hypertrophy and crown-like structures were not present in lean Std Chow control animals (**Figure 3-1C**). Additionally, gene expression of the monocyte chemotactic protein CCL2 (**Figure 3-1E**; $t(9) = 4.81$, $P = 0.001$) and the macrophage-specific antigen CD68 (**Figure 3-1F**; $t(9) = 5.43$, $P = 0.0004$) were significantly increased, 88% and 75% respectively, in adipose tissue from obese HFD animals as compared to lean Std Chow controls.

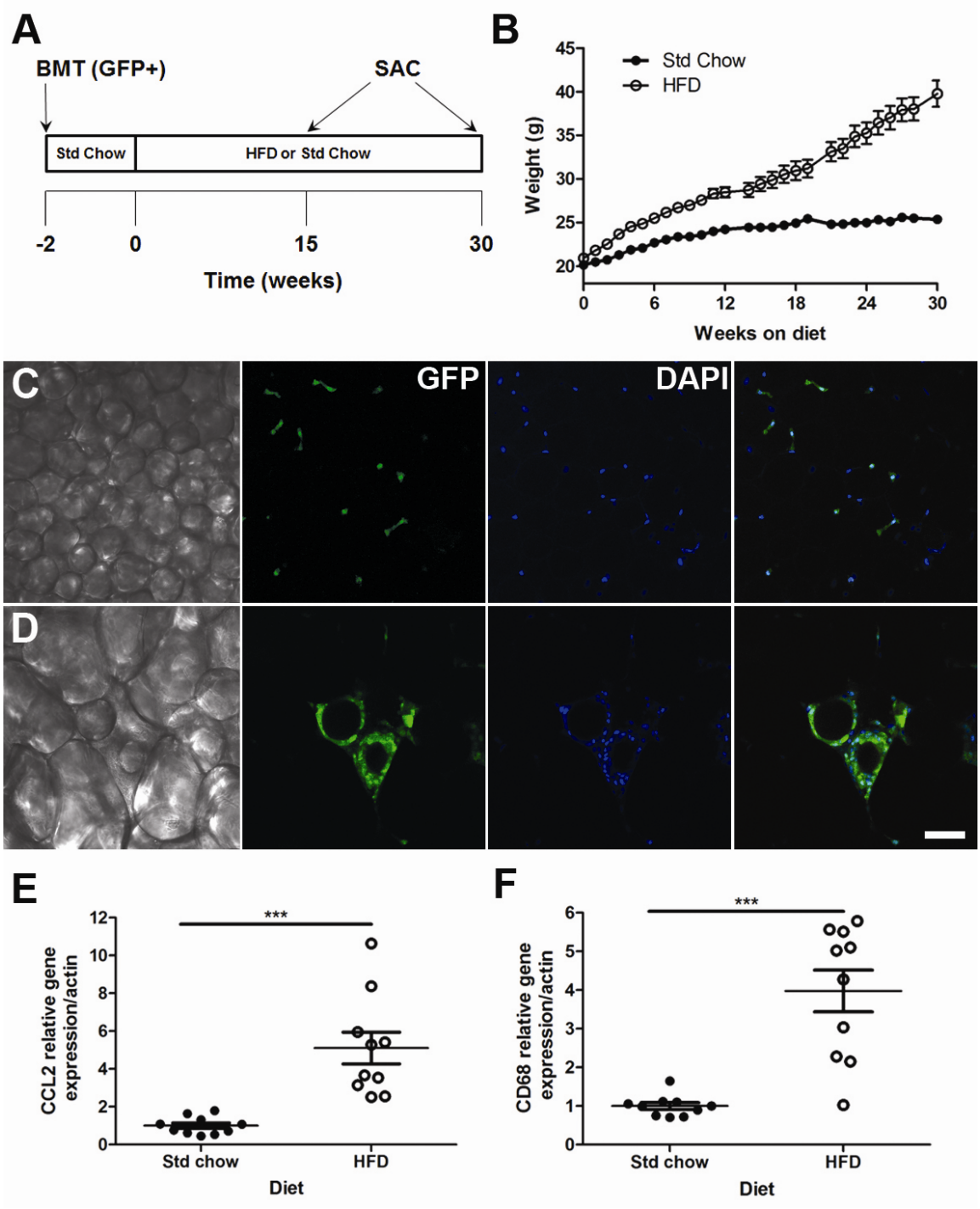
A
BMT (GFP+)
SAC
Std Chow
HFD or Std Chow
-2
0
15
30
Time (weeks)
B
Std Chow
HFD
Weight (g)
45
40
35
30
25
20
0
6
12
18
24
30
Weeks on diet
C
GFP
DAPI
D
E
CCL2 relative gene expression/actin
12
10
8
6
4
2
0
***
Std chow
HFD
Diet
F
CD68 relative gene expression/actin
6
5
4
3
2
1
0
***
Std chow
HFD
Diet

Figure 3-1. Bone Marrow chimeras show obesity and adipose tissue inflammation in response to a high-fat diet. C57BL/6J mice transplanted with GFP^+ (donor) bone marrow were randomly divided into two groups and fed either a 60% high-fat (HFD) or standard chow (Std Chow) diet for 15 or 30 weeks (A). Body weight was increased by high-fat diet (B). Confocal imaging demonstrated adipocyte hypertrophy (C, Std chow; D, HFD) and recruitment of GFP^+ (green) cells into white adipose. DAPI nuclear stain indicated in blue. White adipose tissue gene expression of inflammatory markers CCL2 (E) and CD68 (F) was significantly higher in mice fed a HF diet after 30 weeks. For real-time RT-PCR data, data are presented as mean ± S.E.M., n=10 mice per diet. An unpaired Student's *t*-test was performed for statistical evaluation of the data. *** $P<0.001$. Scale bar = 50μm.

Table 3-1. The body composition of the radiation bone marrow chimeric mice after 15 or 30 weeks on high-fat (HFD) or standard laboratory chow (Std Chow).

15 weeks (n=11/diet)				
Group	**Weight (g)**	**Fat mass (g)**	**Fat mass (%)**	**Muscle mass (g)**
Std Chow	23.64 ± 0.50	1.81 ± 0.14	7.64 ± 0.53	16.26 ± 0.16
HFD	29.27 ± 0.97	5.37 ± 0.75	18.62 ± 2.78	17.28 ± 0.52
	t(14)=5.15, *P*=0.0001	*t*(10)=4.68, *P*=0.0009	*t*(10)=3.89, *P*=0.003	*t*(11)=1.87, *P*=0.09
30 weeks (n=10/diet)				
Group	**Weight (g)**	**Fat mass (g)**	**Fat mass (%)**	**Muscle mass (g)**
Std Chow	25.05 ± 0.37	2.41 ± 0.17	9.56 ± 0.60	18.15 ± 0.32
HFD	38.52 ± 1.99	13.33 ± 1.51	33.61 ± 2.33	21.14 ± 0.54
	t(9)=6.64, *P*<0.0001	*t*(9)=7.20, *P*<0.0001	*t*(10)=10.01, *P*<0.0001	*t*(18)=4.78, *P*=0.0001

[a]Data are expressed as mean ± SEM.

High-fat diet-induced obesity is associated with increased recruitment of peripheral leukocytes into the CNS

The percentage of GFP^+ leukocytes in the blood after bone marrow transplant was examined in order to confirm that the cells that repopulated the peripheral immune system in the chimeric mice were of donor (GFP^+) origin (**Figure 3-2**). The mean percentage of GFP^+ peripheral leukocytes was greater than 90% across all animals (range 78–98%). There was no significant difference in the % GFP^+ leukocytes between the Std chow and HFD fed animals at 30 weeks (Std chow = 91.86 ± 1.75, HFD = 94.36 ± 0.65; P = 0.21, t(11) = 1.13). While there was a small, but statistically significant, difference in the % GFP^+ leukocytes between the Std chow and HFD fed animals at 15 weeks (Std chow = 92.29 ± 8.27, HFD = 95.9 ± 0.68; P = 0.003, t(19) = 3.40), there was no statistically significant correlation observed between the percentage of GFP^+ peripheral leukocytes and the number of GFP^+ single cell events in the CNS (**Figure 3-2**; ρ = 0.014, 95% CI = −0.30–0.33, P = 0.93).

Analysis of the peripheral blood leukocytes demonstrated that mice fed HFD have increased numbers of monocytes and total blood leukocytes as compared to Std chow controls, consistent with previously published data [136]. Therefore, we next investigated whether the appearance of donor-derived monocytes in the brain is attributed to monocytosis induced by a high-fat diet. We found elevated peripheral blood monocytes and total white blood cells (leukocytes) in obese compared to lean mice (**Figure 3-3**), yet the peak leukocyte or monocyte count did not correlate with the number of GFP^+ single cell events in the CNS, suggesting cerebral monocyte infiltration is not solely due to the total number of monocytes in peripheral blood.

The presence of peripheral immune cells in the brains of Std Chow and HFD mice was quantified using flow cytometry of isolated cells that were gated for their intrinsic GFP expression.

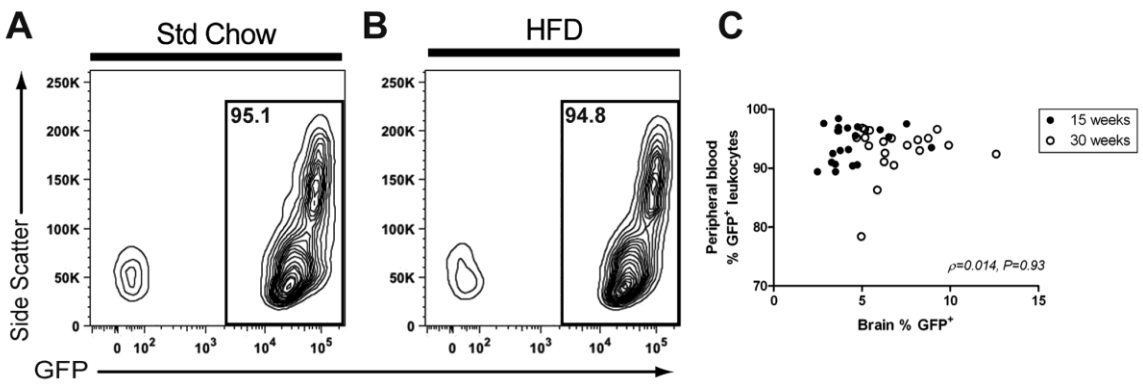

Figure 3-2. The mean percentage of GFP$^+$ peripheral blood leukocytes was greater than 90% across all animals. Donor-derived GFP$^+$ cells in the blood of recipient animals were assessed by flow cytometry and ranged from 78%-98% of total peripheral blood leukocytes. Representative contour plots are shown gated for GFP$^+$ cells (A-B). No correlation was observed between the percentage of GFP$^+$ cells in the brains and peripheral blood of BM chimeras (C). Spearman correlation was performed for statistical evaluation of the data across all animals, including mice fed high fat and standard laboratory chow. ρ and P values for association indicated on graph (n=10-11/diet/timepoint).

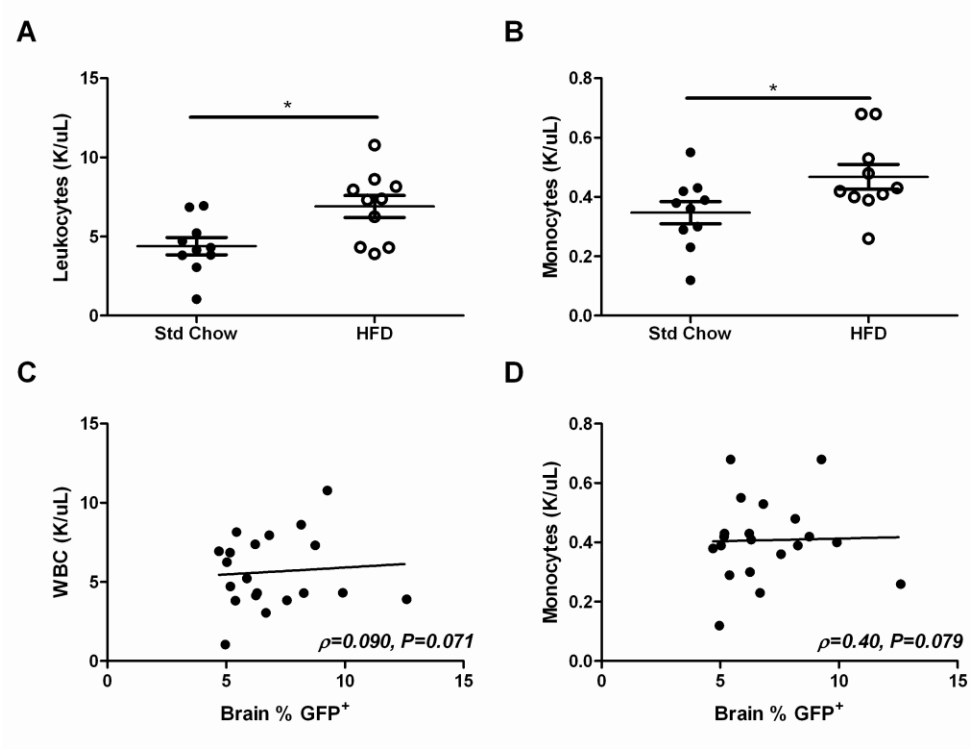

Figure 3-3. The total number of peripheral blood leukocytes and monocytes was significantly increased in HFD animals. Analysis of complete blood counts revealed increases in total leukocytes (A) and monocytes (B) in HFD animals as compared with Standard Chow controls. No correlation was observed between the percentage of GFP^+ cells in the brain and the numbers of peripheral blood leukocytes or monocytes of BM chimeras (C-D). Spearman correlation was performed for statistical evaluation of the data. ρ and P values for association indicated on graph (n=10-11/diet/timepoint).

Quantitative analysis revealed that the percentage of donor-derived GFP^+ peripheral cell infiltrates in the CNS was increased significantly in obese HFD mice at both 15 (**Figure 3-4A**; $t(12) = 2.21$, $P = 0.05$) and 30 weeks (**Figure 3-4B**; $t(18) = 2.22$, $P = 0.04$) as compared to their lean Std Chow controls when expressed as a percentage of single cell events (**Figure 3-4A and B**) or as a percentage of cells that were also positive for the hematopoietic lineage marker CD45 (**Figure 3-4C** – 15 weeks, $t(20) = 2.24$, $P = 0.04$; **Figure 3-4D** – 30 weeks, $t(18) = 3.29$, $P = 0.004$). We further analyzed the GFP^+ cells in the brain for expression of microglia/macrophage marker CD11b. The mean percentage of GFP^+ cells that were positive for both $CD11b^+$ and $CD45^+$ was greater than 80% in both Std Chow and HFD fed groups (**Figure 3-4E and F**).

High-fat feeding is associated with an increased number of $CD45^{hi}$ expressing microglia/macrophages in the brain

CD45 is expressed on all cells of the hematopoietic lineage; however, with respect to microglia, regulation of CD45 expression occurs in an activation-dependent manner. For example, ramified/resting microglia have a CD45 low phenotype ($CD45^{lo}$) and increase their cell surface expression to a high level ($CD45^{hi}$) upon activation [137, 138]. In contrast, macrophages in peripheral tissues constitutively express high levels of CD45; consequently CD45hi expression levels also characterize CNS-infiltrating peripheral monocytes. In this study we observed two distinct CD45 expressing populations: $CD11b^+/CD45^{lo}$ cells and $CD11b^+/CD45^{hi}$ cells. There was a significant increase in the ratio of $CD11b^+CD45^{hi}$ cells to $CD11b^+CD45^{lo}$ cells in the brains of obese compared to lean mice at both 15 (**Figure 3-5A**; $t(20) = 2.53$, $P = 0.02$) and 30 (**Figure 3-5B**; $t(18) = 3.24$, $P = 0.005$) weeks post-HFD. Fewer than 10% of the cells found in the $CD45^{hi}$ gates were GFP^-, suggesting that the majority of the $CD45^{hi}$ cells were GFP^+ CNS-infiltrating peripheral monocytes.

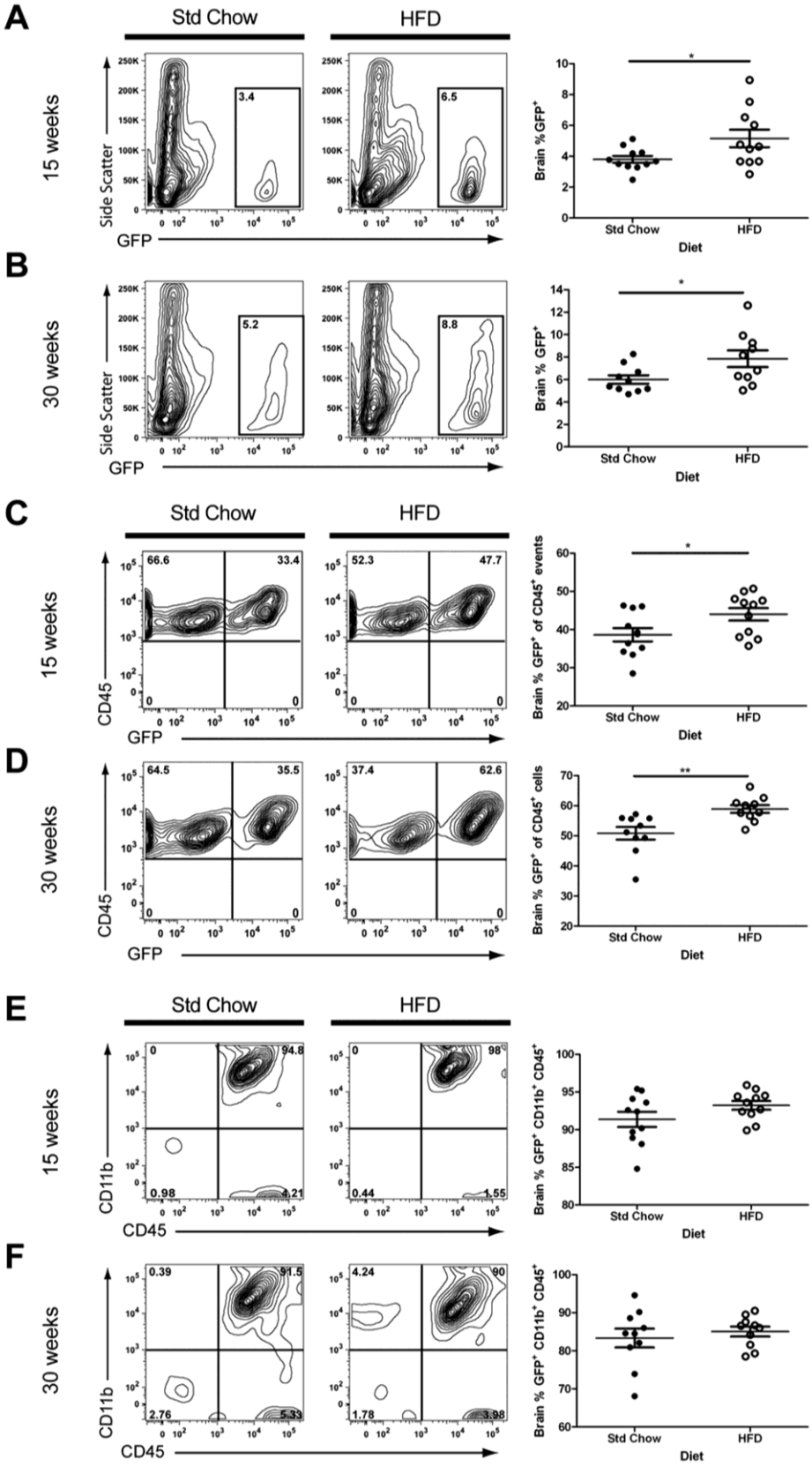
A
Std Chow
HFD
15 weeks
Side Scatter
GFP
3.4
6.5
Brain %GFP+
Std Chow
HFD
Diet
B
30 weeks
5.2
8.8
Brain % GFP+
C
CD45
66.6
33.4
52.3
47.7
Brain % GFP+ of CD45+ events
D
64.5
35.5
37.4
62.6
Brain % GFP+ of CD45+ cells
E
CD11b
94.8
98
0.98
0.21
0.44
1.55
Brain % GFP+ CD11b+ CD45+
F
0.39
91.5
4.24
90
2.76
5.33
1.78
3.98

Figure 3-4. Obesity is associated with increased immune cell entry into the CNS. Brain cells were isolated from recipient mice after 15 or 30 weeks on a HFD or Std Chow diet and analyzed by flow cytometry. High-fat feeding led to increased CNS infiltration of GFP^+ immune cells at both the 15 and 30 week time points, shown as a percentage of single cell events (A, B) or as a percentage of cells that were positive for the hematopoietic lineage marker CD45 (C, D). Greater than 80% of the GFP^+ cells expressed microglial markers CD11b and CD45 (E and F, upper right quadrants). Representative contour plots are shown for each diet/time point. Data are presented as mean ± S.E.M. (n=10-11). An unpaired Student's *t*-test was performed for statistical evaluation of the data. **P*<0.05.

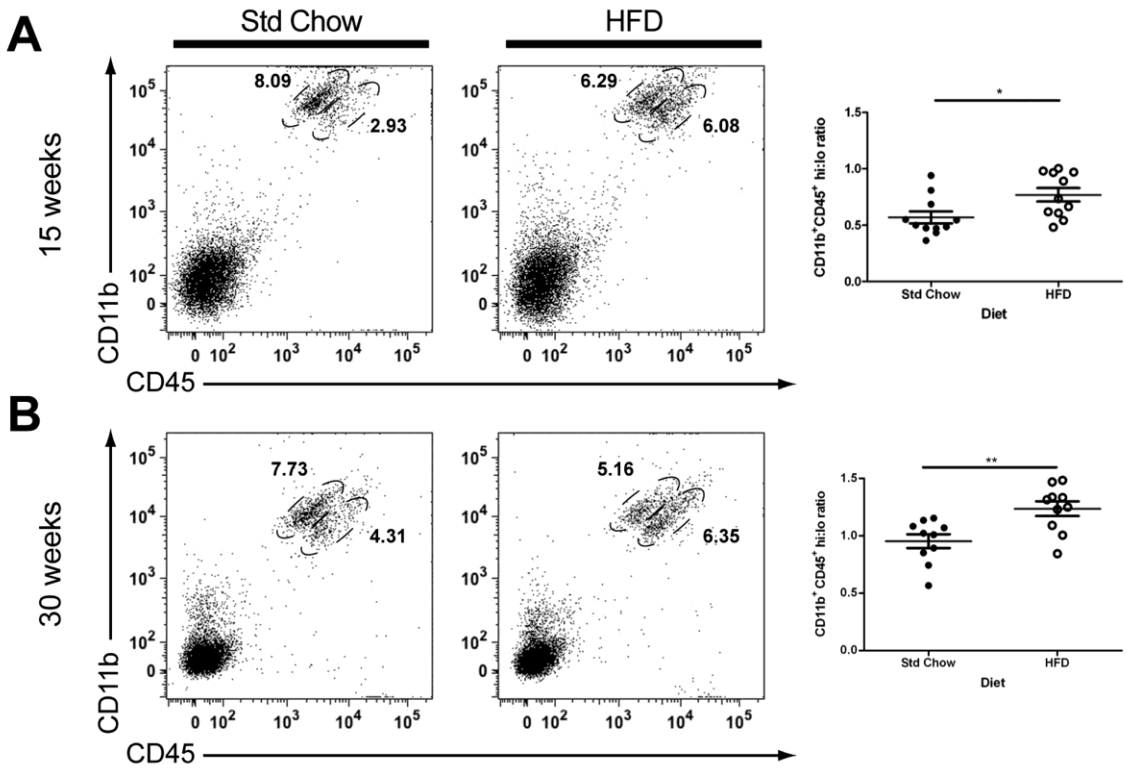

Figure 3-5. Obesity is associated with increased CD45^{hi}-expressing microglia/macrophages in the CNS. Flow cytometric analysis revealed that the percentage of CD11b^{+} cells that expressed high levels of CD45 was increased in HFD- induced obese mice at 15 (A) and 30 (B) week time points as compared to lean Std Chow-fed controls. Representative dot plots are shown gated for CD45^{hi} and CD45^{lo} cells. Data are presented as mean ± S.E.M. (n=10-11). An unpaired Student's *t*-test was performed for statistical evaluation of the data. **P*<0.05; ***P*<0.01.

Donor-derived GFP+ cells in the brain express the microglial marker Iba-1

Using immunohistochemistry we determined that the regional distribution of GFP^+ cells in the CNS was comparable with what has previously been reported using the radiation bone marrow chimera model [139]. Greater than 92% of the GFP^+ cells across both standard chow and HFD groups were found in the parenchyma and had a stellate morphology. In agreement with the flow cytometry data there was a statistically significant increase in the number of GFP^+ cells in the brains of the HFD animals compared with Std Chow fed controls, and this was due to an increase in the number of stellate cells as opposed to cells with an elongated or amoeboid morphology (**Figure 3-6**: $F_{diet}(1,8) = 9.28$, $P = 0.02$; $F_{morphology}(1,8) = 92.61$, $P < 0.0001$; $F_{interaction}(1,8) = 8.53$, $P = 0.02$).

We next performed double-immunohistochemistry to further validate our previous finding using flow cytometry that >80% donor GFP^+ cells in the brain were $CD11b^+CD45^+$, consistent with a microglia/macrophage phenotype. Immunostaining for the microglial marker ionized calcium-binding adapter molecule 1 (Iba1) revealed that most GFP^+ recruited cells indeed co-localized with Iba1. Furthermore, donor GFP^+ cells that were $Iba1^+$ were morphologically distinct from brain-resident microglia (**Figure 3-7**). Resident GFP^- $Iba1^+$ cells largely demonstrated a resting microglial morphology (**Figure 3-6**, solid white arrowheads), whereas $Iba1^+$ cells that were GFP^+ exhibited a distinct stellate morphology with enlarged somata accompanied by retraction and thickening of processes (**Figure 3-7**, open white arrowheads). In contrast, cells that were GFP^+ but $Iba1^-$ were rare and typically found located close to the microvasculature with an elongated morphology (**Figure 3-7F**) similar to what has been reported for perivascular macrophages [135].

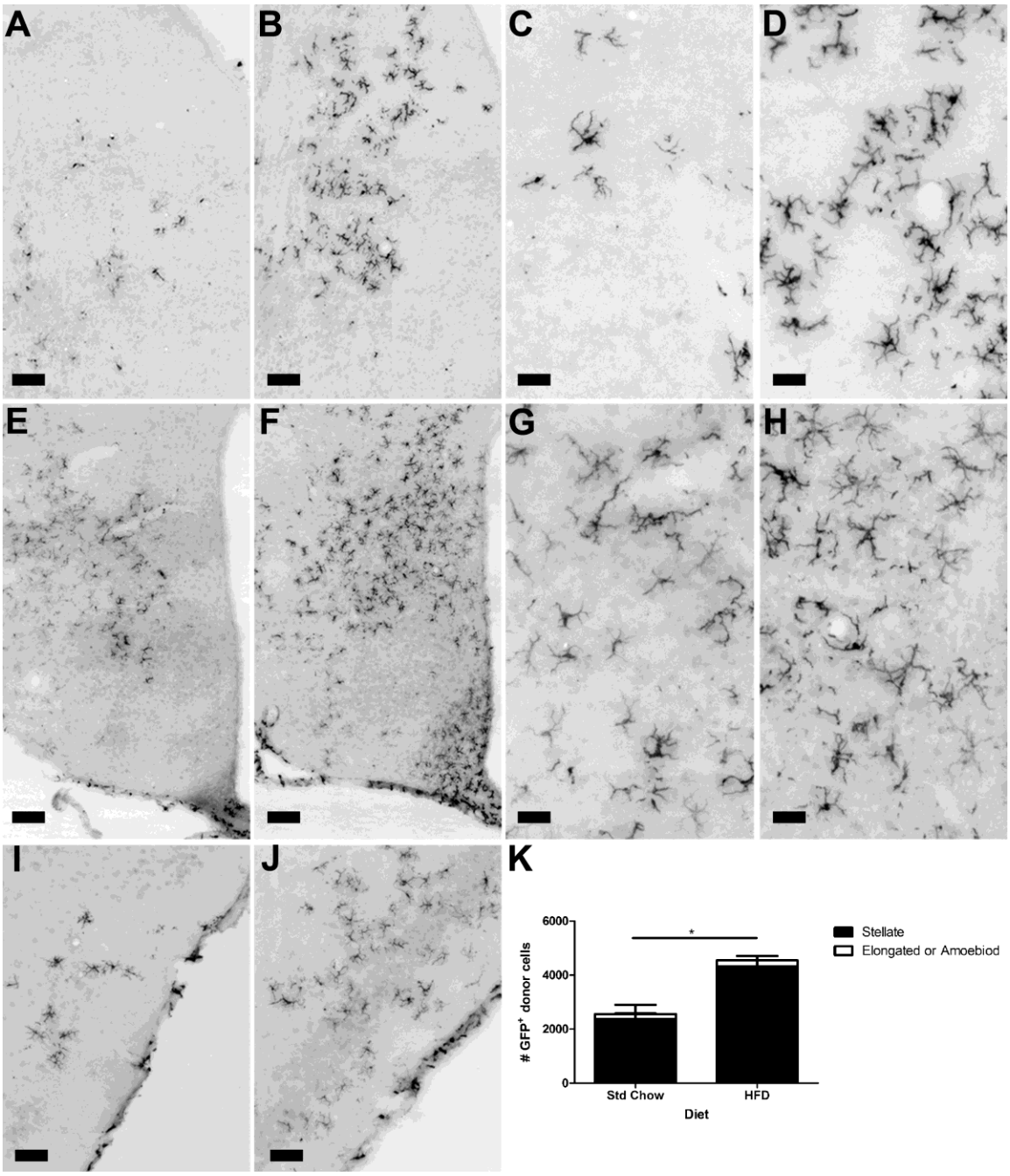
A
B
C
D
E
F
G
H
I
J
K
6000
4000
2000
0
GFP+ donor cells
*
Std Chow
HFD
Diet
Stellate
Elongated or Amoebiod

Figure 3-6. Distribution of GFP$^+$ immune cells in the CNS. Immunohistochemistry for GFP$^+$ cells showed increased recruitment in HFD animals compared with Std Chow controls. Representative images are shown for the septum (Std Chow - A,C; HFD - B, D); hypothalamus (Std Chow - E,G; HFD - F, H) and cortex (Std Chow - I; HFD - J). There was a statistically significant increase in total GFP$^+$ cells in the HFD animals due to an increase in cells of stellate morphology in the parenchyma. Data are presented as mean ± S.E.M. (n=3). Two-way ANOVA was performed for statistical evaluation of the data. *P<0.05. Scale bars: Panels A, B, I and J = 100μm; Panels C, D, G and H = 50μm; Panels E and F = 75μm.

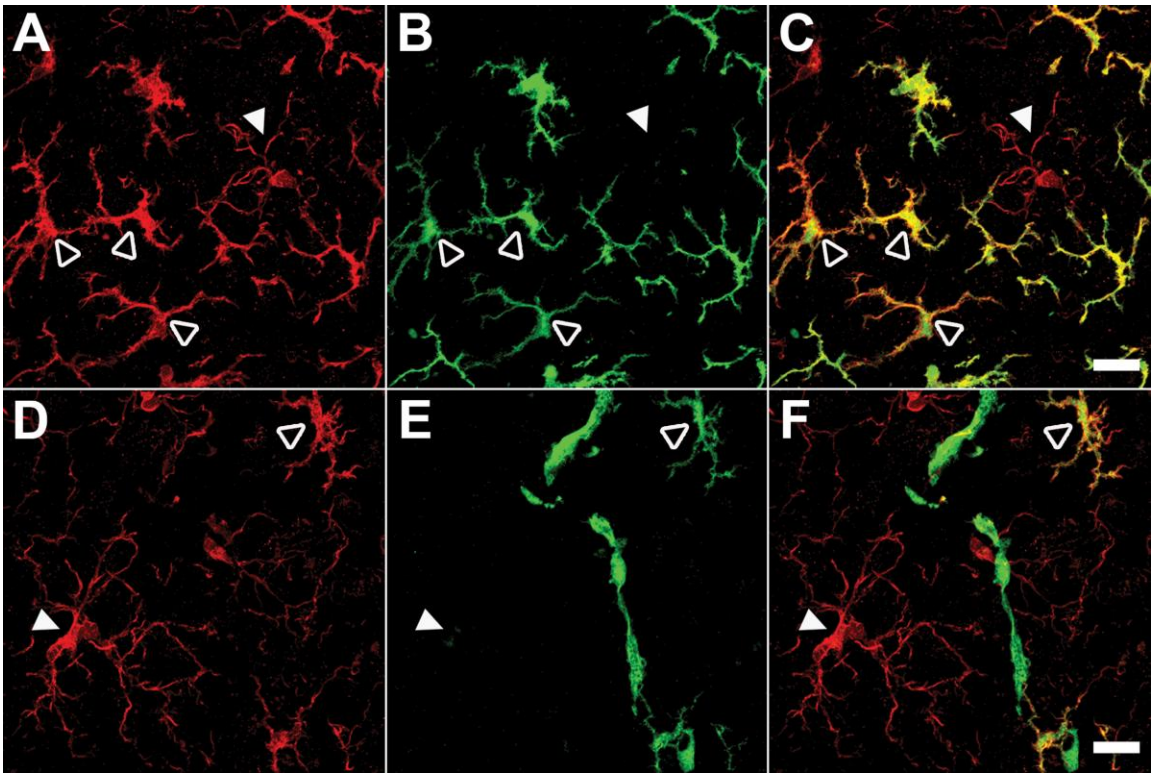

Figure 3-7. Morphology of GFP$^+$ cells recruited to the CNS. Confocal microscopy of CNS sections from recipient mice confirmed that GFP$^+$ cells expressed microglial marker Iba1 and had a stellate appearance (A-F, open arrowheads) compared with resident microglia which displayed a ramified ("resting") phenotype (A-F, closed arrowheads). Representative images showing microglia in red (Iba1; A, D), GFP in green (B, E), and overlay in yellow-orange (C, F). Co-localization of GFP and Iba1 staining was used to distinguish recruited cells (Iba1$^+$GFP$^+$) from resident microglia (Iba1$^+$GFP$^-$) (upper panels). The few GFP$^+$ cells that were negative for Iba1 were associated with blood vessels with an elongated morphology similar to perivascular macrophages (lower panels). Scale bars = 20µm.

Body weight, adiposity and white adipose tissue inflammation positively correlate with the number of GFP$^+$ immune cells in the CNS

Macrophage recruitment to white adipose tissue is an early event in obesity, which drives the development of low-grade systemic inflammation in both humans and mice [140]. Because macrophages content and inflammatory gene expression are highly correlated with the degree of obesity and metabolic dysfunction, we next looked at the relationship between measures of adiposity and macrophage inflammatory markers with the number of GFP$^+$ peripheral immune cells recruited to the CNS across all groups. In this study, we found that the degree of GFP$^+$ peripheral immune cell infiltrates in the CNS positively correlated with increases in body weight (**Figure 3-8A**; $\rho = 0.49$, 95% CI = 0.21–0.70, $P < 0.001$) and fat mass (**Figure 3-8B**; $\rho = 0.55$, 95% CI = 0.28–0.73, $P < 0.001$). Additionally, relative mRNA levels of CD68 (**Figure 3-8C**; $\rho = 0.36$, 95% CI = 0.05–0.60, $P < 0.01$) and CCL2 (**Figure 3-8D**; $\rho = 0.41$, 95% CI = 0.11–0.64, $P < 0.01$), markers of inflammation in white adipose tissue, were both positively correlated with the number of brain-infiltrating GFP$^+$ immune cells.

Discussion

We have demonstrated that high-fat diet induced obesity enhances recruitment of bone marrow-derived monocytes to the CNS. Radiation bone marrow chimera strategies have been highly effective for studying the role of leukocytes in the pathophysiology of obesity [141-148], including one of the initial studies demonstrating recruitment of macrophages into adipose tissue with obesity [140]. In agreement with these studies, our results indicate that bone marrow chimeric mice fed a high-fat diet exhibited the normal physiological response to high-fat feeding including increased body weight gain, adipose tissue macrophage recruitment and white

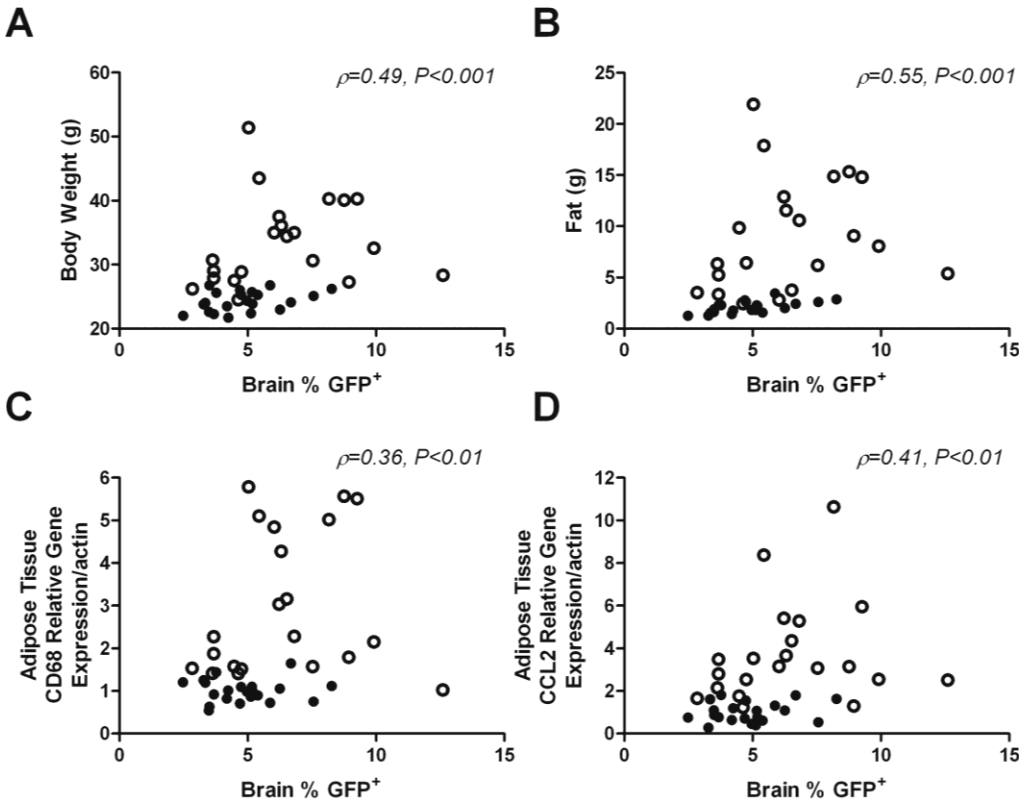

Figure 3-8. Infiltration of GFP$^+$ peripheral immune cells into the CNS is positively correlated with measures of adiposity and white adipose tissue inflammation. The relationship between the percentage of GFP$^+$ cells in the brains of chimeric mice with body weight (A), fat mass (B) and adipose tissue CD68 (C) and CCL2 (D) mRNA expression, across all groups. Data were analyzed using Spearman correlation. ρ and *P* values for associations indicated on graphs (n=10-11/diet/timepoint). ○, HF; ●, Std Chow.

adipose tissue inflammation. Furthermore, we found that the number of CNS-infiltrating monocytes was positively correlated with body weight, fat mass and markers of inflammation in adipose tissue (CD68 and CCL2 gene expression). These data point to a relationship between adiposity and adipose tissue inflammation, and the recruitment of immune cells to the CNS.

Obesity has previously been shown to be associated with microglial activation as assessed by immunohistochemistry [34, 40, 42] and positron emission tomography [40]. In the normal/non-inflamed brain, microglia exist primarily in a resting state with low levels of CD45 expression, which increases to high levels upon activation by inflammatory stimuli such as lipopolysaccharide and during neuropathology [149-151]. For this reason, it is not possible to unequivocally separate activated microglia and bone marrow-derived cells in the CNS by differences in CD45 expression alone. We observed a 30–35% increase in the ratio of $CD11b^{+}CD45^{hi}$ to $CD11b^{+}CD45^{lo}$ cells in our high-fat fed animals compared with the standard chow controls. This may reflect an increase in activation of resident microglia and/or the increase in bone marrow-derived cells in the CNS as non-CNS monocytes/macrophages that constitutively express high levels of CD45; however, our finding that fewer than 10% of the $CD11b^{+}CD45^{hi}$ cells were GFP^{-} suggests that it is likely that the increased recruitment of bone-marrow derived cells to the CNS in the obese animals largely underlies the increase in the $CD11b^{+}CD45^{hi}$ to $CD11b^{+}CD45^{lo}$ cell ratio seen in our study.

Immunohistochemistry revealed that 93% of the bone marrow-derived cells in the CNS were found in the parenchyma, but were not associated with vessels, and had a distinct stellate morphology characterized by enlarged somata accompanied by retraction and thickening of processes similar to what has previously been reported [135, 139, 152]. This is in contrast to resident microglia, which primarily had the ramified morphology characteristic of resting cells

[70]. While we have not proven it definitively by co-staining for activation markers, these morphological changes typically correlate with alterations in microglial action towards a macrophage-like phenotype including increased motility, migration, phagocytosis and cytokine production; however, it is not uncommon that microglial function changes independent of morphology [66]. Activated microglial morphology may alternatively indicate a lack of maturation of infiltrating cells following recruitment to the CNS. Undifferentiated microglia have an amoeboid morphology similar to activated microglia and thus have the ability to distribute across different CNS sites where they transition into a mature morphological ramified/resting phenotype [153, 154].

In support of the idea that bone marrow-derived monocytes behave like macrophages in the CNS, Simard and colleagues [132] demonstrated that bone marrow-derived monocytes/macrophages enter the CNS and phagocytose and degrade amyloid more effectively than resident microglia in a mouse model of Alzheimer's disease. The function of the bone marrow-derived monocytes and their potential contribution to disease pathology in obesity remains to be elucidated. High-fat feeding has been shown to be associated with increased apoptosis of hypothalamic neurons [155]; thus, it is feasible that bone marrow-derived monocytes are recruited to the CNS in obesity in response to this neuronal apoptosis and that they function like macrophages to clear neuronal debris. However, the finding that the increase in GFP^+ infiltrating cells was seen throughout the brain, and not exclusively in the hypothalamus, suggests that other mechanisms are likely to be involved. In the peripheral vasculature, obesity and high-fat feeding are associated with endothelial cell "activation" characterized by changes in expression of proinflammatory cytokines and cell adhesion molecules (for review see [156]), which is thought to be mediated, at least in part, by the activation of the toll-like receptor-4

pathway by diet-derived saturated fatty acids [157]. It is feasible that a similar mechanism may be causing changes in cerebral endothelial cells and thus contributing to the increased recruitment of monocytes to the CNS. Other potential mechanisms include obesity associated changes in CNS vascularity [158], blood–brain barrier permeability [33] and/or elevated CNS expression of chemokines such as MCP-1.

Due to their common cell surface markers it is difficult to accurately distinguish between resident microglia and peripheral immune cells recruited to the CNS during disease. To overcome this we used a radiation bone marrow chimera model, using GFP-labeled bone marrow to unequivocally distinguish between resident microglia and bone marrow-derived monocytes. The same strategy has also been used in a number of other disease models [132, 134, 152, 159-162]; however, it remains controversial whether the irradiation associated with the procedure influences recruitment of myeloid cells to the brain [163, 164]. Nonetheless, in our study both groups received equivalent treatment prior to the diet switch indicating that, in common with other neuroinflammatory conditions, diet-induced obesity increases recruitment of bone marrow-derived monocytes to the brain within this experimental paradigm.

In summary, our study demonstrates increased recruitment of bone marrow-derived monocytes into the CNS during high-fat diet induced obesity. Future work is needed to determine the physiological significance of immune cell recruitment to the CNS during obesity and whether these cells are recruited as a consequence of obesity-induced neuroinflammation and/or contribute to the neuropathology associated with obesity.

CHAPTER 4

Regional astrogliosis in the mouse hypothalamus in response to obesity

Laura B. Buckman*[1], Misty M. Thompson*[1], Heidi N. Moreno[1] and Kate L.J. Ellacott[1]

[1] Department of Molecular Physiology and Biophysics, Vanderbilt University Medical Center, Nashville, TN

*Contributed equally to this work

The contents of this chapter have been published in J Comp Neurol, vol. 521 , no. 6 , pp. 1322-1333; April 15, 2013.

Introduction

Astrocytes play a key role in maintaining the parenchymal environment in the brain and are also a critical component of the neurovascular unit of the blood-brain barrier (BBB) which regulates the influx and efflux of substances from the brain [46]. Astrocytic end feet are in close opposition to endothelial cells of the cerebral vasculature and *in vitro* astrocytes have been shown to regulate the physical tightness of the BBB as well as the expression of key transporters and enzymes [165-168]. Astrocytes are also known to functionally regulate synaptic plasticity via their interactions with neurons [169-172]. The hypertrophy and hyperplasia of astrocytes in response to acute or chronic insults in the brain is known as reactive astrogliosis. Astrogliosis can range from mild changes in astrocyte form and function to severe alterations characterized by the formation of a glial-scar which serves as a barrier between healthy and damaged tissues [59]. Astrogliosis is a feature of numerous neuropathologies including stroke, Alzheimer's disease, spinal cord and traumatic brain injury.

In the rodent hypothalamus, diet-induced obesity results in increased expression of proinflammatory cytokines TNFα and IL-1β [32, 34] and activation of the Ikkβ/NFkβ system [36], which is considered one of the key transcriptional pathways mediating inflammation. Evidence of gliosis (the hypertrophy and hyperplasia of glial cells) in response to high-fat feeding in rodents [33, 34, 40, 41, 173] is also suggestive of the presence of obesity-associated CNS inflammation. Whether this obesity-associated neuroinflammation arises *de novo* or in response to the well-characterized peripheral inflammation is not clear.

While astrogliosis in response to obesity has been reported in rodents, little information is available about the distribution of astrogliosis in the CNS in response to obesity. The expression

of glial-fibrillary acid protein (GFAP), an intermediate filament protein, is a commonly used as a marker of astrocytes. When examining obesity-associated astrogliosis previous studies have either used Western blotting for GFAP in homogenates of whole brain [33] or hippocampus [173], or have examined GFAP-immunoreactivity by immunohistochemistry exclusively in the arcuate nucleus of the hypothalamus (ARC; [34, 41, 169]). Due to the distinct roles of different hypothalamic nuclei in the regulation of energy homeostasis and other neuroendocrine processes, we sought to examine the pattern of astrogliosis across the region.

In this chapter we test the hypothesis that in response to obesity, astrocyte activation, as marked by increased GFAP expression, increases in key hypothalamic nuclei associated with energy homeostasis. We compare the distribution of immunoreactivity for GFAP throughout the hypothalamus in two distinct mouse models of obesity, diet-induced (DIO) and genetic melanocortin-4 receptor (MC4R) deficiency [130].

Results

Validation of the glial-fibrillary acidic protein (GFAP) antibody

In this study we used GFAP-immunoreactivity to examine the distribution of astrogliosis across the hypothalamus in response to obesity. **Tables 4-1 and 4-2** provide information on the antibodies used for conducting these studies. By western blotting the GFAP antibody detected a single band at ~51 kDa in brain homogenate, corresponding to the predicted size of the GFAP protein (**Figure 4-1A**). Furthermore, the GFAP immunoreactivity seen in brain slices corresponded to the known morphology of astrocytes (**Figure 4-1B**) [60]. Some GFAP immunoreactivity was also detected in ependymal cells around the third ventricle. When the secondary antibody was incubated with the tissue in the absence of the GFAP primary antibody

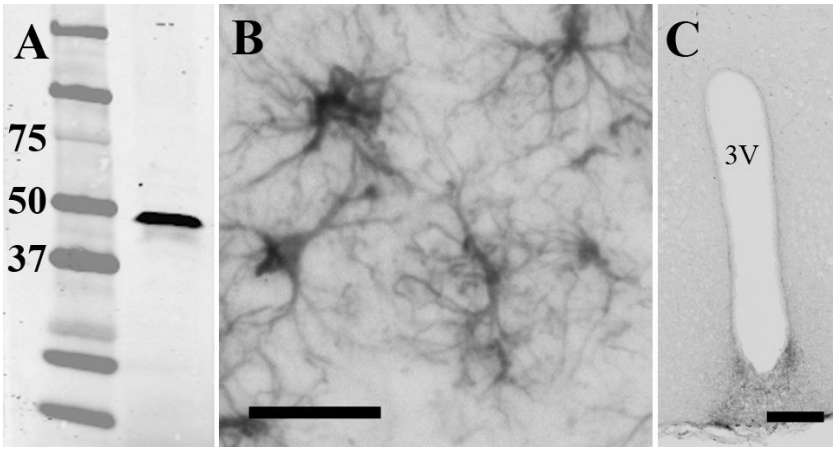

Figure 4-1. Characterization of the glial-fibrillary acidic protein (GFAP) antibody. A) Western blotting for GFAP in whole brain homogenate resulted in a band at 51 kDa corresponding to the predicted size of GFAP; B) GFAP-immunoreactivity seen in brain slices corresponded to the known morphology of astrocytes. Scale bar = 25 µm; C) Incubation of the tissue with secondary antibody in the absence of primary did not result in any cellular staining, indicating that the immunoreactivity seen was not due to non-specific binding of the secondary antibody to the tissue. Scale bar = 200 µm.

Table 4-1. Primary antibodies used in these studies.

Primary Antibodies			
Name	**Immunogen**	**Manufacturer**	**Host Species**
Glial-Fibrillary Acidic Protein (GFAP)	Purified GFAP from bovine spinal cord	Cat. # MAB360, Millipore Inc., MA	Mouse monoclonal, Clone GA5
Green-fluorescent Protein (GFP)	Purified GFP from *Aequorea victoria*	Cat. # A-11122, Invitrogen Life Technologies Corporation, CA	Rabbit polyclonal, IgG fraction

Table 4-2. Secondary antibodies used in these studies.

Name	**Manufacturer**	**Host Species**
Anti-mouse IgG (H+L) HRP	Cat. # W4021, Promega Corporation, WI	Donkey
Anti-rabbit IgG (H+L) AlexaFluor 488	Cat. # A-21206, Invitrogen Life Technologies Corporation, CA	Donkey
Anti-mouse IgG (H+L) AlexaFluor 594	Cat. # A-21203, Invitrogen Life Technologies Corporation, CA	Donkey
Anti-mouse IgG (H+L) IRDye 800CW	Cat #. 926-32212, Li-Cor Biosciences, NE	Donkey

no cellular staining was detected, indicating that the immunoreactivity seen was not due to nonspecific binding of the secondary antibody to the tissue (**Figure 4-1C**). A small amount of noncellular staining was seen at the median eminence, which was likely due the detection of mouse IgG that enters the brain at this circumventricular site.

Distribution of GFAP-immunoreactivity in the hypothalamus of lean and diet-induced obese mice

After 20 weeks of high-fat feeding the mean body weight of the DIO C57BL6/J mice was 42.1 ± 1.8 g, which was significantly greater than the standard chow fed lean group, 20.8 ± 0.8 g ($P<0.001$, two-tailed unpaired t-test). In the lean animals GFAP-immunoreactivity was seen at comparatively low levels throughout the hypothalamus, with the highest level seen around the arcuate nucleus (ARC; **Figures 4-2-4-3**). In obese animals, increased GFAP-immunoreactivity was also seen throughout the rostral-caudal extent of the hypothalamus; however, the astrogliosis was not uniform across all nuclei (**Table 4-3**). The most pronounced increases in GFAP-immunoreactivity were in nuclei proximal to the third ventricle (3V). In particular, high levels of expression were seen in the medial preoptic area (MPOm, vMPO; **Figure 4-2A and B**), paraventricular (Pa; **Figure 4-2C-F, Figure 4-4C and D**) and dorsomedial nuclei (DMN; **Figure 4-3A-F, Figure 4-4 E and F**) of the hypothalamus. High levels of GFAP-immunoreactivity were also seen in the ARC (**Figure 4-3E and F, Figure 4-4G and H**); however, in the medial portion of the ARC adjacent to the median eminence (ME; **Figure 4-3E and F**) the difference between the lean and DIO animals was less pronounced than in the rostral portion of the nucleus (**Figure 4-3A and B**). The areas with the highest level of GFAP-immunoreactivity often fell within in the distinct anatomic boundaries of hypothalamic nuclei. For example, while high levels of GFAP-immunoreactivity were seen in the DMN and ARC, the obesity-associated increase in expression

Table 4-3. Relative expression of glial-fibrillary acidic protein (GFAP) immunoreactivity in lean compared with diet-induced obese (DIO) mice.

Region	Bregma	Mean Lean	Mean DIO
Anteroventral periventricular nucleus (AVPe)	0.38 – 0.02	+/-	+
Anterodorsal preoptic nucleus (ADP)	0.14 - 0.02	+/-	+,+/-
Ventromedial and Medial preoptic nuclei (vMPO, MPOM & MPOL)	0.38 - -0.46	+	+,+/-
Medial preoptic area (MPA)	0.26 - -0.58	+	+
Periventricular hypothalamic nucleus (Pe)			
rostral	0.26 - -0.46	+	+,+/-
medial	-0.58 - - 1.34	+, +/-	+,+/-
caudal	-1.46 - -1.94	+/-	+, +/-
Suprachiasmatic nucleus (Sch)	-0.22- -0.82	+,+/-	++,+/-
Paraventricular hypothalamic nucleus (Pa)			
rostral	-0.58 - -0.82	+,+/-	++,+/-
caudal	-0.94 - -1.22	+	++
Anterior hypothalamic area (AH)			
Anterior	-0.34 - -0.58	+	+
Central	-0.70 - -0.82	+	+
Posterior	-0.94 - -1.34	+	+
Lateroanterior hypothalamic nucleus (LA)	-0.34 - -0.70	+	+
Lateral hypothalamic area (LH)			
rostral	-0.34 - -0.94	+/-	+

medial	-1.06 - - 1.70	+/-	+,+/-
caudal	-1.82 - - 2.46	+/-	+/-
Arcuate hypothalamic nucleus (ARC)			
rostral	-1.22 - -1.82	+++	+++
caudal	-1.94 - -2.46	++,+/-	++,+/-
Dorsomedial hypothalamic nucleus (DMN)			
rostral	-1.34 - -1.70	+	++,+/-
caudal	-1.82 - -2.18	+,+/-	++, +/-
Posterior hypothalamic area (PH)	-1.82 - -2.46	+	+
Premammillary nucleus, ventral part (PMV)	-2.30 - -2.46	+/-	+
Ventromedial hypothalamic area (VMH)			
rostral	-1.06 - -1.58	+	+, +/-
caudal	-1.70 - -2.06	+	+, +/-

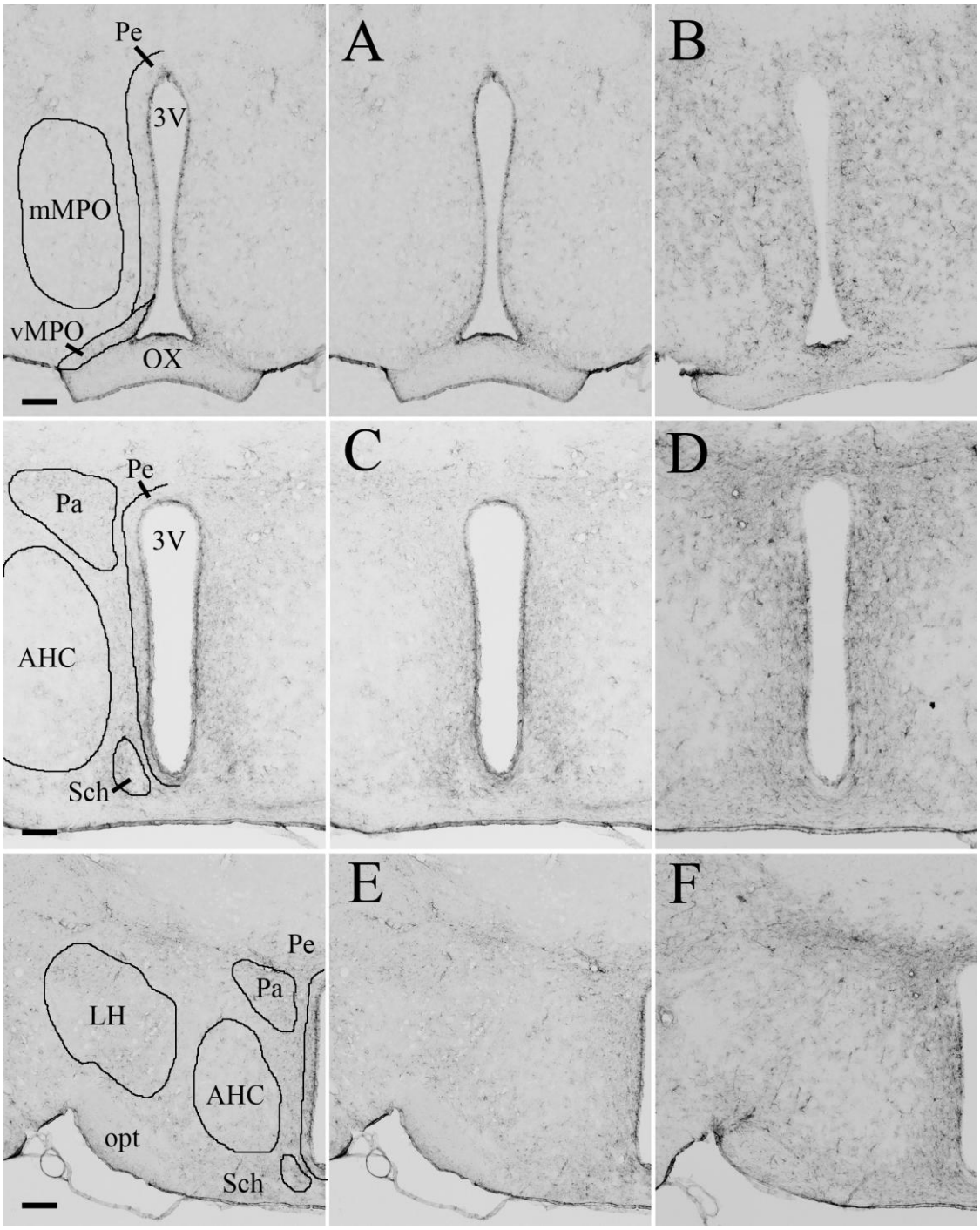
A
B
C
D
E
F
Pe
3V
mMPO
vMPO
OX
Pa
AHC
Sch
LH
opt

Figure 4-2. Regional increases in glial-fibrillary acidic protein (GFAP) immunoreactivity in the rostral hypothalamus in diet-induced obese compared with lean mice. Diet-induced obesity was associated with the most pronounced increases in GFAP immunoreactivity in the medial preoptic nucleus (A, lean; B obese), periventricular nucleus (A, C & E lean; B, D & F, obese) and paraventricular nucleus (C & E, lean; D & F, obese) compared with the anterior and lateral hypothalamic areas (C & E, lean; D & F, obese) which showed a lower relative increase. Third ventricle = 3V, Medial preoptic nucleus = MPO [medial portion = MPOm; ventromedial portion = vMPO], OX = optic chiasm, Pe = Periventricular nucleus, Pa = paraventricular nucleus, Sch = suprachiasmatic nucleus, AHC = anterior hypothalamic area central portion, LH = lateral hypothalamic area, opt = optic tract. Distance from bregma is as according to Paxinos and Franklin [131]: A & B = bregma -0.1mm; C-F = bregma -0.82. Scale bars = 100 µm.

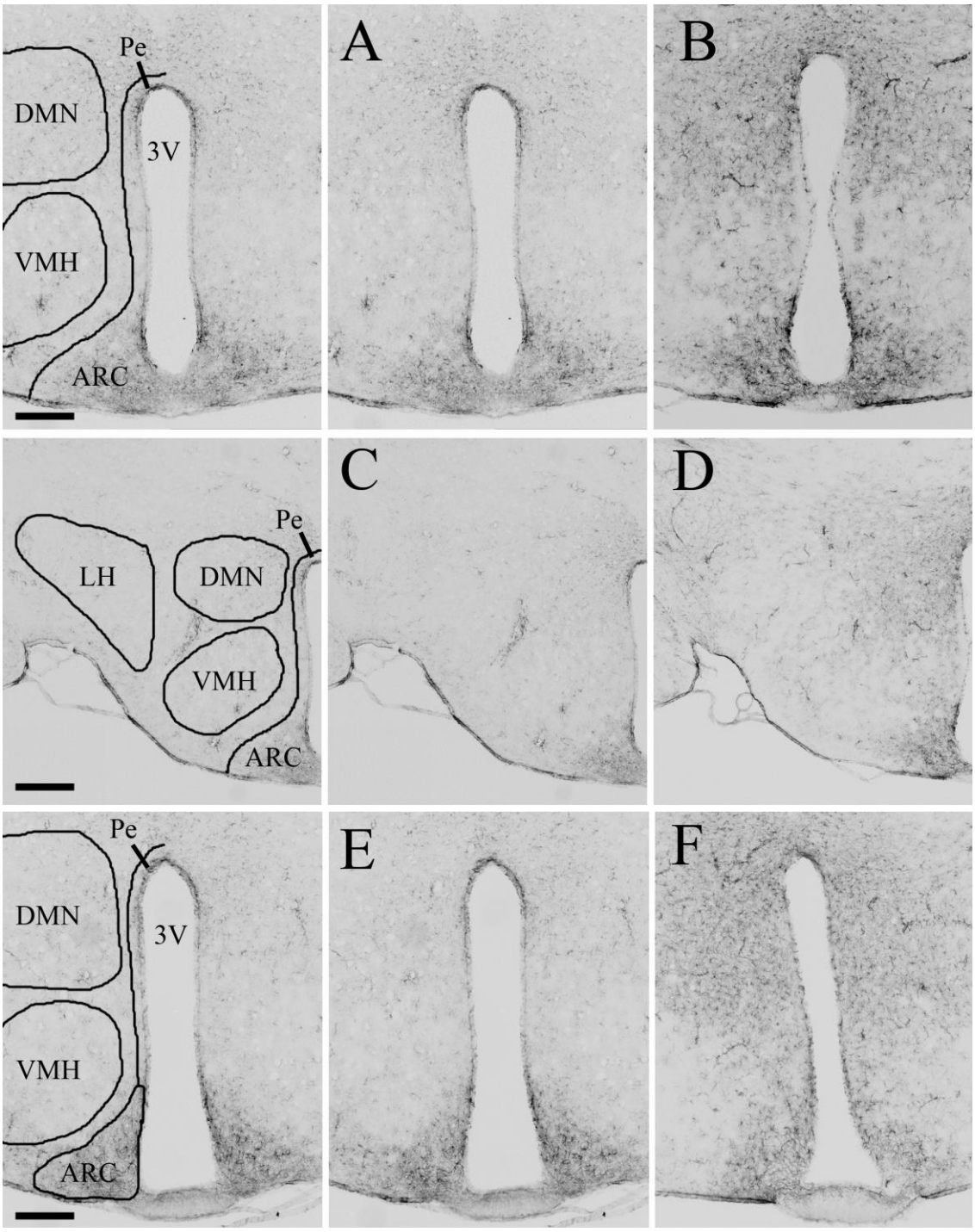
Pe
DMN
3V
VMH
ARC
A
B
LH
DMN
Pe
VMH
ARC
C
D
Pe
DMN
3V
VMH
ARC
E
F

Figure 4-3. Regional increases in glial-fibrillary acidic protein (GFAP) immunoreactivity in the medial hypothalamus in diet-induced obese compared with lean mice. Diet-induced obesity was associated with the most pronounced increases in GFAP immunoreactivity in the dorsomedial hypothalamus (A,C & E, lean; B, D & F, obese) and periventricular nucleus (A,C & E, lean; B, D & F, obese) compared with the ventromedial and lateral hypothalamic areas (A,C & E, lean; B, D & F, obese) which showed a lower relative increase. Third ventricle = 3V, ARC = arcuate nucleus, DMN = Dorsomedial hypothalamus, LH = lateral hypothalamic area, Pe = Periventricular nucleus, opt = optic tract, VMH = ventromedial hypothalamus. Distance from bregma is as according to Paxinos and Franklin [131]: A-D = bregma -1.46mm; E & F = bregma -1.94mm. Scale bars = 200 μm.

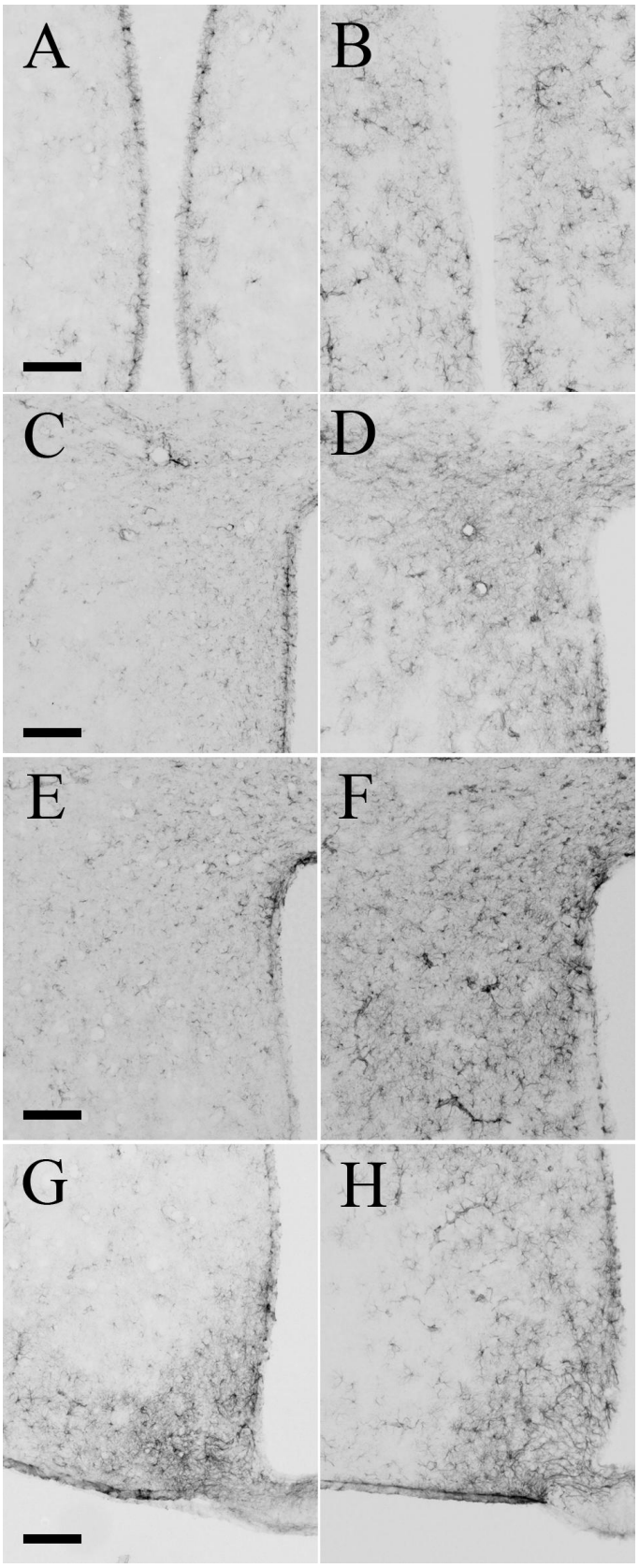
A
B
C
D
E
F
G
H

Figure 4-4. Higher-magnification images of regions with the most pronounced difference in glial-fibrillary acidic protein (GFAP) immunoreactivity between lean and diet-induced obese mice. Medial preoptic area (A, lean; B, obese); Paraventricular nucleus (C, lean; D, obese); Dorsomedial hypothalamus (E, lean; F, obese) and Arcuate nucleus (G, lean; H, obese). Distance from bregma as according to Paxinos and Franklin [131]: A & B = -0.1mm; C & D = -0.82mm; E & F = -1.46mm; G & H = -1.94. Scale bars = 100 μm.

In the ventromedial hypothalamic nucleus (VMH) was more modest (**Figure 4-3A-F**). The anterior (AH; **Figure 4-2C-F**) and lateral hypothalamic (LH; **Figure 4-2E and F, Figure 4-3C and D**) areas also showed a less pronounced difference in GFAP-immunoreactivity between the lean and DIO groups.

Distribution of GFAP-immunoreactivity in the hypothalamus of MC4R+/+ and obese MC4R-/- mice

In an independent experiment we examined GFAP-immunoreactivity in a genetic model of obesity, the MC4R-/- mouse. The MC4R-/- mice showed a significant increase in body weight (50.1 ± 1.6 g) compared to their wild-type littermates (MC4R+/+; 21.8 ± 0.5 g, $P<0.001$ by two tailed unpaired t-test). In common with the DIO animals, the MC4R-/- mice showed increased GFAP-immunoreactivity throughout the rostral-caudal extent of the hypothalamus, reflecting a similar distribution pattern characterized by high levels of GFAP-immunoreactivity in the MPO nuclei, Pa and DMN (**Table 4-4**). In contrast to the DIO study there was a more pronounced difference in GFAP-immunoreactivity in the ARC between the lean MC4R+/+ and obese MC4R-/- animals (**Figure 4-5**).

GFAP-immunoreactivity associated with microvessels

In areas of high GFAP-immunoreactivity the cell bodies of the astrocytes were swollen and their processes in close proximity, in some cases overlapping, indicative of moderate to severe astrogliosis [59]. Furthermore, GFAP-immunoreactivity was also seen forming distinct staining patterns that resembled the outline of microvessels (**Figure 4-6**). These structures were found predominantly in the obese animals with less pronounced microvascular-associated staining seen in the lean groups. In order to confirm that this distinct GFAP-immunoreactivity was in fact

Table 4-4. Relative expression of glial-fibrillary acidic protein (GFAP) immunoreactivity in obese melanocortin-4 receptor deficient mice (MC4R-/-) compared with lean wild-type (MC4R+/+) littermates.

Region	Bregma	MC4R+/+	MC4R-/-
Anteroventral periventricular nucleus (AVPe)	0.38 - 0.02	+/-	++,+/-
Anterodorsal preoptic nucleus (ADP)	0.14 - 0.02	+/-	+,+/-
Ventromedial and Medial preoptic nuclei (vMPO, MPOM & MPOL)	0.38 - -0.46	+	+,+/-
Medial preoptic area (MPA)	0.26 - -0.58	+	+,+/-
Periventricular hypothalamic nucleus (Pe)			
rostral	0.26 - -0.46	+	+
medial	-0.58 - -1.34	+, +/-	++
caudal	-1.46 - -1.94	+	+, +/-
Suprachiasmatic nucleus (Sch)	-0.22 - -0.82	++	++,+/-
Paraventricular hypothalamic nucleus (Pa)			
rostral	-0.58 - -0.82	+,+/-	+++
caudal	-0.94 - -1.22	++	++
Anterior hypothalamic area (AH)			
Anterior	-0.34 - -0.58	+	+
Central	-0.70 - -0.82	+	+
Posterior	-0.94 - -1.34	+	+, +/-
Lateroanterior hypothalamic nucleus (LA)	-0.34 - -0.70	+	+

Lateral hypothalamic area (LH)			
rostral	-0.34 - -0.94	+	+
medial	-1.06 - - 1.70	+	+
caudal	-1.82 - - 2.46	+/-	+
Arcuate hypothalamic nucleus (ARC)			
rostral	-1.22 - -1.82	++	+++, +/-
caudal	-2.06 - -2.46	+,+/-	+++
Dorsomedial hypothalamic nucleus (DMN)			
rostral	-1.34 - -1.70	+,+/-	++, +/-
caudal	-1.82 - -2.18	+,+/-	++, +/-
Posterior hypothalamic area (PH)	-1.82 - -2.46	+	+
Premammillary nucleus, ventral part (PMV)	-2.30 - -2.46	+	+,+/-
Ventromedial hypothalamic area (VMH)			
rostral	-1.06 - -1.58	+	++
caudal	-1.70 - -2.06	+	++

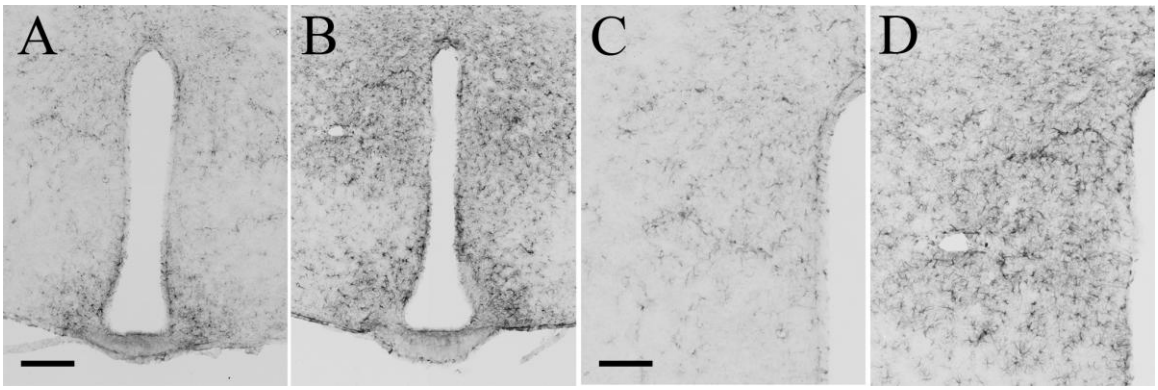

Figure 4-5. Regional increases in glial-fibrillary acidic protein (GFAP) immunoreactivity in the medial hypothalamus of melanocortin-4 receptor deficient (MC4R-/-) mice compared with wild-type (MC4R+/+) littermates. Genetic obesity caused by loss of MC4R signaling was associated with the most pronounced increases in GFAP-immunoreactivity in the dorsomedial hypothalamus (A-D) and arcuate nucleus (A&B) compared with the ventromedial and lateral hypothalamic areas, which showed a lower relative increase. MC4R+/+ = Panels A & C; MC4R-/- = panels B & D. Bregma = -1.46mm, as according to Paxinos and Franklin [131]. Panels A & B scale bar = 200 μm. Panels C & D scale bar = 50 μm.

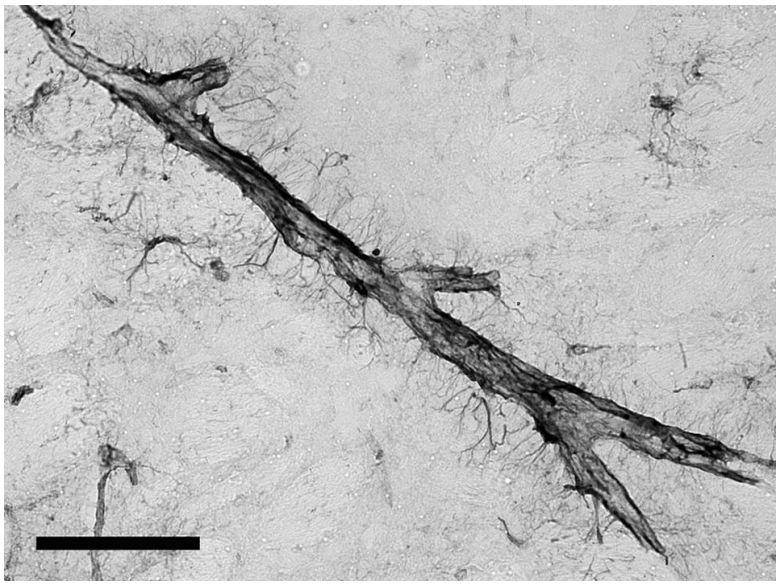

Figure 4-6. Obesity is associated with increased microvascular associated glial-fibrillary acidic protein (GFAP) immunoreactivity. A representative image taken from a diet-induced obese mouse illustrating the distinct pattern of microvascular associated GFAP staining. Scale bar = 100 µm.

associated with microvessels we repeated the DIO experiment in animals expressing green fluorescent protein (GFP) under the control of the promotor for the endothelial marker Tie2 (Tie2-GFP mice [174]).

In the DIO Tie2-GFP mice this microvascular-associated GFAP-immunoreactivity was adjacent to areas of Tie2-GFP expression confirming that the GFAP-staining was proximal to microvessels (**Figure 4-7**). In this study the immunoreactivity of the GFP antibody corresponded to the endogenous fluorescence in the Tie2-GFP transgenic mice and was used to intensify the existing signal.

Distribution of GFAP-immunoreactivity in extra-hypothalamic areas in lean compared with obese mice

The goal of this study was to characterize the distribution of GFAP-immunoreactivity in the hypothalamus of lean and obese mice. While a detailed examination of the whole brain is beyond the scope of this study we did see some differences in staining in extra-hypothalamic brain regions such as the hippocampus and thalamus, particularly the medial habenula, internal capsule and reticular thalamic nucleus (**Figure 4-8**). Areas of the forebrain more rostral to the hypothalamus or caudal areas in the midbrain, pons and medulla were not examined in this study.

Discussion

Inflammation in the hypothalamus is being increasingly recognized as a pathologic feature of obesity in animals [32, 34, 36, 41, 169] and possibly humans [34]. Reactive astrogliosis occurs in response to inflammation and injury to the CNS. While changes in GFAP-immunoreactivity have

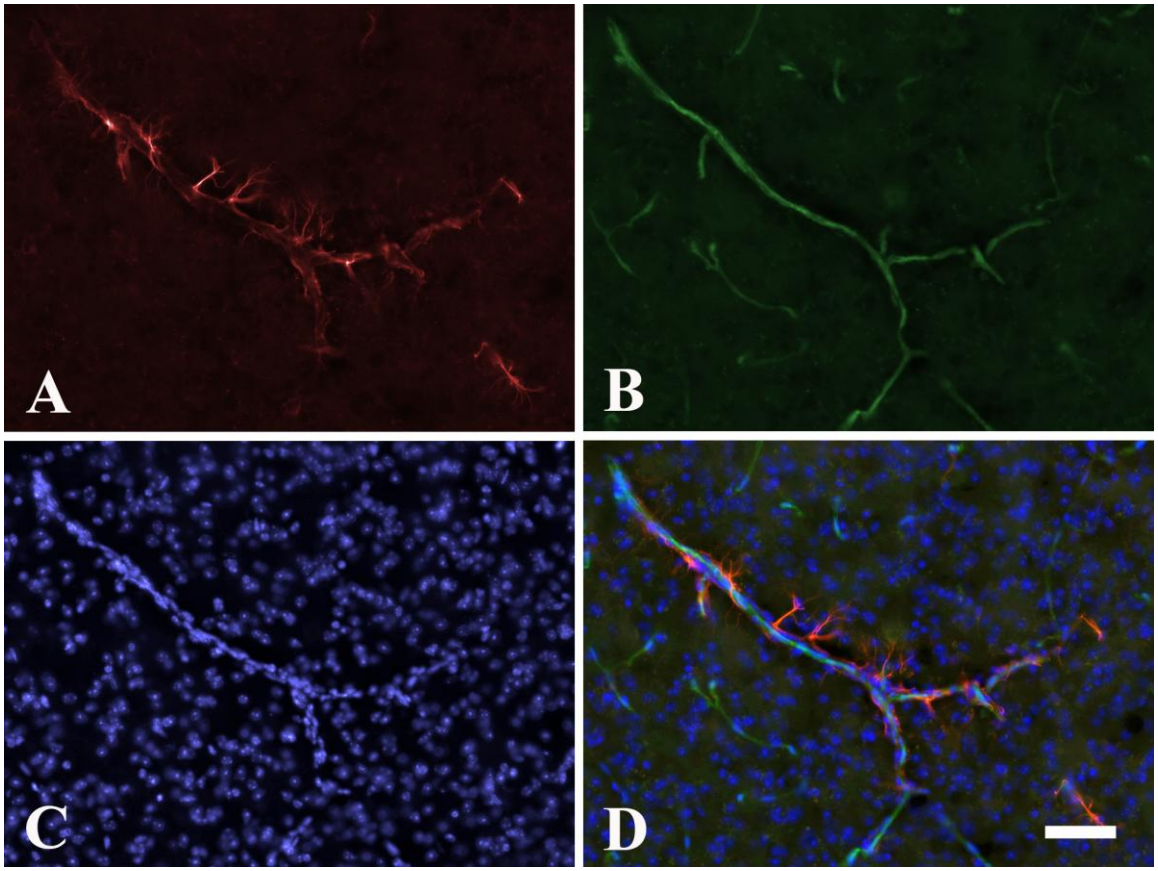

Figure 4-7. Increased glial-fibrillary acidic protein (GFAP) immunoreactivity is seen surrounding endothelial cells in diet-induced obese Tie2-GFP animals. A distinct pattern of GFAP immunoreactivity (A) is seen surrounding endothelial cells (B; Tie2-GFP expression) in diet-induced obese mice. Panel C indicates nuclei stained with DAPI. Panel D is all panels overlaid. Scale bar = 50 μm.

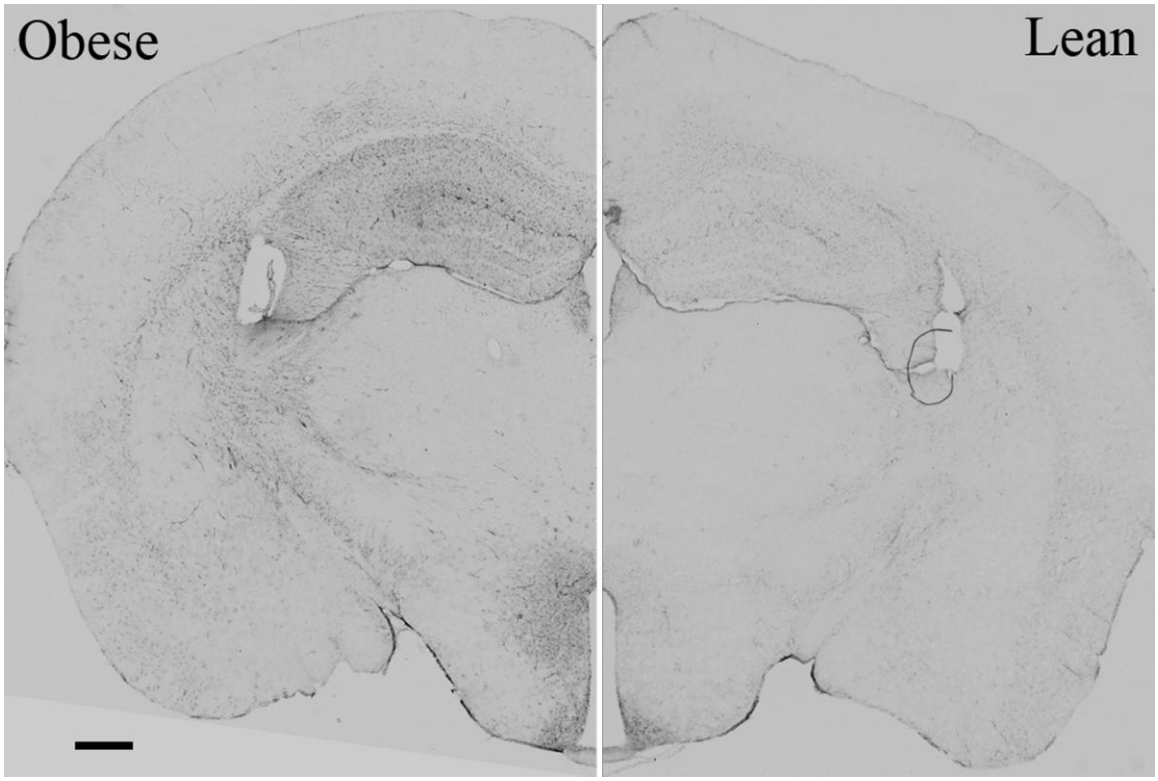

Figure 4-8. Increased expression of glial-fibrillary acidic protein (GFAP) is also seen in extra-hypothalamic regions in obese compared with lean animals. A side by side comparison of GFAP-immunoreactivity across an entire brain slice reveals an increased expression in the multiple brain regions in the diet-induced obese animals including the hippocampus, medial habenula, internal capsule and reticular thalamic nuclei. Scale bar = 500 µm.

been documented using immunohistochemistry in the ARC in response to obesity [34, 41, 169] this study is the first to examine the relative distribution of reactive astrogliosis throughout the hypothalamus. The finding that some hypothalamic nuclei, such as the MPO, Pa, and DMN show a profound up regulation in GFAP-immunoreactivity in response to obesity compared with other areas, such as the VMH, AH, and LH, which showed comparatively less astrogliosis, suggests that these nuclei have distinctly different inflammatory responses to obesity. One potential reason for this difference may be the proximity of the different nuclei to the third ventricle. In general, the hypothalamic nuclei that showed the highest increases in GFAP-immunoreactivity in this study were situated proximal to the third ventricle. The relative expression (lean vs. obese) and distribution of GFAP-immunoreactivity was very similar between the diet and genetic (MC4R-/-) obesity models suggesting that it is the obesity, not the high-fat diet *per se*, that leads to the increased GFAP-immunoreactivity.

In this study we used GFAP-immunoreactivity as a marker of astrocytes/astrogliosis. While GFAP-immunoreactivity is commonly used for this purpose we acknowledge that GFAP is not a completely comprehensive marker of astrocytes and that some astrocytes do not express GFAP [99]; however, for the purposes of this study we believe that GFAP-immunoreactivity provides an indication of the behavior of this sub-set of astrocytes in response to obesity.

In this study we utilized female mice. Glial plasticity has been shown to vary with the stage in the estrous cycle [171, 175]. The stage of the estrous cycle of the animals used in this study was not controlled; thus, may be partially responsible for the relatively higher GFAP-immunoreactivity seen in ARC of the lean female mice compared to other hypothalamic nuclei. Other studies have utilized male mice, and while they did not document nuclei outside of the ARC, they did see increases in GFAP-immunoreactivity in the ARC of high-fat fed mice in their

study [34, 169]. The goal of the present study was not to examine the sexual dimorphism in GFAP-immunoreactivity in response to obesity so only one sex was used. This study will need to be repeated in male mice in order to confirm that the same pattern of GFAP-immunoreactivity is seen in response to obesity.

Whether hypothalamic inflammation in obesity arises *de novo* or in response to the well-documented peripheral inflammation has not been completely elucidated. A recent study by Thaler and colleagues [34] performed a time-course of the development of inflammation and reactive astrogliosis in the CNS. Their study indicates that the hypothalamic inflammation in response to high-fat feeding in rats precedes the onset of white adipose tissue inflammation; however, as adipose tissue inflammation was only examined at a single time point, further investigation is needed. The distinct pattern of GFAP-immunoreactivity seen in this study associated with microvessels (**Figures 4-6 and 4-7**) suggests that the reactive astrogliosis can occur, at least in part, in response to changes at the level of the blood-brain barrier/periphery. It is likely that in chronic obesity inflammation in the brain occurs both *de novo* and in response to chronic adipose tissue derived inflammation. As our study only examined a single time point, reflecting chronic obesity, further studies are needed to characterize the development of reactive astrogliosis in the different hypothalamic nuclei over time.

The regional differences in astrogliosis in response to obesity may have important consequences for the regulation of energy homeostasis. Astrocytes are known to regulate synaptic plasticity in other neuroendocrine systems such as the reproductive axis [171, 175] and hypothalamo-neurohypophysial system [170, 172]; thus, astrogliosis seen in response to obesity may have a significant impact on modulating neuronal communication. Indeed, this has already been demonstrated for the melanocortin system of the ARC [169], which is critical for the regulation

of energy homeostasis [176]. The consequences of obesity-associated astrogliosis outside of the ARC have yet to be determined but are likely to have wide-ranging implications for the control of metabolism [177] and other neuroendocrine axes.

CHAPTER 5

Regulation of S100B in white adipose tissue by obesity in mice

Laura B. Buckman[1], Emily K. Anderson-Baucum[1, 2], Alyssa H. Hasty[1] and Kate L.J. Ellacott[1, 3]

[1]Department of Molecular Physiology & Biophysics, Vanderbilt University Medical Center, Nashville, TN 37232

[2]Present address: Department of Medicine, Indiana University School of Medicine, Indianapolis, IN 46202

[3]Corresponding author, present address: Biomedical Neuroscience Research Group, University of Exeter Medical School, Exeter, Devon, EX4 4PS, UK

The contents of this chapter have been published in Adipocyte, vol. 3, no. 3; *In press*.

Introduction

S100B is a member of S100 calcium-binding proteins, which is abundantly produced in the CNS, primarily by astrocytes and, to a lesser extent, neurons and oligodendrocytes [178]. When secreted by astrocytes at low levels, S100B acts as a neurotrophic factor by stimulating neurite outgrowth and enhancing neuronal survival. Conversely, high S100B concentrations induce a pro-inflammatory response that exerts cytotoxic effects through binding its cell surface receptor, the receptor for advanced glycation end-products (RAGE) [178]. In this regard, an increase in the levels of S100B is generally used as a marker of reactive astrogliosis, a hallmark of inflammation and injury in the brain. Thus, an increased circulating serum level of S100B is a feature not only of astrocyte dysfunction, but also of CNS disorders and pathologies.

During the last decade, S100B has been validated in clinical studies as a non-invasive peripheral biomarker of neuroinflammation and CNS injury that is readily measured in the blood and cerebrospinal fluid (CSF). Elevated levels of circulating S100B have been reported in humans affected by a wide array of neuropatholoigcal conditions including cerebral ischemia, trauma and psychiatric illness [179-182]. High levels have also been reported in obese human subjects [183], as compared to their normal-weight counterparts. The presence of elevated S100B in the serum of obese human subjects may reflect astrocyte activation; however, expression of S100B expression is also found in non-CNS tissues, such as adipose tissue and skin, where S100B levels can increase independent of CNS injury.

Recently, it has been suggested that the S100B-RAGE axis may be an important regulator of chronic low-grade adipose tissue inflammation during obesity. This is exemplified by *in vitro* studies in which adipocyte-derived S100B can act as an inflammatory cytokine via RAGE,

stimulating a pro-inflammatory, M1-polarized phenotype of macrophages in a co-culture system [184]. However, in obesity direct evidence for *in vivo* regulation of S100B in adipose tissue or the CNS is limited. The objective of this study was to test the hypothesis that increased plasma S100B contributes to obesity-associated inflammation in a diet-induced obese (DIO) mouse model. On the basis that both brain and adipose tissue may influence circulating S100B levels, we examined the expression and regulation of S100B in these tissues by obesity and determined whether these effects were reversible by weight loss.

Results

Plasma and white adipose tissue S100B levels were increased by diet-induced obesity in mice

We examined the regulation of plasma S100B protein levels and adipose tissue *s100b* gene expression in a DIO mouse model. Fifteen weeks of high-fat feeding resulted in a statistically significant increase in body weight (Lean: 30.9 ± 0.5g; DIO: 44.7 ± 0.9g; P<0.001) and adiposity (Lean: 2.2 ± 0.3g; DIO: 14.3 ± 0.7g; P<0.001) compared with lean standard chow-fed control animals. DIO animals had a statistically significant increase in plasma S100B protein levels as measured by ELISA (**Figure 5-1A;** lean: 7.2 ± 0.8 pg/ml; DIO: 19.5 ± 2.5 pg/ml; P<0.001), supporting what has previously been shown in human subjects [183]. To determine if WAT S100B expression was also regulated by obesity we measured *S100b* gene expression in whole WAT by qPCR. There was a statistically significant increase in *S100b* gene expression in WAT of DIO animals compared to lean controls (**Figure 5-1B**; P<0.05). In addition, there was a statistically significant increase in WAT gene expression of *Tnf* (**Figure 5-1C**; P<0.001), *Ccl2* (**Figure 5-1D**; P<0.001) and *Emr1* (the gene for the macrophage marker F4/80; **Figure 5-1D**; P<0.001), indicating the presence of WAT inflammation in DIO animals. WAT *Rage* gene

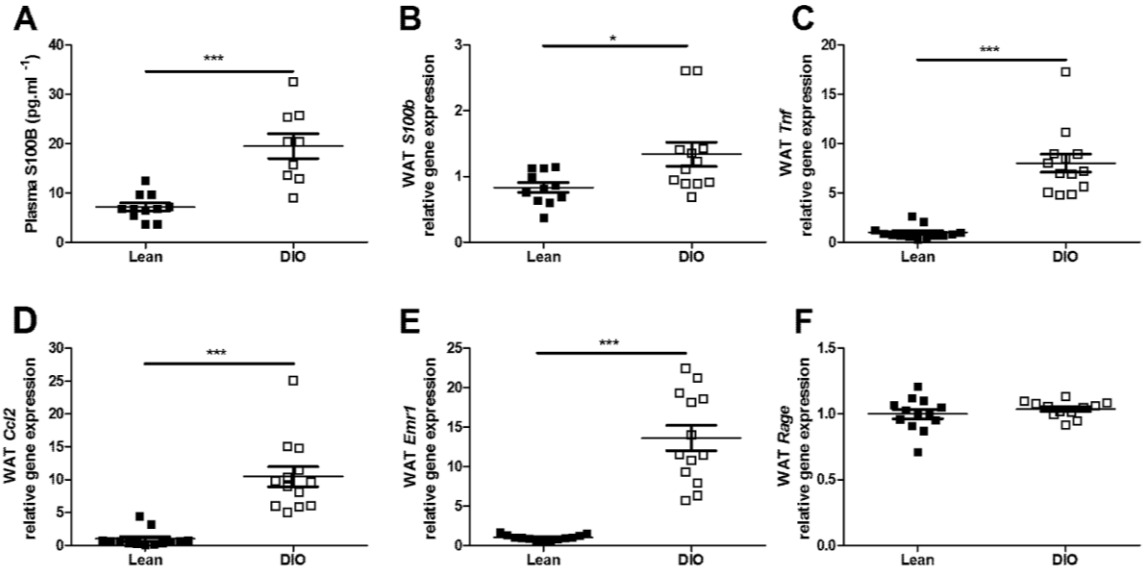

Figure 5-1. Plasma and white adipose tissue (WAT) S100B levels in diet-induced obese (DIO) mice. Plasma S100B protein (A) and WAT *s100b* gene expression (B) are increased in DIO mice compared with lean standard chow fed controls. DIO mice showed WAT inflammation as indicated by increased gene expression for *Tnf* (C), *Ccl2* (D) and *Emr1* (E). WAT gene expression for the S100B receptor, RAGE was not altered by diet-induced obesity (F). *P<0.05; ***P<0.001. N=12-13/group.

expression was not significantly different between the lean and DIO groups (**Figure 5-1E**). Together, these data indicate that, in common with markers of adipose tissue inflammation, WAT s100b gene expression was increased by diet-induced obesity.

Obesity-associated increases in plasma and white adipose tissue S100B levels were reversed by weight-loss in mice

In obese animals, adipose tissue dysfunction and WAT inflammation decrease following weight-loss [185]. To further examine the potential contribution of S100B to adipose tissue dysfunction during obesity, we determined whether the increased plasma and WAT S100B levels in DIO mice could be reversed by weight-loss. Switching DIO mice to standard chow for 5 weeks after 15 weeks of HFD (weight-loss group) resulted in weight-loss compared with the animals that remained on HFD (DIO; **Figure 5-2**); however, at euthanasia the animals in the weight-loss group were still significantly heavier than the control lean animals that were fed standard chow throughout the study (Lean: 29.9 ± 0.6g; Weight-loss: 36.3 ± 1.5g; $P<0.001$). The difference in terminal body weight between groups was due to differences in adiposity, with all three groups having statistically significant differences in body fat content (Lean: 2.5 ± 0.4g; Weight-loss: 7.6 ± 1.2g; DIO: 16.8 ± 0.5g; $P<0.001$).

In contrast, there were no significant differences in WAT gene expression of the S100B receptor *Rage* between groups (**Figure 5-3F**; $P>0.05$). These data demonstrate that, in common with markers of adipose tissue inflammation, *s100b* gene expression is reversed following weight-loss in mice.

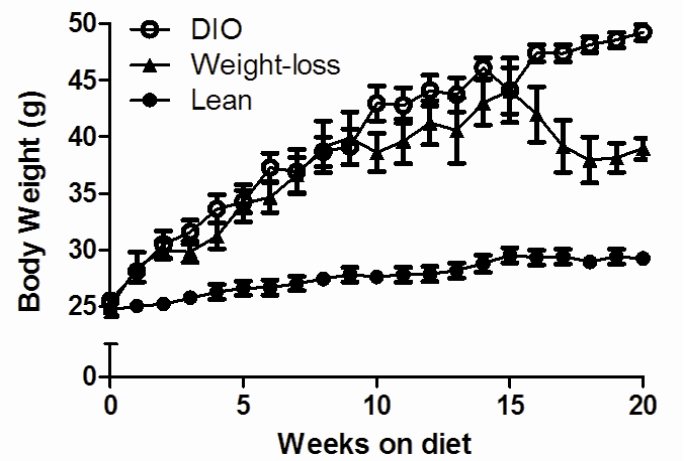

Figure 5-2. Body-weight curves of mice used for weight-loss study. Changing mice from high-fat diet back to standard chow for five weeks resulted in weight-loss (weight-loss group) compared with mice maintained on high-fat diet (DIO). Both groups remained heavier than the lean group that was maintained on standard chow throughout the study. N= 7-9/group

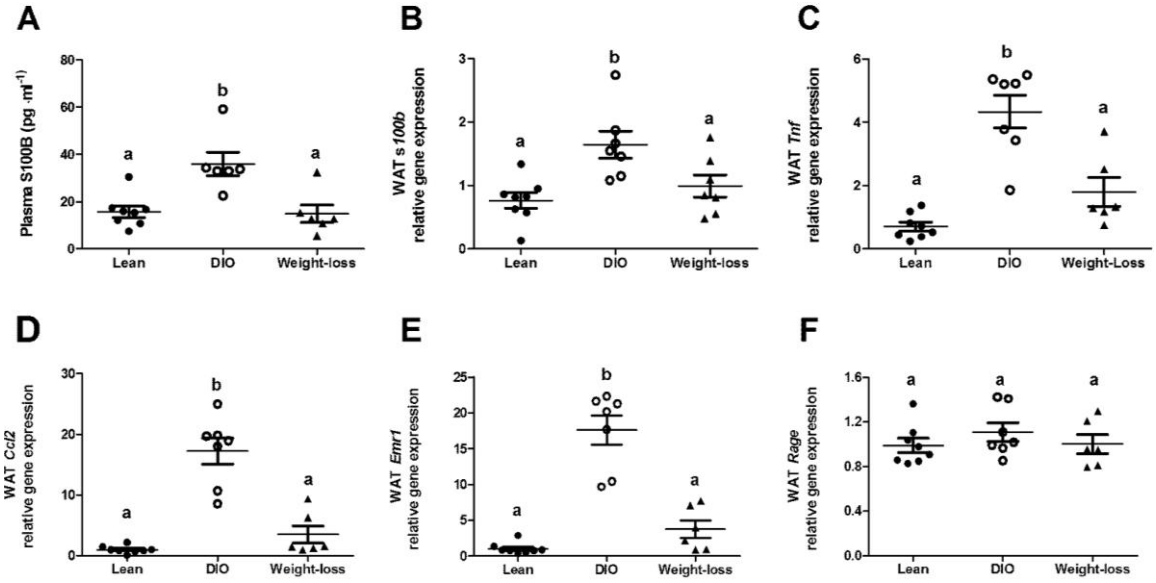

Figure 5-3. Plasma and white adipose tissue (WAT) S100B levels after weight-loss in mice. Weight-loss reversed the diet-induced obesity-associated increase in plasma S100B protein (A), WAT *s100b* gene expression (B), and markers of WAT inflammation (*Tnf* [C], *Ccl2* [D] and *Emr1* [E]). Gene expression for the S100B receptor RAGE was not significantly different between the groups (F). Data sets with different letters are significantly different from each other. N=7-9/group. DIO = diet-induced obese.

CNS levels of S100B were not altered by diet-induced obesity or following weight-loss in mice

Our previous work (**Chapter 4**) provided anatomical evidence of reactive astrogliosis in obese mice within several nuclei of the hypothalamus involved in energy homeostasis, suggesting that astrocytes contribute to metabolic inflammation in this brain region. On the basis of these findings, we examined *in vivo* regulation of S100B protein content in the DMN and MBH, in DIO compared with lean animals. These areas were selected as they had previously shown high levels of GFAP-immunoreactivity in obese animals (**Chapter 4**). Surprisingly, no significant changes in S100B levels were detected in the DIO animals as compared to the lean controls (**Figure 5-4A**; $P<0.05$). Furthermore, no significant differences in S100B levels were found in the weight-loss group as compared with the animals that remained on HFD or standard chow (**Figure 5-4B**; $P<0.05$).

S100B-immunoreactivity was detected in both adipocytes and adipose tissue macrophages

Although secretion of S100B has been shown in adipose tissue, very little is known about the cell type specification of its expression within this organ. Therefore, we performed immunohistochemistry on whole mount WAT to determine the localization of S100B within adipose tissue from lean and DIO animals. Adipocytes in DIO animals were hypertrophied (**Figure 5-5A**) compared with lean controls (**Figure 5-5F**). In agreement with our qPCR data, WAT immunohistochemistry reveled increased immunoreactivity for S100B (**Figure 5-5B**) and F4/80 (**Figure 5-5C**) in the DIO animals compared with lean controls (**Figure 5-5G and H**). Co-localization of S100B-immunoreactivity with F4/80-immunoreactivity revealed expression of S100B in adipose-tissue macrophages in lean (**Figure 5-5J**) and DIO animals (**Figure 5-5E**).

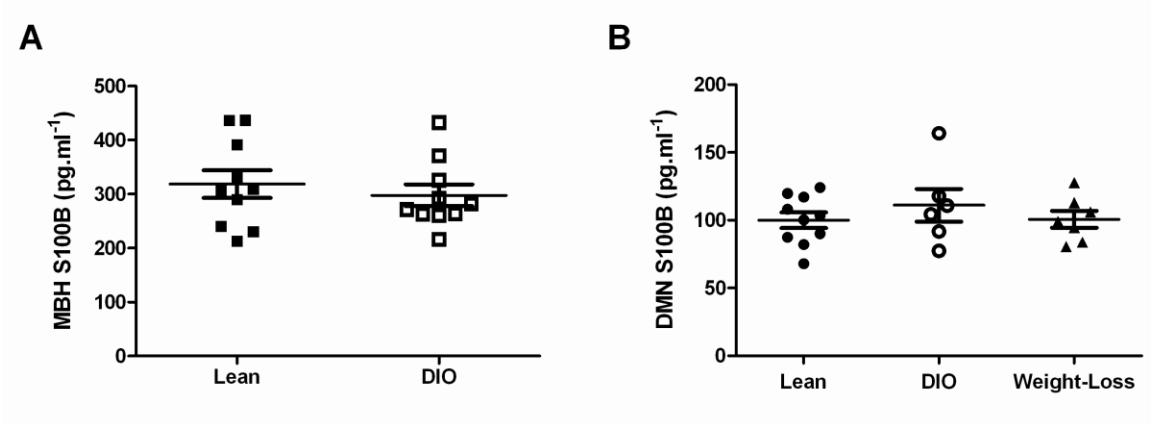

Figure 5-4. Protein levels of hypothalamic S100B in mice with diet-induced obesity and after weight loss. Brain S100B protein levels in the mediobasal hypothalamus (MBH) and dorsomedial hypothalamic nucleus (DMN) were unchanged in DIO mice relative to those in lean and weight-loss groups. N=7-9/group. DIO = diet-induced obese.

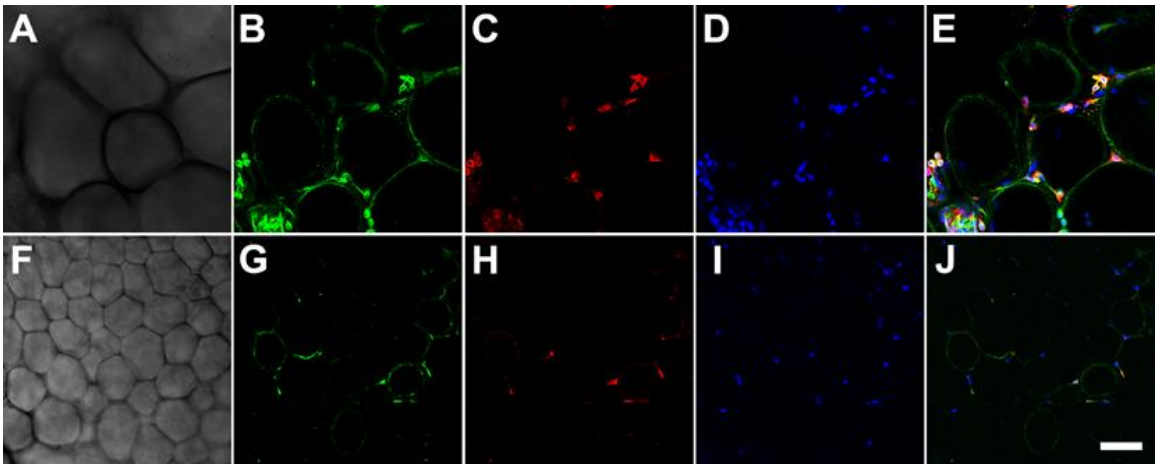

Figure 5-5. Immunohistochemistry for S100B in adipose tissue from lean and diet-induced obese mice. Differential interference contrast (DIC) microscopy revealed that diet-induced obesity was associated with adipocyte hypertrophy (A) compared with lean controls (F). Immunoreactivity for S100B (green) was seen in both adipocytes and non-adipocytes in both diet-induced obese (DIO; B) and lean control mice (G) with levels increased in the DIO animals. Increased F4/80 immunoreactivity (red) was seen in DIO (C) compared with lean control mice (H). Co-localization of S100B and F4/80-immunoreactivity (yellow/white) revealed expression of S100B in both adipocytes and F4/80-positive macrophages in both DIO (E) and lean (J) mice. DAPI (blue) was used to indicate cell nuclei. Upper panels A-E are representative images from a DIO mouse. Lower panels F-J are representative images from a lean control. Scale bar = 50µm.

S100b gene expression was increased in the adipocyte-enriched fraction of adipose tissue by obesity

WAT is a heterogeneous organ that can be separated into an adipocyte-enriched fraction and a stromal-vascular fraction (SVF), containing pre-adipocytes, endothelial and immune cells. Using a subset of the animals from the weight-loss study we quantified the relative gene expression of *s100b* and *Rage* in the adipocyte-enriched and SVFs of lean and DIO mice by qPCR. First we determined the efficiency of our cellular fractionation by examining the relative gene expression of the adipocyte marker, adiponectin (*Adipoq*), and the macrophage marker, *Emr1,* in the different fractions. *Adipoq* gene expression was high in the adipocyte-enriched fractions but barely detectable in the SVFs, independent of diet (**Figure 5-6A**; $P_{(fraction)}<0.01$, $P_{(diet)}>0.05$, $P_{(interaction)}>0.05$), indicating efficient separation of the adipocytes into the adipocyte-enriched fraction. As expected, the SVF contained higher levels of the macrophage marker *Emr1* compared with the adipocyte-enriched fractions across all groups (**Figure 5-6B**; $P_{(fraction)}<0.05$, $P_{(diet)}<0.01$, $P_{(interaction)}>0.05$); however, likely due to the presence of lipid-laden macrophages in the DIO animals [186], the efficiency of the separation was reduced and statistically significant levels of the macrophage marker *Emr1* were still detected in the adipocyte-enriched fractions from DIO animals (**Figure 5-6B**; $P<0.05$). In agreement with our immunhistochemical study, using qPCR we detected *s100b* gene expression in both the adipocyte-enriched fractions and SVFs in lean and DIO mice (**Figure 5-6C**). In response to high-fat feeding there was a statistically significant increase in *s100b* gene expression in the adipocyte-enriched fraction but not the SVF fraction (**Figure 5-6C**; $P_{(fraction)}<0.001$, $P_{(diet)}<0.05$, $P_{(interaction)}<0.01$). Gene expression of *Rage* was also detected in both adipocyte-enriched and SVF (**Figure 5-6D**; $P_{(fraction)}<0.01$, $P_{(diet)}>0.05$, $P_{(interaction)}<0.05$). Bonferroni *post-hoc* analysis revealed a statistically significant decrease in *Rage* gene expression in the SVF fraction from DIO mice (**Figure 5-6D**; $P<0.01$); however, there were

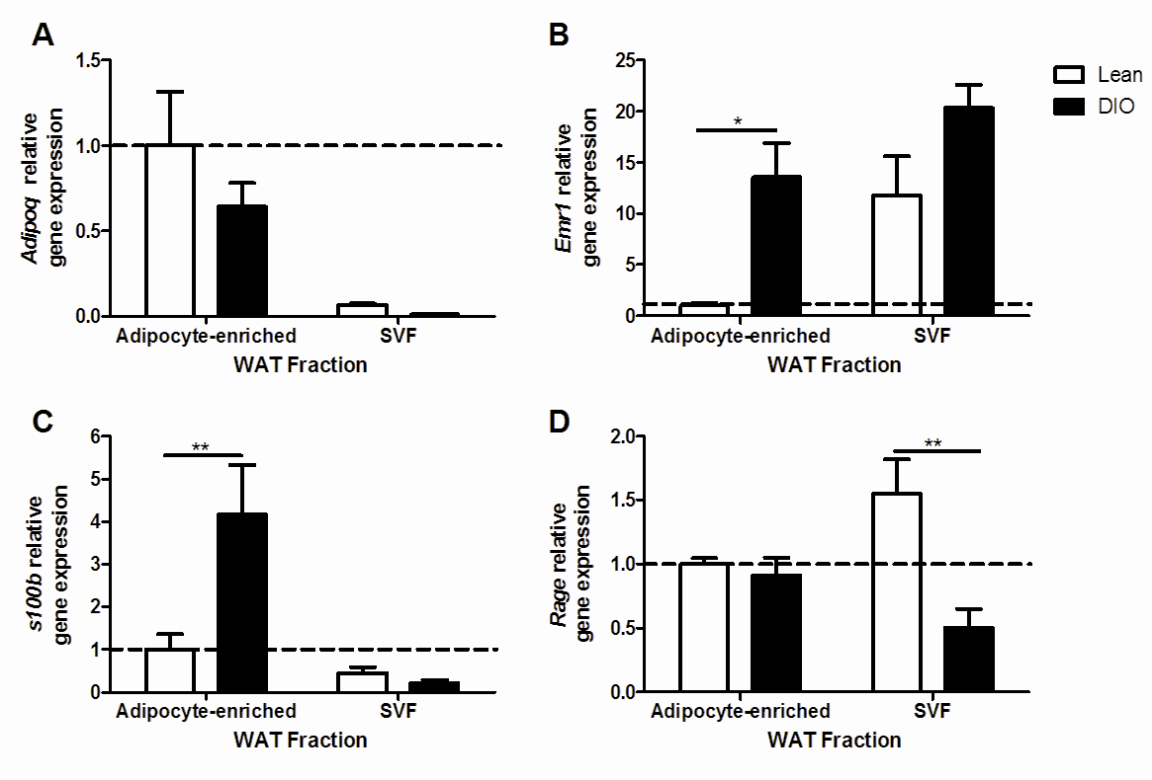

Figure 5-6. Regulation of S100B gene expression in different white adipose tissue (WAT) compartments. Fractionation of WAT into adipocyte-enriched and stromal-vascular fractions (SVF) was verified by examining gene expression for the adipocyte marker adiponectin (A) and the macrophage marker *emr1* (B). In diet-induced obese (DIO) mice, *s100b* gene expression was selectively increased in the adipocyte-enriched fraction (C) while *Rage* gene expression was selectively decreased in the SVF fraction. N=3-5/group. *P<0.05; **P<0.01.

no obesity-associated changes in *Rage* gene expression in the adipocyte-enriched fraction. These data suggest that obesity-associated changes in WAT *s100b* gene expression are due to increased expression in adipocytes and/or the lipid-laden macrophages that fractionate with the adipocytes in DIO animals.

Discussion

WAT dysfunction during obesity contributes to the development of insulin resistance and cardiovascular disease [19]. An improved understanding of factors that mediate WAT dysfunction will enable the development of novel therapeutics for these detrimental comorbidities. Here we demonstrate that plasma S100B concentration and whole WAT *s100b* gene expression are increased by obesity in mice and that these increases can be reversed by weight-loss. Further we provide evidence that obesity-associated increases in WAT S100B expression are likely specific to adipocytes and/or the lipid-laden macrophages that fractionate with the adipocytes from obese animals.

One limitation of this work stems from the WAT fraction study. Due to the presence of lipid-laden macrophages that fractionate with adipocytes in DIO animals [186] we were unable to generate an adipocyte-enriched fraction that did not contain a statistically significant increase in macrophages compared with the lean group. This means that we cannot unequivocally say that the DIO-associated increase in *s100b* gene expression in the adipocyte-enriched fraction is due to changes in adipocytes rather than the lipid-laden macrophages that fractionate with the adipocytes in the obese animals.

While the presence of S100B was first reported in adipose tissue in 1983 [187] its physiologic

function in this organ is not well characterized. In the CNS, S100B is documented to act as an inflammatory cytokine [188] via its interaction with RAGE. Due to the known proinflammatory role of S100B in the CNS it has been proposed that adipose-derived S100B may play a role in the recruitment and subsequent activation of innate immune cells in adipose tissue [189]. This hypothesis is supported by our findings that provide evidence of an increase in adipose *S100b* gene expression in WAT during obesity, which, in common with markers of adipose tissue inflammation, can be reversed following weight loss. Our findings provide an *in vivo* complement to a recent a study by Fujiya and colleagues [184] who demonstrated *in vitro* that S100B released from adipocytes acts as a proinflammatory cytokine promoting "M1" polarization of macrophages via the RAGE receptor. Interestingly, we also noted a reduction in *Rage* gene expression in the SVFs from obese animals, which may represent a compensatory mechanism to reduce inflammation in the face of increased S100B and other RAGE ligands [190] in adipose tissue during obesity. Together our data and published studies provide evidence suggesting that the activation of the S100B-RAGE axis may contribute to the chronic low-grade adipose tissue inflammation during obesity.

In addition to increased adipose tissue *s100b* gene expression we also demonstrated that obesity is associated with elevated plasma S100B in mice. This is in agreement with published data reporting a positive correlation between plasma S100B levels and BMI in humans [183, 191-193]. However, this finding has been disputed by others [194]. The source of the elevated plasma S100B during obesity remains to be determined. In addition to WAT, another potential source is the brain, as increased gene expression for *s100b* [33] and other markers of inflammation [32, 34] as well as glial cell activation [33, 34] have been reported in response to chronic diet-induced obesity in rodents. Surprisingly, changes in S100B levels were not present

within regions of the hypothalamus, including the DMN or MBH, following chronic high-fat feeding despite significant elevations of S100B in both plasma and WAT. Thus, in this study it is unlikely that the CNS contributes substantially to the high levels of circulating S100B in obesity; however, our study did not evaluate or exclude participation of other brain regions.

The elevated plasma S100B levels seen in obesity suggest the potential for endocrine activation of the S100B-RAGE axis. Inhibition of RAGE following administration of soluble RAGE or neutralizing antibodies has been shown to be protective in mouse models of atherosclerosis [195, 196] and diabetes-associated kidney disease [197] suggesting that elevated plasma S100B during obesity, whatever its source, may contribute to the well-characterized vascular inflammation and compromise associated with obesity.

In summary, our data suggests that the activation of the S100B-RAGE axis may be a previously undescribed mechanism contributing to WAT dysfunction during obesity that warrants further study. As such, the S100B-RAGE axis may be a potential therapeutic target for obesity-associated comorbidities.

CHAPTER 6

Evidence for novel functional role of astrocytes in the acute homeostatic response to high-fat diet intake in mice

Laura B. Buckman*[a], Misty M. Thompson*[a,d], Rachel N. Lippert[a], Timothy S. Blackwell[bc], Fiona E. Yull[c] and Kate L. J. Ellacott[a,e]

*Contributed equally to this work

[a] Department of Molecular Physiology and Biophysics, Vanderbilt University Medical Center, 702 Light Hall, 2213 Garland Ave, Nashville, TN 37232, USA

[b] Division of Allergy, Pulmonary and Critical Care Medicine, Department of Medicine, Vanderbilt University School of Medicine, 1161 21st Ave. South, Suite T-1217 MCN, Nashville, TN 37232, USA

[c] Department of Cancer Biology, Vanderbilt University Medical Center, 691 Preston Research Building, 2220 Pierce Ave, Nashville, TN 37232, USA

[d] Present address: Department of Neurology, University of Tennessee Health Science Center, 415 Link Building, 855 Monroe Avenue, Memphis, TN 38163, USA

[e] Corresponding author, present address: University of Exeter Medical School, Medical Research, RILD Level 3, Royal Devon & Exeter NHS Foundation Trust, Barrack Road, Exeter, Devon, EX2 5DW, UK

The contents of this chapter have been submitted for publication and are in revision.

Introduction

Obesity is a leading public health problem worldwide and is caused by a dysregulation of energy homeostasis, the balance between food intake and energy expenditure. The central nervous system (CNS) controls body weight by homeostatic regulation of energy intake and expenditure. Genetic and pharmacologic studies in rodents have identified a number of neuronal circuits critical for the regulation of energy homeostasis [198, 199]. However, to date the vast majority of research on the central regulation of energy homeostasis has focused on the contribution of neurons, with the potential contribution of non-neuronal CNS cells, including glia, only beginning to be appreciated [34, 107, 177, 200].

Studies from our laboratory and others demonstrate that in rodents high-fat feeding resulting in obesity causes CNS inflammation [32-34] and astrocyte activation, known as reactive astrogliosis [34, 41, 169, 201]. Astrocytes are the most abundant glial cell type in the CNS and are essential for regulation of the CNS microenvironment and neuronal synaptic plasticity [60]. In the arcuate nucleus of the medial basal hypothalamus (MBH) chronic obesity-associated reactive astrogliosis has been implicated in modulating synaptic organization of the melanocortin circuitry [169], thus contributing to obesity by modulating the tone of melanocortin neurons. In addition to being elevated by chronic high-fat feeding, CNS inflammation and reactive astrogliosis are also evident in the rodent hypothalamus at only 24h after the introduction of a high-fat diet [34]. During the initial 24h period after the introduction of a highly-palatable high-fat diet mice undergo a period of voracious food intake, known as hyperphagia, before homeostatic mechanisms prevail to restore energy intake to an isocaloric level. The increase in CNS inflammation and astrocyte activation during this period suggests a potential contribution of these cells in this homeostatic response; however, the physiologic significance of acute

astrocyte activation after high-fat feeding is not clear.

The objective of this study was to determine the contribution of astrocytes to the acute homeostatic response to high-fat feeding. In other CNS disorders, inflammation is both protective and detrimental depending on the context [75]. We hypothesized that high-fat diet-induced activation of inflammatory signaling pathways in astrocytes is part of a homeostatic response, which restrains food intake in response to the diet. The corollary to this hypothesis is that inhibiting inflammatory signaling in astrocytes should ameliorate this homeostatic response resulting in increased food intake during the initial acute hyperphagic response to the high-fat diet. In CNS injury the nuclear-factor kappa B (NFκB) transcription pathway in astrocytes plays a key role in the production of proinflammatory cytokines and the development of reactive astrogliosis [37, 38]. To determine the contribution of astrocytes to the acute homeostatic response to high-fat feeding we bred a mouse model with doxycycline-inducible inhibition of the NFκB transcription pathway under the control of the astrocyte specific glial-fibrillary acidic protein (GFAP) promotor. Using this model we examined how preventing astrocyte activation by inhibiting the NFκB transcription pathway specifically in astrocytes altered the acute homeostatic response to high-fat diet.

Results

Inflammation and astrocyte activation were acutely induced in the medial basal hypothalamus of wild-type mice following introduction of a high-fat diet

Initially we examined changes in markers of inflammation and astrocyte activity in the MBH at 24h after HFD was first introduced to the mice; the time point at which the peak hyperphagic response is documented. As predicted, switching wild-type mice from standard chow to highly-

palatable HFD resulted in hyperphagia; in the first 24h after introduction of the HFD the mean caloric intake of the mice increased by 75% (**Figure 6-1A**; P<0.001). This increased caloric intake was accompanied by statistically significant increases in MBH levels of the proinflammatory cytokine TNFα (**Figure 6-1B**; P<0.05) and markers of astrocyte activation, S100B (**Figure 6-1C**; P<0.01) and GFAP (**Figure 6-1D**; P<0.05). These findings support published work demonstrating acute hypothalamic inflammation and astrocyte activation in rodents after 24h of high-fat feeding [34].

Acute high-fat diet induced astrocyte activation in the medial basal hypothalamus was absent in melanocortin-4 receptor deficient mice

MC4R-deficient mice have an exaggerated hyperphagic response to high-fat feeding [202, 203]. This is caused, at least in part, by a failure to initiate appropriate homeostatic mechanisms, to compensate for the increased caloric content of the diet. We postulated that if HFD-induced astrocyte activation is part of a homeostatic response aimed at restraining food intake then astrocyte activation in response to HFD would be attenuated or absent in the MC4R-deficient mouse. MC4R-deficient mice showed a 118% increase in caloric intake 24h after introduction of the HFD (**Figure 6-2A**; P<0.001). In contrast to our earlier study in wild-type mice (**Figure 6-1**), the basal levels of S100B and GFAP were higher in the MC4R-deficient mice and the animals failed to further increase MBH S100B (**Figure 6-2B**; P>0.05) or GFAP (**Figure 6-2C**; P>0.05) levels in response to HFD. Thus, in the MC4R-deficient mouse exaggerated hyperphagia in response to introduction of a HFD was associated with the absence of HFD-induced MBH astrocyte activation.

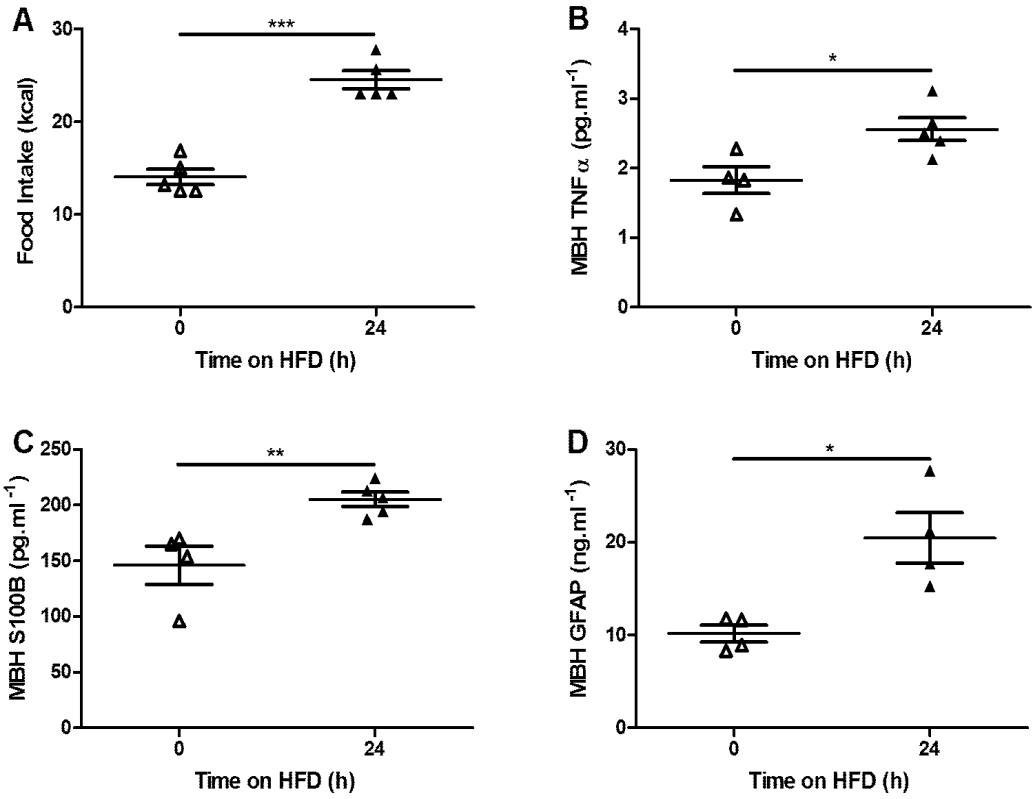

Figure 6-1. Inflammation and astrocyte activation were acutely induced in the medial basal hypothalamus of wild-type mice following introduction of a high-fat diet. 24h of high-fat feeding resulted in hyperphagia (A) accompanied by increased levels of tumor necrosis factor-α (TNFα; B), S100B (C) and glial-fibrillary acidic protein (GFAP; D) in the medial basal hypothalamus (MBH). *P<0.05, **P<0.01, ***P<0.001. n=4-5/group.

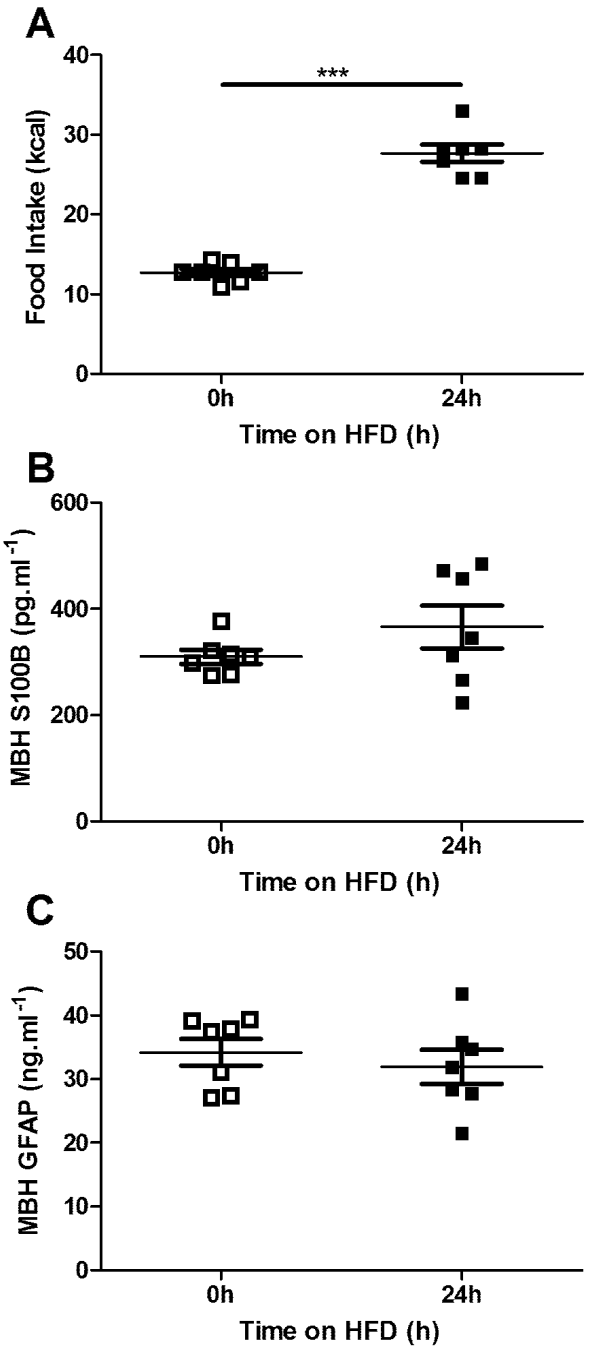

Figure 6-2. Acute high-fat diet induced astrocyte activation in the medial basal hypothalamus was absent in melanocortin-4 receptor deficient mice. In agreement with published literature [202, 203] melanocortin-4 receptor deficient mice showed exaggerated hyperphagia 24h after introduction of the high-fat diet (A). However, in the medial basal hypothalamus (MBH) there was no HFD-induced increase in the level of markers of astrocyte activation S100B (B) and glial-fibrillary acidic protein (GFAP; C). ***P<0.001, n=7/group.

Inhibition of astrocyte activation increased high-fat diet induced hyperphagia

To determine the physiologic significance of MBH astrocyte activation in response to acute high-fat feeding in mice, we blocked reactive astrogliosis using a transgenic mouse model. We bred mice with doxycycline-inducible expression of a dominant-negative form of the NFκB inhibitor IκBα under the control of the astrocyte specific GFAP promotor. We verified that transgene expression was present only in the brains in the IκB-DN^{+} animals after treatment with doxycycline using PCR (**Figure 6-3**). No expression was detected in either control IκB-DN^{-} mice or IκB-DN^{+} in the absence of doxycycline. Furthermore, the expression of the dominant-negative transgene was not detected in the liver.

We verified the successful inhibition of astrocyte activation in our transgenic mouse model by measuring levels of S100B and GFAP in the MBH. IκB-DN^{+} mice did not show the HFD-induced increase in MBH S100B (**Figure 6-4A**; P>0.05) and GFAP (**Figure 6-4B**; P>0.05) seen in control IκB-DN^{-} littermates 24h after introduction of the HFD (S100B - **Figure 6-4A**; P<0.05, GFAP - **Figure 6-4B**; P<0.01). There was a statistically significant effect of genotype on baseline S100B (**Figure 6-4A**; $P_{(genotype)}$<0.01) and GFAP (**Figure 6-4B**; $P_{(genotype)}$<0.001) expression in IκB-DN^{+} mice on standard chow, which was not unexpected since NFκB is a transcription factor that controls the expression of key glial marker genes, including GFAP [204, 205] and several members of the S100 protein family [206, 207]. However, the reduction in S100B and GFAP levels in IκB-DN^{+} animals was not associated with any overt differences in standard chow intake prior to introduction of the HFD (**Figure 6-4C**). Inhibiting the NFκB transcription pathway in astrocytes resulted in an increase in peak food intake 24h after introduction of HFD in IκB-DN^{+} animals, compared with littermate controls (IκB-DN^{-}; **Figure 6-4D**; P<0.01). The increased food intake was only seen at 24h after introduction of the HFD after which point there was no statistically

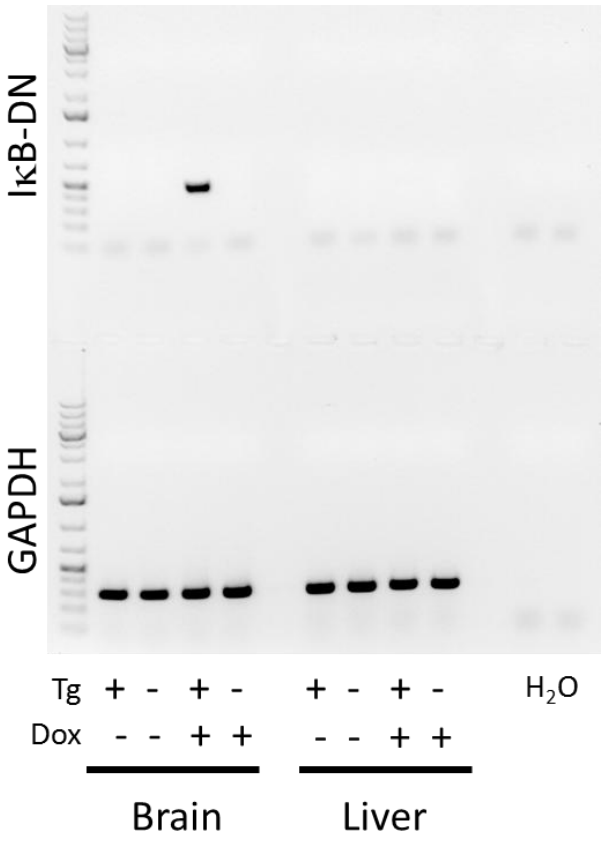

Figure 6-3. IκB-DN transgene expression was induced in the brain but not liver of IκB-DN+ mice upon exposure to doxycycline. PCR for the IκB-DN transgene was performed in cDNA made from brain or liver of IκB-DN+ and IκB-DN- mice with or without doxycycline treatment. Tg = transgene; Dox = doxycycline exposure.

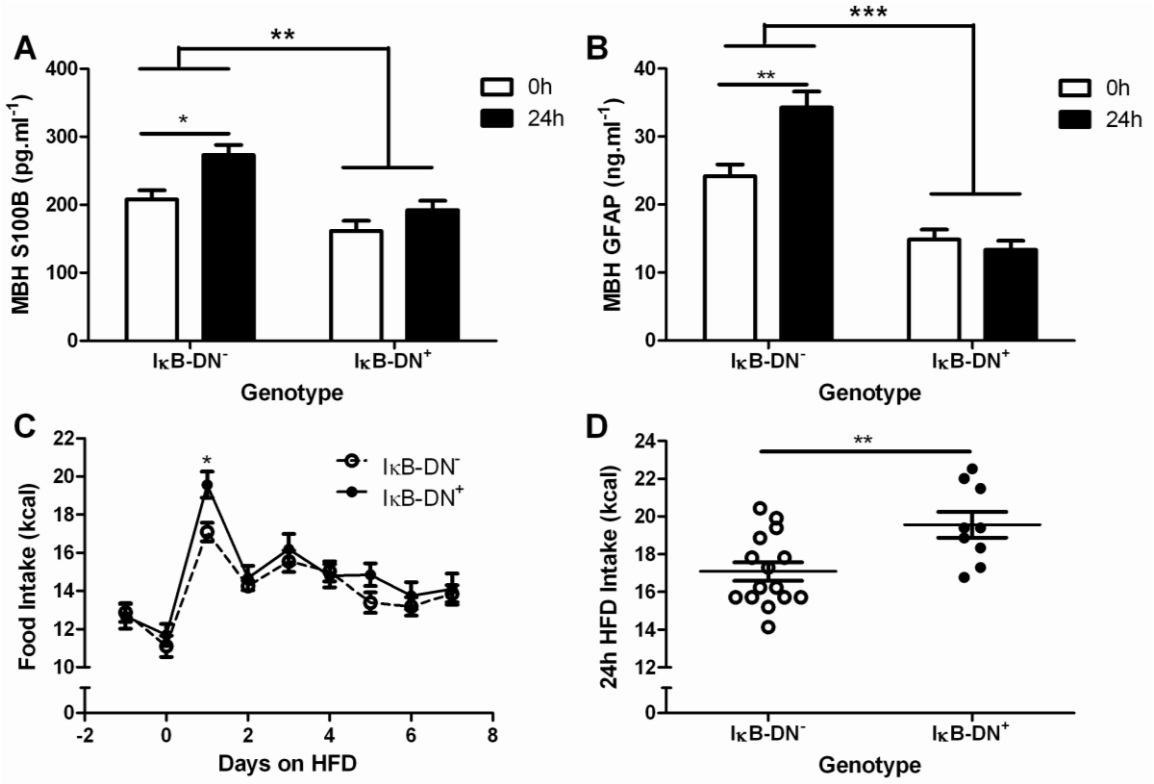

Figure 6-4. Inhibition of astrocyte activation increased high-fat diet induced hyperphagia. Inhibiting astrocyte activation by inducing expression of a dominant negative form of the inhibitor of NFκB signaling, IκBα, under the control of the glial-fibrillary acidic protein (GFAP) promotor (IκB-DN$^+$ mice) prevented the high-fat diet induced increase in markers of astrocyte activation, S100B (A) and GFAP (B) in the medial basal hypothalamus (MBH) 24h after introduction of the diet. This was associated with an increase in high-fat diet intake at 24h (C and D). *P<0.05, **P<0.01. n=3-15/group.

significant difference between the groups (**Figure 6-4C**). Together these data support our hypothesis that acute astrocyte activation 24h after introduction of a HFD is part of a homeostatic response that restrains food intake and that loss of astrocyte activation results in elevated food intake.

The IκB-DN^{+} mice and their IκB-DN^{-} littermate controls showed lower overall caloric intake on both standard chow and in response to introduction of the HFD (**Figure 6-4**), compared with the wild-type mice used to generate the data in **Figure 6-1**. To test whether this was due to doxycycline exposure we performed an acute high-fat feeding study in IκB-DN^{-} mice that were not exposed to the drug. In the absence of doxycycline the peak HFD intake of IκB-DN^{-} mice at 24h was 17.2 ± 0.6 kcal (**Figure 6-5**) compared with 17.1 ± 0.49 kcal in the IκB-DN^{-} mice exposed to doxycycline (**Figures 6-4C and D**). This suggests that the genetic background of the animals (C57BL6/J in the case of the wild-type mice used to generate the data in **Figure 6-1**, compared with F1 C57BL6/J X FVB hybrids in the case of the transgenic mice used to generate the data in **Figure 6-4**) likely contributed to the differences in caloric intake seen between the studies.

Discussion

Dysfunction in the homeostatic regulation of food intake is a key contributor to the pathogenesis of obesity. As such an improved understanding of how food intake is regulated, particularly in response to highly-palatable calorically dense foods, is necessary for the development of effective therapeutic interventions. The presence of hypothalamic inflammation and astrocyte activation acutely after initial exposure to a highly-palatable calorically dense HFD [34] suggests a potential contribution of these cells in the homeostatic response to the diet; however, the physiologic significance of acute astrocyte activation after high-fat feeding is not

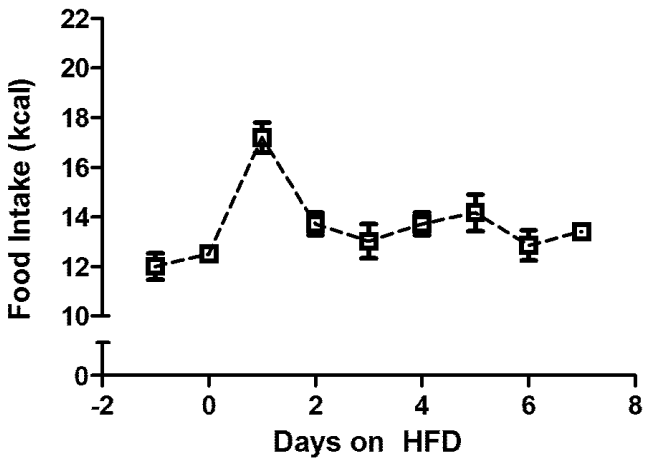

Figure 6-5. Doxycycline treatment did not influence the peak hyperphagic response to high-fat diet in IκB-DN⁻ mice. In order to control for potential effects of doxycycline on food intake we examined the response to introduction of a high-fat diet in control IκB-DN⁻ mice in the absence of doxycycline. The pattern and magnitude of food intake was similar to the IκB-DN⁻ mice treated with doxycycline (see **Figure 6-4C**).

clear. In this study we provide evidence that astrocyte activation is part of an acute homeostatic response to introduction of a HFD that restrains food intake and that the absence of HFD-induced astrocyte activation is associated with exaggerated hyperphagia. These findings are significant as they are amongst the first to provide direct experimental evidence for a role of astrocytes in the regulation of food intake.

In this study we utilized the MC4R-deficent mouse as a model of exaggerated HFD hyperphagia [202, 203]. We predicted that if our hypothesis was correct and astrocytes are part of a homeostatic response involved in restraining food intake in response to a HFD then acute astrocyte activation in response to HFD may be attenuated in this model. This was indeed the case as we found that MC4-R deficient mice failed to upregulate GFAP and S100B levels in the MBH 24h after introduction of the HFD. However, this data is complicated by the finding that, in agreement with our previously published work [201], MC4-R deficient mice had higher basal levels of hypothalamic GFAP and S100B than WT mice, indicating the presence of underlying astrogliosis. Astrogliosis in the MC4R-deficient mouse is present in the absence of high-fat feeding and is likely due to the prevailing obesity. Factors which may contribute to the development of astrogliosis in this model include obesity-associated elevations in inflammatory, metabolic and/or humoral signals arising in the periphery or directly in the CNS. It is conceivable that due to the elevated basal activation in MC4R-deficient mouse that the MBH astrocytes are already maximally activated precluding further activation in response to a HFD. It may also be argued that due to the high level of basal activity this data suggests that the exaggerated high-fat hyperphagia in the MC4R-deficient mouse is independent of astrocyte activation. However, data from our IκB-DN^{+} transgenic mouse model demonstrating that preventing HFD-induced astrocyte activation resulted in elevated HFD intake clearly supports a physiologic role for

astrocytes in the acute homeostatic response to HFD.

In this study we focused on the MBH as it is likely to be one of the principal brain regions mediating the effects seen. It has previously been shown that the MBH exhibits rapid changes in glial cell activity in response to high-fat feeding [34] and the presence of a circumventricular site, the median eminence, within this area makes it highly sensitive to changes in hormonal and nutritional inputs. Furthermore, the MBH contains critical neuronal circuitry mediating feeding behavior including the well-characterized melanocortin neurons in the arcuate nucleus. Indeed, astrogliosis associated with chronic high-fat feeding has been implicated in modulating the synaptic organization of melanocortin neurons in this brain region [169]. Like the MBH, caudal brainstem areas such as the nucleus of the solitary tract and dorsal vagal complex also mediate feeding behavior [208] and are in close proximity to another circumventricular organ, the area postrema. To date no one has reported inflammation or glial activation in the brainstem in response to high-fat feeding but the involvement of this or indeed other brain areas, such as nuclei of the mesolimbic dopamine that mediate HFD palatability and reward, cannot be excluded as the transgenic mouse model used in our study targeted all GFAP-expressing cells and not those exclusively in the MBH.

GFAP is principally expressed in the central nervous system; however, peripheral sites of expression including the liver [209], pancreas [210] and enteric nervous system [211] have been documented. While we did not detect any expression of the IκB-DN transgene in the liver in our doxycycline-treated IκB-DN^{+} animals a potential of contribution of non-CNS GFAP-positive cells in mediating the altered acute feeding response to HFD cannot be completely ruled out.

Alterations in synaptic plasticity, exemplified by rapid rewiring of melanocortin neurons in the

arcuate nucleus, have been observed acutely in response to introduction of a HFD [212]. In other neuroendocrine axes, astrocytes regulate synaptic plasticity contributing to the regulation of tone within neuronal circuits [213]. A likely mechanism by which astrocytes contribute to a reduction in acute HFD-induced food intake is via modulation of the activity of neurons that regulate food intake in the arcuate nucleus or another brain region. This neuronal modulation may occur via: 1) the action of astrocyte-derived cytokines or other biochemicals such as ketone bodies; 2) astrocyte ensheathment of neurons physically hindering synaptic connectivity; 3) astrocyte mediated alterations in neurotransmitter reuptake in the synapse; and/or 4) astrocyte induced alterations in blood-brain barrier permeability which change humoral and nutritional inputs to the CNS from the periphery. In a recent study, Le Foll and colleagues presented evidence that astrocytes in the ventral medial hypothalamus play a role in modulating food intake in response to a high-fat diet via the action of ketone bodies [107]. An important mechanistic question that remains unresolved in the field relates to what is causing the high-fat diet induced inflammation and astrocyte activation in the CNS. Candidates include saturated fatty acids [214], endoplasmic reticulum stress [36] and neuronal injury [34].

In summary, we have discovered that reactive astrogliosis is part of a previously undescribed homeostatic response to consumption of a high-fat diet that functions to acutely restrain food intake. This has implications for our understanding of the cellular mechanisms by which food intake is regulated by the CNS.

CHAPTER 7

Conclusions and Future Directions

While research on the neuronal circuitry underlying feeding behavior has been an intense focus of obesity research over the last several decades, glial cells have only recently emerged as potentially important contributing factors in the pathogenesis of the disease. In obese rodent models, markers of inflammation, including oxidative stress and pro-inflammatory cytokine signaling, have been observed in the hypothalamus, a key brain region involved in energy homeostasis [32, 34]. A primary hallmark of neuroinflammation present in obese animals, activated microglia and astrocytes, promotes immediate immune activation and mediates long-term neurotoxic effects that are associated with neuropathology. However, relatively little is known about the influence of diet or obesity on glial cell function and, more importantly, how glial cells may participate in the normal and pathological processes in the central regulation of energy balance. Thus, the overall goal of this dissertation was to advance our understanding of the neuroinflammatory changes triggered by high-fat diet and obesity, and to address the contribution of these responses to the pathogenesis of obesity. We made the following key observations that have contributed to advancing our knowledge in this area:

1. Obesity elicits increased monocyte infiltration into the CNS that correlates with adiposity and measures of adipose tissue inflammation and may contribute to the neuroinflammatory response to the disease (**Chapter 3**).
2. Astrogliosis seen in response to obesity is present throughout several nuclei of the hypothalamus involved in food intake and body weight regulation, as well as the brain capillaries, but does not affect all hypothalamic nuclei equally (**Chapter 4**).

3. Astrocytes are involved in the acute homeostatic response to high-fat diet and mediate protection against acute high-fat-diet-induced hyperphagia, demonstrating for the first time a novel role for astrocytes in the regulation of feeding behavior (**Chapter 6**).

Outstanding Questions/Future Directions

What are the acute consequences of inflammation in mice fed a HFD?

While chronic inflammation has long been viewed as contributing to pathology in obesity, our data suggests that acute inflammation may be protective by promoting a reduction in high-fat food intake. Indeed, in other disease states inflammation is an essential mechanism that protects against infectious agents and plays beneficial, reparative roles during tissue remodeling following injury. In the CNS, this process is coupled with activation of microglia and astrocytes, which is tightly regulated to prevent overactivation and related neurotoxicity. Currently, in the context of energy homeostasis, most of the available knowledge on the role of inflammation is associated with chronic neuroinflammation as a consequence of prolonged exposure to a high-fat diet. In this context, the IKKβ/NF-κB pathway plays a critical role in mediating hypothalamic inflammation and metabolic impairment in chronic diet-induced obese animals. Here, we present a new homeostatic view of obesity-induced neuroinflammation in which astrocytes participate in an acute inflammatory response to promote a return to homeostasis. Consistent with the idea that the acute-phase response represents normal, "homeostatic" activity, we found that blocking astrocyte activation, by the specific inhibition of NF-κB signaling in astroglial cells, enhanced hyperphagia induced by a highly palatable, high-fat diet.

More detailed analyses into the timing and duration of NF-κB and pro-inflammatory cytokines are crucial for determining the effect of these stimuli, which may act additively as potent

enhancers of astrocyte activation to induce transient changes in astrocyte function. Another unanswered question is whether the effects observed in our inducible mouse model are solely attributed to interference of NF-κB signaling in the mediobasal hypothalamus (MBH), since suppression was induced in astrocytes globally throughout the brains of our transgenic mice. Consequently, additional studies are needed to further substantiate that the MBH is the primary site of action for astrocytes in stimulating feeding behavior, as opposed to other brain structures involved in feeding behavior control. Understanding whether there is enhancement of astrocyte activity in other brain regions in response to acute high-fat feeding is crucial to fully elucidate the mechanisms by which acute astrocyte activation affects feeding behavior. Most likely, this homeostatic regulation results from an integration of astrocyte-regulated signals from a number of brain areas that include the brainstem and the mesolimbic dopamine pathway. To determine whether any of these effects can be attributed to the MBH vs. other brain regions, we could selectively modulate astrocytic NF-κB signaling using MBH-directed injections of a lentiviral vector expressing dominant negative IκBα driven by the expression of the astrocyte-specific GFAP promoter.

Evidence for a role of acute neuroinflammation in the homeostatic regulation of neuronal circuitry

In addition to the well-described activation of glial cells in the course of neuropathology, there is growing evidence that *astrocytes* can be directly activated by *increased* neuronal activity [215]. This phenomenon, which is termed "neurogenic neuroinflammation", occurs as a mechanism to protect against neuronal injury. For example, enhanced neuronal activity induces expression of glutamate transporters in astrocytes and thus prevented glutamate spill over to neighboring synapses [216, 217]. This protects against glutamate-induced neurotoxicity. Neurogenic

neuroinflammation can also modulate blood flow, which in turn increases substrate availability to meet the increased cellular energy demands associated with neuronal activity. Application of glutamate to astrocytes *in vitro* induces calcium waves that trigger the release of vasodilators such as ATP [215, 218]. Furthermore, results from *in vitro* studies indicate that inhibition of synaptic activity by tetrodotoxin (TTX) significantly increased TNFα production by glial cells, accompanied by an increase in the surface expression of AMPA receptors on neurons [125]. These effects contribute to synaptic scaling, a form of synaptic plasticity that controls the strength of evoked transmission between neurons. Together these data support the hypothesis that acute neuroinflammation is neuroprotective in the CNS.

What is the Significance of Neuroinflammation in the Pathophysiology of Obesity?

In the previous section, we have discussed the role of early astrocyte activation in the homeostatic regulation of food intake as a protective mechanism to maintain/restore metabolic homeostasis. However, this inflammatory process, when prolonged, can become maladaptive and lead to metabolic dysfunction and chronic disease. According to our findings in **Chapters 3 & 4**, the maladaptive reaction associated with obesity is characterized by activation of astrocytes and infiltration of peripheral immune cells into the CNS. Normal brain function is highly coupled to astrocyte activity. Below are descriptions of three potential mechanisms by which astrocytes may participate in pathological processes underlying neuronal dysfunction and thus dysregulation of energy homeostasis.

Alteration of synaptic plasticity

One potential mechanism is re-organization of the synaptic networks in the hypothalamus, a

phenomenon referred to as synaptic plasticity. Neural plasticity allows neurons to modify and form new connections in response to changes in the microenvironment or as a result of injury to the brain. Interestingly, two key hormones involved in the control of appetite and energy balance (leptin and ghrelin) have been shown to regulate synaptic plasticity by altering the number of synaptic inputs to hypothalamic neurons of the arcuate nucleus that control feeding behavior, including both POMC and NPY-expressing neurons [219, 220]. Astrocytes may be complicit in this process. This possibility is supported in particular by the fact that astrocytes surround and ensheath synapses and regulate key steps in synapse formation and maintenance through both secreted and contact-mediated mechanisms. Moreover, Horvath et al. [169] have shown that exposure to a high-fat diet results in re-wiring of synaptic inputs to melanocortin neurons possibly due to increased astrocyte ensheathment, which can physically hinder synaptic connectivity. Because of the spatial association of astrocytes with synapses, changes in astrocyte morphology are capable of affecting synapse formation and maintenance [172, 221, 222]. Our observations in **Chapter 4** suggest the hypothesis that the increased astrocyte activation associated with chronic HFD-feeding modifies the function of different hypothalamic nuclei by altering astrocyte-neuron interactions, which likely translates into long-term structural changes contributing to the pathogenesis of obesity. The next step is to determine whether suppression of astrocytic NF-κB signaling inhibits reorganization of these neuronal networks in response to high-fat diet.

Alteration of hypothalamic neurogenesis

Another possible mechanism that may induce rapid re-wiring of the hypothalamus is adult neurogenesis, a process by which neural progenitor and stem cells generate new neurons.

Evidence is accumulating that adult neurogenesis contributes to hypothalamic control of food intake, where its dysregulation contributes to and perhaps even initiates obesity. For example, it has been reported that the hypothalamus contains multipotent stem cells that can produce neuronal subtypes that are essential for energy-balance regulation, mainly neuropeptide Y (NPY) and proopiomelanocortin (POMC) hypothalamic neurons [223-226]. In line with these reports, targeted deletion studies have shown that acute ablation of agouti related protein (AGRP)–expressing neurons induces cell proliferation of newborn neurons in the arcuate nucleus, in particular neurons expressing NPY and AGRP, two potent orexigenic (appetite-stimulating) peptides [227]. Moreover, many of the newborn neurons were found to be leptin-responsive [223]. The present data also indicate that the rate of neurogenesis in the hypothalamus can be altered by changes in the physiological state such as obesity. McNay and colleagues [228] employed BrdU labeling to reveal that chronic HFD attenuates hypothalamic neurogenesis in adult mice fed a HFD for 2 months and this is attributed, at least in part, to increased apoptosis of newly divided cells and retention of older hypothalamic neurons.

Although the direct mechanism through which chronic high-fat-diet-feeding attenuates neurogenesis is unknown, there is evidence that suggests the involvement of astrocytes. Astrocytic NF-κB signaling has emerged as a particularly important mediator of hypothalamic neurogenesis. Astrocytes express numerous factors that can influence neural stem cell (NSC) proliferation and differentiation [89, 229], including inflammatory mediators such as TNFα that have been reported to inhibit neurogenesis. Our observation that HFD feeding increased astrocyte activation along with elevated hypothalamic levels of TNFα, which can be blocked by inhibition of NF-κB, raises the possibility that astrocytes may contribute to hypothalamic re-wiring through adult neurogenesis by modulating NF-κB-mediated inflammatory signaling. It is

also plausible that increased NF-κB transcriptional activity in astrocytes prevents the differentiation of cells to the neural pathway, which is supported by reports that pro-inflammatory cytokines IL-6 and TNFα induce an overall increase in glial cell differentiation with less progenitor cells showing preference for the neuronal pathway [230, 231]. Increases in astroglial differentiation may also contribute to the marked increase in astroglial cell number that we observed in HFD-induced and genetically obese mouse models described in **Chapter 4**. Hence, targeted disruption of NF-κB signaling in astrocytes should promote increased differentiation of neural stem cells into a neuronal lineage and increase survival of newly differentiated cells, thereby restoring the capacity to replace older neurons and damaged neural networks. The possibility of these two mechanisms could be tested using our mouse model with genetically induced IKKβ/NF-κB inhibition in astrocytes.

Excitotoxicity

There is also evidence implicating neurochemical processes such as excitotoxicity to the pathology of obesity. Excitotoxicity is an important contributor to neuronal death due to overstimulation with excitatory amino acids, primarily glutamate. An inflammatory stimulus in the brain triggers excessive release of glutamate from both microglia and astrocytes [232, 233]. At the same time, pathological stimuli attenuate astrocyte glutamate uptake by decreasing expression of critical glutamate transport proteins [234, 235] causing further increases in the glutamate concentration. It is therefore tempting to speculate that early activation of astrocytes alters the capacity of neurotransmitter clearance within the synapse, which may play a key role in control of the activity and excitability of neuronal circuits involved in the regulation of food intake and energy balance.

The above-described disorders have also been associated with dysfunction of microglia including excitoxicity as well as reduced neurogenesis and synaptic plasticity. Moreover, microglia express a variety of neurotransmitter receptors that are known to modulate neuronal activity, including glutamate and ATP. Microglia have also been shown to directly interact with synapses as often as every hour [236]. These data suggest that microglia may also contribute to or amplify the neuroinflammatory response to obesity thereby contributing to impaired energy metabolism. Indeed, work in our laboratory has demonstrated that astrocyte activation and peripheral immune cell infiltration are located in brain regions important in the regulation of energy homeostasis, namely the hypothalamus.

What is the Trigger of Obesity-associated Neuroinflammation?

One of the questions still under debate involves the possible mechanisms by which inflammation and gliosis in the hypothalamus are initiated and transition from a potentially protective acute response to harmful chronic effects in the context of obesity. Emerging candidates include lipids, secreted factors from adipocytes (leptin, adiponectin) and cytokines.

Lipids

One major candidate is diet, specifically diets high in saturated fats. Diets rich in saturated fatty acids have been shown to induce cognitive impairments [237]. This is in contrast to diets high in either polyunsaturated fatty acids (PUFAs) or monounsaturated fatty acids (MUFAs) [238]. Conversely, studies performed by Bruce-Keller and colleagues [239] suggest that the effects of HFD on the CNS are partially mediated by the overall percentage of total fat rather than the percentage of saturated fat intake. They demonstrated significantly higher levels of pro-

inflammatory cytokine production (TNFα, IL-6, and MCP-1) and glial cell activation in the brains of mice fed a high-fat diet composed of 60% total dietary fat (37% saturated fat) as compared to mice fed a high-fat diet consisting of 41% total dietary fat (62% saturated fat). Since both diets elicit significant obesity, these data suggest that the percentage of total fat, rather than weight gain or saturated fat content, mediates these effects. A third possibility is the breakdown of dietary fats into free fatty acids (FFAs). Two recent studies have demonstrated that high-fat feeding leads to increased fat accumulation in the hypothalamus [240, 241]. This is further supported by the finding that saturated fatty acids induce pro-inflammatory signaling in cultured astrocytes [242]. Collectively, these data indicate that dietary lipids may play an important role in hypothalamic inflammatory signaling during HFD intake.

Circulating Factors from Adipose Tissue

Induction of neuroinflammation might also be associated with changes in humoral signals, particularly adiponectin and leptin. Adiponectin is an adipokine that exerts protective effects against the development of insulin resistance, dyslipidemia and atherosclerosis [243]. It has significant anti-inflammatory properties that include suppression of adhesion molecule expression on endothelial cells, reduction of inflammatory cytokine signaling, including inhibition of IL6 and TNFα, and suppression of macrophage phagocytosis. Adiponectin has also been reported to contribute to neuroprotection [244] and has demonstrated anti-inflammatory effects in the brain mediated, in part, through inhibition of NF-κB signaling [245, 246]. Notably, there is also adiponectin receptor expression in the brainstem and mouse hypothalamus [245-247]. Therefore, it is plausible that the decrease in plasma adiponectin levels associated with obesity may at least be partially responsible for the increased TNFα production and astrocytic

NF-κB activation in the hypothalamus in response to HFD. Similarly, leptin has also been recognized as contributing to the modulation of inflammatory reactions in the CNS. However, in contrast to adiponectin, leptin levels are increased during obesity in proportion to the increase in fat mass. Leptin has been shown to activate inflammatory signaling in microglia *in vitro* [248, 249]. As such, leptin could induce inflammatory effects triggered by a HFD by modulating microglial activation, which could contribute to release of inflammatory cytokines and cause reactive astrogliosis.

Another potential trigger is adipose derived cytokines. Several mechanisms might account for this possibility. For example, cytokines can enter the CNS via specific transporters present on the endothelial cells that form the blood-brain barrier as well as through capillaries of the choroid plexus and circumventricular organs [56]. Intriguingly, our findings in **chapter 6** revealed early activation of astrocytes within the MBH, which is situated in close proximity to the median eminence (ME), a circumventricular organ that senses and integrates diverse peripheral signals to maintain energy homeostasis. Therefore, it is conceivable that a combination of peripherally derived cytokines may act on the BBB and associated cell types, including microglia, astrocytes, and perivascular cells, to induce the inflammatory effects of HFD in the MBH. An alternative hypothesis is that cytokines signal *via* Toll-like receptor 4 (TLR4) on vagal afferent fibers leading to activation of brainstem neurons that project into the hypothalamus. Indeed, consumption of a HFD increases TLR4 expression in the gut epithelium and decreases alkaline phosphatase activity, a lipopolysaccharide (LPS)-detoxifying enzyme [250]. In addition to cytokines, LPS is a potent stimulator of TLR4 signaling. These data raise the possibility that HFD-induced neuroinflammation may also be initiated by products originating from the gut (such as LPS) that activate vagal afferents.

Does Neuroinflammation Contribute to Obesity-associated Co-morbidities?

The findings of this dissertation provide valuable insights into the increased susceptibility to neurological disorders seen in obese patients. It is well known that obesity is associated with an increased incidence of neurologic disease as well as impairments to long-term memory and cognition [179, 180]. Intriguingly, our findings indicate that obese mice develop persistent neuroinflammation in several extrahypothalamic brain regions such as the hippocampus, which is a critical brain region for memory processing. Additionally, recent studies have reported decreased production of neurotrophic factors and impaired hippocampal neurogenesis in obese rodents [251, 252]. Therefore, modulation of NF-κB signaling in astrocytes might also emerge as a possible mechanism by which HFD impacts cognitive function.

Our findings also have important implications for other neuroendocrine systems involving the hypothalamus, such as the hypothalamo–pituitary–adrenal (HPA), hypothalamo– pituitary–thyroid (HPT) and hypothalamo–pituitary–gonadal (HPG) axes. For example, astrocytic and synaptic remodeling has been shown to occur in the arcuate nucleus in response to gonadal hormones involved in the control of reproduction [175]. At puberty and during the ovarian cycle, the number of synaptic contacts and coverage by glial processes changes in the hypothalamic gonadotropin releasing hormone (GnRH) neurons [175], which are essential for puberty onset, fertility and correct reproductive function [253]. This raises the possibility that HFD-induced neuroinflammatory changes in the hypothalamus might also play a role in increasing susceptibility to disorders of the HPG axis. In fact, obesity is associated with an increased risk for pregnancy complications such as pre-eclampsia, infertility in both men and women, as well as pubertal changes in obese children [254, 255]. Hence, understanding how

HFD intake leads to neuronal injury and remodeling may provide novel insights to advance the treatment of patients with various neuroendocrine disorders.

Final Summary

Overall, the studies described in this thesis have advanced our knowledge of the pathology of obesity and physiological systems responsible for control of food intake. It is clear that the timing and duration of neuroinflammation are critical factors determining outcome. Our findings of chronic immune cell recruitment and reactive astrogliosis in the CNS during obesity are particularly interesting since they parallel findings in other chronic neurodegenerative inflammatory disorders. Whether these CNS manifestations are reversible is a critical unanswered question. Ultimately, identification of therapeutic targets for the treatment of obesity and its comorbidities depends on advancing our understanding of these CNS inflammatory responses including the interplay between cell types in the CNS mediating immune activation and the studies described in this thesis have directly contributed to this goal (**Figure 7-1**).

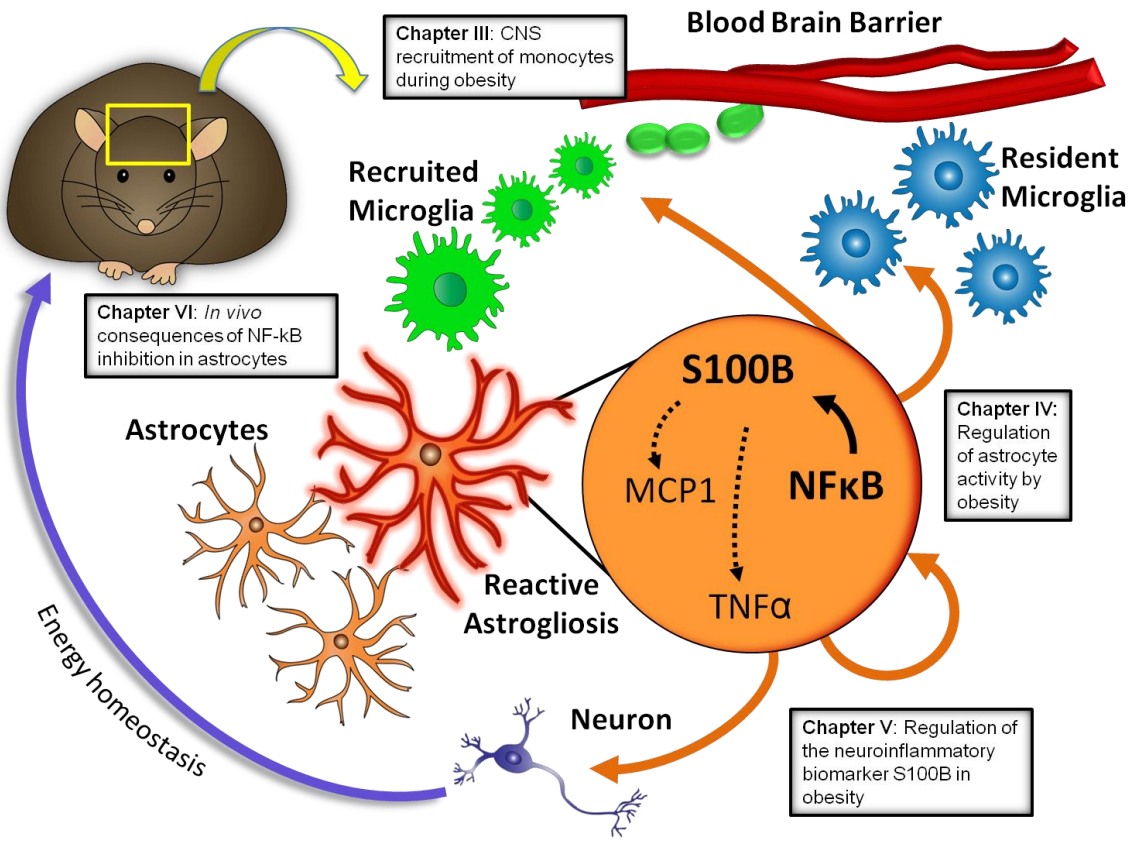

Figure 7-1. A schematic of the findings of this dissertation research. In response to chronic obesity, we found increased monocytes infiltration into the CNS, which assume a characteristic amoeboid morphology that coincides with brain inflammation. We also demonstrate that astrogliosis is induced throughout several nuclei of the hypothalamus involved in energy homeostasis. Finally, we demonstrate for the first time a novel role for astrocytes in the regulation of feeding behavior via NF-κB during acute high-fat-diet-induced hyperphagia.

REFERENCES

1. Flegal, K.M., et al., *Prevalence and trends in obesity among US adults, 1999-2008.* JAMA. **303**(3): p. 235-41.
2. Ogden, C.L., et al., *Prevalence of obesity and trends in body mass index among US children and adolescents, 1999-2010.* JAMA. **307**(5): p. 483-90.
3. Jeffrey Levi LMS, R.S.L., Albert Land, Jack Rayburn, *F as in Fat: How Obesity Threaten's America's Future*. 2012.
4. *Methods for voluntary weight loss and control. NIH Technology Assessment Conference Panel.* Ann Intern Med, 1992. **116**(11): p. 942-9.
5. Mann, T., et al., *Medicare's search for effective obesity treatments: diets are not the answer.* Am Psychol, 2007. **62**(3): p. 220-33.
6. Safer, D.J., *Diet, behavior modification, and exercise: a review of obesity treatments from a long-term perspective.* South Med J, 1991. **84**(12): p. 1470-4.
7. Elmquist, J.K., C.F. Elias, and C.B. Saper, *From lesions to leptin: hypothalamic control of food intake and body weight.* Neuron, 1999. **22**(2): p. 221-32.
8. Gao, Q. and T.L. Horvath, *Neurobiology of feeding and energy expenditure.* Annu Rev Neurosci, 2007. **30**: p. 367-98.
9. Hill, J.W., J.K. Elmquist, and C.F. Elias, *Hypothalamic pathways linking energy balance and reproduction.* Am J Physiol Endocrinol Metab, 2008. **294**(5): p. E827-32.
10. Berthoud, H.R. and C. Morrison, *The brain, appetite, and obesity.* Annu Rev Psychol, 2008. **59**: p. 55-92.
11. Cone, R.D., *Anatomy and regulation of the central melanocortin system.* Nat Neurosci, 2005. **8**(5): p. 571-8.
12. Mountjoy, K.G., et al., *Localization of the melanocortin-4 receptor (MC4-R) in neuroendocrine and autonomic control circuits in the brain.* Mol Endocrinol, 1994. **8**(10): p. 1298-308.

13. Benoit, S.C., et al., *The catabolic action of insulin in the brain is mediated by melanocortins.* J Neurosci, 2002. **22**(20): p. 9048-52.
14. Cowley, M.A., et al., *Leptin activates anorexigenic POMC neurons through a neural network in the arcuate nucleus.* Nature, 2001. **411**(6836): p. 480-4.
15. Blevins, J.E. and D.G. Baskin, *Hypothalamic-brainstem circuits controlling eating.* Forum Nutr. **63**: p. 133-40.
16. Yi, C.X. and M.H. Tschop, *Brain-gut-adipose-tissue communication pathways at a glance.* Dis Model Mech. **5**(5): p. 583-7.
17. Grill, H.J., et al., *Evidence that the caudal brainstem is a target for the inhibitory effect of leptin on food intake.* Endocrinology, 2002. **143**(1): p. 239-46.
18. Williams, D.L., J.M. Kaplan, and H.J. Grill, *The role of the dorsal vagal complex and the vagus nerve in feeding effects of melanocortin-3/4 receptor stimulation.* Endocrinology, 2000. **141**(4): p. 1332-7.
19. Hotamisligil, G.S., *Inflammation and metabolic disorders.* Nature, 2006. **444**(7121): p. 860-7.
20. Gregor, M.F. and G.S. Hotamisligil, *Inflammatory mechanisms in obesity.* Annu Rev Immunol, 2011. **29**: p. 415-45.
21. Mohamed-Ali, V., et al., *Subcutaneous adipose tissue releases interleukin-6, but not tumor necrosis factor-alpha, in vivo.* J Clin Endocrinol Metab, 1997. **82**(12): p. 4196-200.
22. Kim, F., et al., *Vascular inflammation, insulin resistance, and reduced nitric oxide production precede the onset of peripheral insulin resistance.* Arterioscler Thromb Vasc Biol, 2008. **28**(11): p. 1982-8.
23. McArdle, M.A., et al., *Mechanisms of obesity-induced inflammation and insulin resistance: insights into the emerging role of nutritional strategies.* Front Endocrinol (Lausanne). **4**: p. 52.
24. Gual, P., Y. Le Marchand-Brustel, and J.F. Tanti, *Positive and negative regulation of insulin signaling through IRS-1 phosphorylation.* Biochimie, 2005. **87**(1): p. 99-109.

25. White, M.F., *The IRS-signaling system: a network of docking proteins that mediate insulin and cytokine action.* Recent Prog Horm Res, 1998. **53**: p. 119-38.

26. Chang, L., S.H. Chiang, and A.R. Saltiel, *Insulin signaling and the regulation of glucose transport.* Mol Med, 2004. **10**(7-12): p. 65-71.

27. Vitkovic, L., et al., *Cytokine signals propagate through the brain.* Mol Psychiatry, 2000. **5**(6): p. 604-15.

28. Dantzer, R., *Cytokine, sickness behavior, and depression.* Immunol Allergy Clin North Am, 2009. **29**(2): p. 247-64.

29. Tazi, A., et al., *Interleukin-1 induces conditioned taste aversion in rats: a possible explanation for its pituitary-adrenal stimulating activity.* Brain Res, 1988. **473**(2): p. 369-71.

30. Plata-Salaman, C.R., Y. Oomura, and Y. Kai, *Tumor necrosis factor and interleukin-1 beta: suppression of food intake by direct action in the central nervous system.* Brain Res, 1988. **448**(1): p. 106-14.

31. Scarlett, J.M., et al., *Regulation of central melanocortin signaling by interleukin-1 beta.* Endocrinology, 2007. **148**(9): p. 4217-25.

32. De Souza, C.T., et al., *Consumption of a fat-rich diet activates a proinflammatory response and induces insulin resistance in the hypothalamus.* Endocrinology, 2005. **146**(10): p. 4192-9.

33. Nerurkar, P.V., et al., *Momordica charantia (bitter melon) attenuates high-fat diet-associated oxidative stress and neuroinflammation.* J Neuroinflammation, 2011. **8**: p. 64.

34. Thaler, J.P., et al., *Obesity is associated with hypothalamic injury in rodents and humans.* J Clin Invest, 2012. **122**(1): p. 153-62.

35. Zhang, X., et al., *High dietary fat induces NADPH oxidase-associated oxidative stress and inflammation in rat cerebral cortex.* Exp Neurol, 2005. **191**(2): p. 318-25.

36. Zhang, X., et al., *Hypothalamic IKKbeta/NF-kappaB and ER stress link overnutrition to energy imbalance and obesity.* Cell, 2008. **135**(1): p. 61-73.

37. Brambilla, R., et al., *Inhibition of astroglial nuclear factor kappaB reduces inflammation and improves functional recovery after spinal cord injury.* J Exp Med, 2005. **202**(1): p. 145-56.
38. Lian, H., et al., *IkappaBalpha deficiency in brain leads to elevated basal neuroinflammation and attenuated response following traumatic brain injury: implications for functional recovery.* Mol Neurodegener, 2012. **7**: p. 47.
39. Oeckinghaus, A., M.S. Hayden, and S. Ghosh, *Crosstalk in NF-kappaB signaling pathways.* Nat Immunol. **12**(8): p. 695-708.
40. Drake, C., et al., *Brain inflammation is induced by co-morbidities and risk factors for stroke.* Brain Behav Immun, 2011. **25**(6): p. 1113-22.
41. Hsuchou, H., et al., *Obesity induces functional astrocytic leptin receptors in hypothalamus.* Brain, 2009. **132**(Pt 4): p. 889-902.
42. Yi, C.X., et al., *Exercise protects against high-fat diet-induced hypothalamic inflammation.* Physiol Behav, 2012. **106**(4): p. 485-90.
43. Tracey, K.J., *Reflex control of immunity.* Nat Rev Immunol, 2009. **9**(6): p. 418-28.
44. Hickey, W.F., *Basic principles of immunological surveillance of the normal central nervous system.* Glia, 2001. **36**(2): p. 118-24.
45. Medawar, P.B., *Immunity to homologous grafted skin; the fate of skin homografts transplanted to the brain, to subcutaneous tissue, and to the anterior chamber of the eye.* Br J Exp Pathol, 1948. **29**(1): p. 58-69.
46. Abbott, N.J., L. Ronnback, and E. Hansson, *Astrocyte-endothelial interactions at the blood-brain barrier.* Nat Rev Neurosci, 2006. **7**(1): p. 41-53.
47. Carson, M.J., et al., *CNS immune privilege: hiding in plain sight.* Immunol Rev, 2006. **213**: p. 48-65.
48. Ransohoff, R.M. and B. Engelhardt, *The anatomical and cellular basis of immune surveillance in the central nervous system.* Nat Rev Immunol. **12**(9): p. 623-35.
49. Engblom, D., et al., *Prostaglandins as inflammatory messengers across the blood-brain barrier.* J Mol Med (Berl), 2002. **80**(1): p. 5-15.

50. Engelhardt, B. and R.M. Ransohoff, *The ins and outs of T-lymphocyte trafficking to the CNS: anatomical sites and molecular mechanisms.* Trends Immunol, 2005. **26**(9): p. 485-95.

51. Tracey, K.J., *The inflammatory reflex.* Nature, 2002. **420**(6917): p. 853-9.

52. Lampa, J., et al., *Peripheral inflammatory disease associated with centrally activated IL-1 system in humans and mice.* Proc Natl Acad Sci U S A. **109**(31): p. 12728-33.

53. Quan, N., S.K. Sundar, and J.M. Weiss, *Induction of interleukin-1 in various brain regions after peripheral and central injections of lipopolysaccharide.* J Neuroimmunol, 1994. **49**(1-2): p. 125-34.

54. van Dam, A.M., et al., *Appearance of interleukin-1 in macrophages and in ramified microglia in the brain of endotoxin-treated rats: a pathway for the induction of non-specific symptoms of sickness?* Brain Res, 1992. **588**(2): p. 291-6.

55. Tian, L., et al., *Neuroimmune crosstalk in the central nervous system and its significance for neurological diseases.* J Neuroinflammation. **9**: p. 155.

56. Dantzer, R., et al., *From inflammation to sickness and depression: when the immune system subjugates the brain.* Nat Rev Neurosci, 2008. **9**(1): p. 46-56.

57. Eskandari, F., J.I. Webster, and E.M. Sternberg, *Neural immune pathways and their connection to inflammatory diseases.* Arthritis Res Ther, 2003. **5**(6): p. 251-65.

58. Frank-Cannon, T.C., et al., *Does neuroinflammation fan the flame in neurodegenerative diseases?* Mol Neurodegener, 2009. **4**: p. 47.

59. Sofroniew, M.V., *Molecular dissection of reactive astrogliosis and glial scar formation.* Trends Neurosci, 2009. **32**(12): p. 638-47.

60. Sofroniew, M.V. and H.V. Vinters, *Astrocytes: biology and pathology.* Acta Neuropathol, 2010. **119**(1): p. 7-35.

61. Popovich, P.G. and E.E. Longbrake, *Can the immune system be harnessed to repair the CNS?* Nat Rev Neurosci, 2008. **9**(6): p. 481-93.

62. Lawson, L.J., et al., *Heterogeneity in the distribution and morphology of microglia in the normal adult mouse brain.* Neuroscience, 1990. **39**(1): p. 151-70.

63. Ginhoux, F., et al., *Fate mapping analysis reveals that adult microglia derive from primitive macrophages.* Science, 2010. **330**(6005): p. 841-5.

64. Ginhoux, F., et al., *Origin and differentiation of microglia.* Front Cell Neurosci. **7**: p. 45.

65. Gordon, S. and P.R. Taylor, *Monocyte and macrophage heterogeneity.* Nat Rev Immunol, 2005. **5**(12): p. 953-64.

66. Ransohoff, R.M. and V.H. Perry, *Microglial physiology: unique stimuli, specialized responses.* Annu Rev Immunol, 2009. **27**: p. 119-45.

67. Lawson, L.J., V.H. Perry, and S. Gordon, *Turnover of resident microglia in the normal adult mouse brain.* Neuroscience, 1992. **48**(2): p. 405-15.

68. Stence, N., M. Waite, and M.E. Dailey, *Dynamics of microglial activation: a confocal time-lapse analysis in hippocampal slices.* Glia, 2001. **33**(3): p. 256-66.

69. Davalos, D., et al., *ATP mediates rapid microglial response to local brain injury in vivo.* Nat Neurosci, 2005. **8**(6): p. 752-8.

70. Nimmerjahn, A., F. Kirchhoff, and F. Helmchen, *Resting microglial cells are highly dynamic surveillants of brain parenchyma in vivo.* Science, 2005. **308**(5726): p. 1314-8.

71. Hanisch, U.K. and H. Kettenmann, *Microglia: active sensor and versatile effector cells in the normal and pathologic brain.* Nat Neurosci, 2007. **10**(11): p. 1387-94.

72. Guillemin, G.J. and B.J. Brew, *Microglia, macrophages, perivascular macrophages, and pericytes: a review of function and identification.* J Leukoc Biol, 2004. **75**(3): p. 388-97.

73. Saijo, K., et al., *A Nurr1/CoREST pathway in microglia and astrocytes protects dopaminergic neurons from inflammation-induced death.* Cell, 2009. **137**(1): p. 47-59.

74. Dominguez, E., et al., *SOCS3-mediated blockade of JAK/STAT3 signaling pathway reveals its major contribution to spinal cord neuroinflammation and mechanical allodynia after peripheral nerve injury.* J Neurosci. **30**(16): p. 5754-66.

75. Czeh, M., P. Gressens, and A.M. Kaindl, *The yin and yang of microglia.* Dev Neurosci, 2011. **33**(3-4): p. 199-209.

76. Cardona, A.E., et al., *Control of microglial neurotoxicity by the fractalkine receptor.* Nat Neurosci, 2006. **9**(7): p. 917-24.

77. Hoek, R.M., et al., *Down-regulation of the macrophage lineage through interaction with OX2 (CD200).* Science, 2000. **290**(5497): p. 1768-71.

78. Cherry, J.D., J.A. Olschowka, and M.K. O'Banion, *Neuroinflammation and M2 microglia: the good, the bad, and the inflamed.* J Neuroinflammation. **11**(1): p. 98.

79. Luo, X.G. and S.D. Chen, *The changing phenotype of microglia from homeostasis to disease.* Transl Neurodegener. **1**(1): p. 9.

80. Olah, M., et al., *Microglia phenotype diversity.* CNS Neurol Disord Drug Targets. **10**(1): p. 108-18.

81. Boche, D., V.H. Perry, and J.A. Nicoll, *Review: activation patterns of microglia and their identification in the human brain.* Neuropathol Appl Neurobiol. **39**(1): p. 3-18.

82. Perez-de Puig, I., et al., *IL-10 deficiency exacerbates the brain inflammatory response to permanent ischemia without preventing resolution of the lesion.* J Cereb Blood Flow Metab. **33**(12): p. 1955-66.

83. Xiong, X., et al., *Increased brain injury and worsened neurological outcome in interleukin-4 knockout mice after transient focal cerebral ischemia.* Stroke. **42**(7): p. 2026-32.

84. Bao, F., et al., *Increased oxidative activity in human blood neutrophils and monocytes after spinal cord injury.* Exp Neurol, 2009. **215**(2): p. 308-16.

85. Kigerl, K.A., et al., *Identification of two distinct macrophage subsets with divergent effects causing either neurotoxicity or regeneration in the injured mouse spinal cord.* J Neurosci, 2009. **29**(43): p. 13435-44.

86. Nayak, D., et al., *In vivo dynamics of innate immune sentinels in the CNS.* Intravital. **1**(2): p. 95-106.

87. Perry, V.H., *A revised view of the central nervous system microenvironment and major histocompatibility complex class II antigen presentation.* J Neuroimmunol, 1998. **90**(2): p. 113-21.

88. Kettenmann, H. and A. Verkhratsky, *Neuroglia: the 150 years after.* Trends Neurosci, 2008. **31**(12): p. 653-9.

89. Song, H., C.F. Stevens, and F.H. Gage, *Astroglia induce neurogenesis from adult neural stem cells.* Nature, 2002. **417**(6884): p. 39-44.

90. Miller, R.H. and M.C. Raff, *Fibrous and protoplasmic astrocytes are biochemically and developmentally distinct.* J Neurosci, 1984. **4**(2): p. 585-92.

91. Hewett, J.A., *Determinants of regional and local diversity within the astroglial lineage of the normal central nervous system.* J Neurochem, 2009. **110**(6): p. 1717-36.

92. Charles, A.C., et al., *Intercellular signaling in glial cells: calcium waves and oscillations in response to mechanical stimulation and glutamate.* Neuron, 1991. **6**(6): p. 983-92.

93. Nedergaard, M., B. Ransom, and S.A. Goldman, *New roles for astrocytes: redefining the functional architecture of the brain.* Trends Neurosci, 2003. **26**(10): p. 523-30.

94. Batter, D.K., et al., *Heterogeneity in gap junction expression in astrocytes cultured from different brain regions.* Glia, 1992. **6**(3): p. 213-21.

95. Venance, L., et al., *Gap junctional communication and pharmacological heterogeneity in astrocytes cultured from the rat striatum.* J Physiol, 1998. **510 (Pt 2)**: p. 429-40.

96. Eng, L.F., R.S. Ghirnikar, and Y.L. Lee, *Glial fibrillary acidic protein: GFAP-thirty-one years (1969-2000).* Neurochem Res, 2000. **25**(9-10): p. 1439-51.

97. Eng, L.F., et al., *An acidic protein isolated from fibrous astrocytes.* Brain Res, 1971. **28**(2): p. 351-4.

98. Goncalves, C.A., M.C. Leite, and P. Nardin, *Biological and methodological features of the measurement of S100B, a putative marker of brain injury.* Clin Biochem, 2008. **41**(10-11): p. 755-63.

99. Cahoy, J.D., et al., *A transcriptome database for astrocytes, neurons, and oligodendrocytes: a new resource for understanding brain development and function.* J Neurosci, 2008. **28**(1): p. 264-78.

100. Oberheim, N.A., et al., *Astrocytic complexity distinguishes the human brain.* Trends Neurosci, 2006. **29**(10): p. 547-53.

101. Araque, A., G. Carmignoto, and P.G. Haydon, *Dynamic signaling between astrocytes and neurons.* Annu Rev Physiol, 2001. **63**: p. 795-813.

102. Simard, M. and M. Nedergaard, *The neurobiology of glia in the context of water and ion homeostasis.* Neuroscience, 2004. **129**(4): p. 877-96.

103. Iadecola, C. and M. Nedergaard, *Glial regulation of the cerebral microvasculature.* Nat Neurosci, 2007. **10**(11): p. 1369-76.

104. Tsacopoulos, M. and P.J. Magistretti, *Metabolic coupling between glia and neurons.* J Neurosci, 1996. **16**(3): p. 877-85.

105. Wender, R., et al., *Astrocytic glycogen influences axon function and survival during glucose deprivation in central white matter.* J Neurosci, 2000. **20**(18): p. 6804-10.

106. Guzman, M. and C. Blazquez, *Ketone body synthesis in the brain: possible neuroprotective effects.* Prostaglandins Leukot Essent Fatty Acids, 2004. **70**(3): p. 287-92.

107. Le Foll, C., et al., *Regulation of Hypothalamic Neuronal Sensing and Food Intake By Ketone Bodies and Fatty Acids.* Diabetes, 2013.

108. Boyles, J.K., et al., *Apolipoprotein E associated with astrocytic glia of the central nervous system and with nonmyelinating glia of the peripheral nervous system.* J Clin Invest, 1985. **76**(4): p. 1501-13.

109. Poirier, J., et al., *Cholesterol synthesis and lipoprotein reuptake during synaptic remodelling in hippocampus in adult rats.* Neuroscience, 1993. **55**(1): p. 81-90.

110. Suzuki, A., et al., *Astrocyte-neuron lactate transport is required for long-term memory formation.* Cell. **144**(5): p. 810-23.

111. Pekny, M. and M. Nilsson, *Astrocyte activation and reactive gliosis.* Glia, 2005. **50**(4): p. 427-34.

112. Soos, J.M., et al., *Differential expression of B7 co-stimulatory molecules by astrocytes correlates with T cell activation and cytokine production.* Int Immunol, 1999. **11**(7): p. 1169-79.

113. Austin, P.J. and G. Moalem-Taylor, *The neuro-immune balance in neuropathic pain: involvement of inflammatory immune cells, immune-like glial cells and cytokines.* J Neuroimmunol. **229**(1-2): p. 26-50.

114. Lepore, A.C., et al., *Reduction in expression of the astrocyte glutamate transporter, GLT1, worsens functional and histological outcomes following traumatic spinal cord injury.* Glia. **59**(12): p. 1996-2005.

115. Myer, D.J., et al., *Essential protective roles of reactive astrocytes in traumatic brain injury.* Brain, 2006. **129**(Pt 10): p. 2761-72.

116. Sheridan, G.K. and K.J. Murphy, *Neuron-glia crosstalk in health and disease: fractalkine and CX3CR1 take centre stage.* Open Biol, 2013. **3**(12): p. 130181.

117. Harrison, J.K., et al., *Role for neuronally derived fractalkine in mediating interactions between neurons and CX3CR1-expressing microglia.* Proc Natl Acad Sci U S A, 1998. **95**(18): p. 10896-901.

118. Chapman, G.A., et al., *Fractalkine cleavage from neuronal membranes represents an acute event in the inflammatory response to excitotoxic brain damage.* J Neurosci, 2000. **20**(15): p. RC87.

119. Zhan, Y., et al., *Deficient neuron-microglia signaling results in impaired functional brain connectivity and social behavior.* Nat Neurosci, 2014. **17**(3): p. 400-6.

120. Suzumura, A., et al., *Transforming growth factor-beta suppresses activation and proliferation of microglia in vitro.* J Immunol, 1993. **151**(4): p. 2150-8.

121. Sawada, M., et al., *Interleukin-10 inhibits both production of cytokines and expression of cytokine receptors in microglia.* J Neurochem, 1999. **72**(4): p. 1466-71.

122. Heyen, J.R., et al., *Interleukin (IL)-10 inhibits IL-6 production in microglia by preventing activation of NF-kappaB.* Brain Res Mol Brain Res, 2000. **77**(1): p. 138-47.

123. Szelenyi, J., *Cytokines and the central nervous system.* Brain Res Bull, 2001. **54**(4): p. 329-38.

124. Santello, M., P. Bezzi, and A. Volterra, *TNFalpha controls glutamatergic gliotransmission in the hippocampal dentate gyrus.* Neuron, 2011. **69**(5): p. 988-1001.

125. Stellwagen, D. and R.C. Malenka, *Synaptic scaling mediated by glial TNF-alpha.* Nature, 2006. **440**(7087): p. 1054-9.

126. Perea, G., M. Navarrete, and A. Araque, *Tripartite synapses: astrocytes process and control synaptic information.* Trends Neurosci, 2009. **32**(8): p. 421-31.

127. Beattie, E.C., et al., *Control of synaptic strength by glial TNFalpha.* Science, 2002. **295**(5563): p. 2282-5.

128. Pascual, O., et al., *Microglia activation triggers astrocyte-mediated modulation of excitatory neurotransmission.* Proc Natl Acad Sci U S A, 2012. **109**(4): p. E197-205.

129. Min, K.J., et al., *Astrocytes induce hemeoxygenase-1 expression in microglia: a feasible mechanism for preventing excessive brain inflammation.* J Neurosci, 2006. **26**(6): p. 1880-7.

130. Huszar, D., et al., *Targeted disruption of the melanocortin-4 receptor results in obesity in mice.* Cell, 1997. **88**(1): p. 131-41.

131. Paxinos, G. and K.B.J. Franklin, *The mouse brain in stereotaxic coordinates*. 2nd ed. 2001: Academic Press.

132. Simard, A.R., et al., *Bone marrow-derived microglia play a critical role in restricting senile plaque formation in Alzheimer's disease.* Neuron, 2006. **49**(4): p. 489-502.

133. Priller, J., et al., *Targeting gene-modified hematopoietic cells to the central nervous system: use of green fluorescent protein uncovers microglial engraftment.* Nat Med, 2001. **7**(12): p. 1356-61.

134. Getts, D.R., et al., *Ly6c+ "inflammatory monocytes" are microglial precursors recruited in a pathogenic manner in West Nile virus encephalitis.* J Exp Med, 2008. **205**(10): p. 2319-37.

135. Vallieres, L. and P.E. Sawchenko, *Bone marrow-derived cells that populate the adult mouse brain preserve their hematopoietic identity.* J Neurosci, 2003. **23**(12): p. 5197-207.

136. Trottier, M.D., et al., *Enhancement of hematopoiesis and lymphopoiesis in diet-induced obese mice.* Proc Natl Acad Sci U S A. **109**(20): p. 7622-9.

137. Sedgwick, J.D., et al., *Isolation and direct characterization of resident microglial cells from the normal and inflamed central nervous system.* Proc Natl Acad Sci U S A, 1991. **88**(16): p. 7438-42.

138. Zhang, G.X., et al., *Parenchymal microglia of naive adult C57BL/6J mice express high levels of B7.1, B7.2, and MHC class II.* Exp Mol Pathol, 2002. **73**(1): p. 35-45.

139. Simard, A.R. and S. Rivest, *Bone marrow stem cells have the ability to populate the entire central nervous system into fully differentiated parenchymal microglia.* FASEB J, 2004. **18**(9): p. 998-1000.

140. Weisberg, S.P., et al., *Obesity is associated with macrophage accumulation in adipose tissue.* J Clin Invest, 2003. **112**(12): p. 1796-808.

141. Coenen, K.R., et al., *Impact of macrophage toll-like receptor 4 deficiency on macrophage infiltration into adipose tissue and the artery wall in mice.* Diabetologia, 2009. **52**(2): p. 318-28.

142. De Taeye, B.M., et al., *Macrophage TNF-alpha contributes to insulin resistance and hepatic steatosis in diet-induced obesity.* Am J Physiol Endocrinol Metab, 2007. **293**(3): p. E713-25.

143. Furuhashi, M., et al., *Adipocyte/macrophage fatty acid-binding proteins contribute to metabolic deterioration through actions in both macrophages and adipocytes in mice.* J Clin Invest, 2008. **118**(7): p. 2640-50.

144. Kowalski, G.M., et al., *Deficiency of haematopoietic-cell-derived IL-10 does not exacerbate high-fat-diet-induced inflammation or insulin resistance in mice.* Diabetologia, 2011. **54**(4): p. 888-99.

145. Nicholls, H.T., et al., *Hematopoietic cell-restricted deletion of CD36 reduces high-fat diet-induced macrophage infiltration and improves insulin signaling in adipose tissue.* Diabetes, 2011. **60**(4): p. 1100-10.

146. Orr, J.S., et al., *Toll-like Receptor 4 Deficiency Promotes the Alternative Activation of Adipose Tissue Macrophages.* Diabetes, 2012. **61**(11): p. 2718-27.

147. Saberi, M., et al., *Hematopoietic cell-specific deletion of toll-like receptor 4 ameliorates hepatic and adipose tissue insulin resistance in high-fat-fed mice.* Cell Metab, 2009. **10**(5): p. 419-29.

148. Xu, J., et al., *GPR105 ablation prevents inflammation and improves insulin sensitivity in mice with diet-induced obesity.* J Immunol, 2012. **189**(4): p. 1992-9.

149. Akiyama, H., et al., *Expression of MRP14, 27E10, interferon-alpha and leukocyte common antigen by reactive microglia in postmortem human brain tissue.* J Neuroimmunol, 1994. **50**(2): p. 195-201.

150. Nikodemova, M. and J.J. Watters, *Efficient isolation of live microglia with preserved phenotypes from adult mouse brain.* J Neuroinflammation. **9**: p. 147.

151. Sedgwick, J.D., et al., *Central nervous system microglial cell activation and proliferation follows direct interaction with tissue-infiltrating T cell blasts.* J Immunol, 1998. **160**(11): p. 5320-30.

152. Djukic, M., et al., *Circulating monocytes engraft in the brain, differentiate into microglia and contribute to the pathology following meningitis in mice.* Brain, 2006. **129**(Pt 9): p. 2394-403.

153. Perry, V.H. and S. Gordon, *Macrophages and microglia in the nervous system.* Trends Neurosci, 1988. **11**(6): p. 273-7.

154. Rezaie, P., K. Patel, and D.K. Male, *Microglia in the human fetal spinal cord--patterns of distribution, morphology and phenotype.* Brain Res Dev Brain Res, 1999. **115**(1): p. 71-81.

155. Moraes, J.C., et al., *High-fat diet induces apoptosis of hypothalamic neurons.* PLoS One, 2009. **4**(4): p. e5045.

156. Rutkowski, J.M., K.E. Davis, and P.E. Scherer, *Mechanisms of obesity and related pathologies: the macro- and microcirculation of adipose tissue.* FEBS J, 2009. **276**(20): p. 5738-46.

157. Kim, F., et al., *Toll-like receptor-4 mediates vascular inflammation and insulin resistance in diet-induced obesity.* Circ Res, 2007. **100**(11): p. 1589-96.

158. Yi, C.X., et al., *High calorie diet triggers hypothalamic angiopathy.* Mol Metab. **1**(1-2): p. 95-100.

159. Albrecht, J., B. Wroblewska, and M.J. Mossakowski, *The binding of insulin to cerebral capillaries and astrocytes of the rat.* Neurochem Res, 1982. **7**(4): p. 489-94.

160. Kokovay, E. and L.A. Cunningham, *Bone marrow-derived microglia contribute to the neuroinflammatory response and express iNOS in the MPTP mouse model of Parkinson's disease.* Neurobiol Dis, 2005. **19**(3): p. 471-8.

161. Malm, T.M., et al., *Bone-marrow-derived cells contribute to the recruitment of microglial cells in response to beta-amyloid deposition in APP/PS1 double transgenic Alzheimer mice.* Neurobiol Dis, 2005. **18**(1): p. 134-42.

162. Priller, J., et al., *Early and rapid engraftment of bone marrow-derived microglia in scrapie.* J Neurosci, 2006. **26**(45): p. 11753-62.

163. Ajami, B., et al., *Local self-renewal can sustain CNS microglia maintenance and function throughout adult life.* Nat Neurosci, 2007. **10**(12): p. 1538-43.

164. Mildner, A., et al., *Microglia in the adult brain arise from Ly-6ChiCCR2+ monocytes only under defined host conditions.* Nat Neurosci, 2007. **10**(12): p. 1544-53.

165. Haseloff, R.F., et al., *In search of the astrocytic factor(s) modulating blood-brain barrier functions in brain capillary endothelial cells in vitro.* Cell Mol Neurobiol, 2005. **25**(1): p. 25-39.

166. McAllister, M.S., et al., *Mechanisms of glucose transport at the blood-brain barrier: an in vitro study.* Brain Res, 2001. **904**(1): p. 20-30.

167. Ramsauer, M., D. Krause, and R. Dermietzel, *Angiogenesis of the blood-brain barrier in vitro and the function of cerebral pericytes.* FASEB J, 2002. **16**(10): p. 1274-6.

168. Sobue, K., et al., *Induction of blood-brain barrier properties in immortalized bovine brain endothelial cells by astrocytic factors.* Neurosci Res, 1999. **35**(2): p. 155-64.

169. Horvath, T.L., et al., *Synaptic input organization of the melanocortin system predicts diet-induced hypothalamic reactive gliosis and obesity.* Proc Natl Acad Sci U S A, 2010. **107**(33): p. 14875-80.

170. Panatier, A., *Glial cells: indispensable partners of hypothalamic magnocellular neurones.* J Neuroendocrinol, 2009. **21**(7): p. 665-72.

171. Prevot, V., et al., *Neuronal-glial-endothelial interactions and cell plasticity in the postnatal hypothalamus: implications for the neuroendocrine control of reproduction.* Psychoneuroendocrinology, 2007. **32 Suppl 1**: p. S46-51.

172. Theodosis, D.T., A. Trailin, and D.A. Poulain, *Remodeling of astrocytes, a prerequisite for synapse turnover in the adult brain? Insights from the oxytocin system of the hypothalamus.* Am J Physiol Regul Integr Comp Physiol, 2006. **290**(5): p. R1175-82.

173. Pistell, P.J., et al., *Cognitive impairment following high fat diet consumption is associated with brain inflammation.* J Neuroimmunol, 2010. **219**(1-2): p. 25-32.

174. Motoike, T., et al., *Universal GFP reporter for the study of vascular development.* Genesis, 2000. **28**(2): p. 75-81.

175. Garcia-Segura, L.M., B. Lorenz, and L.L. DonCarlos, *The role of glia in the hypothalamus: implications for gonadal steroid feedback and reproductive neuroendocrine output.* Reproduction, 2008. **135**(4): p. 419-29.

176. Cone, R.D., *Studies on the physiological functions of the melanocortin system.* Endocr Rev, 2006. **27**(7): p. 736-49.

177. Yi, C.X., et al., *A role for astrocytes in the central control of metabolism.* Neuroendocrinology, 2011. **93**(3): p. 143-9.

178. Donato, R., et al., *S100B's double life: intracellular regulator and extracellular signal.* Biochim Biophys Acta, 2009. **1793**(6): p. 1008-22.

179. Whitmer, R.A., et al., *Obesity in middle age and future risk of dementia: a 27 year longitudinal population based study.* BMJ, 2005. **330**(7504): p. 1360.

180. Whitmer, R.A., et al., *Central obesity and increased risk of dementia more than three decades later.* Neurology, 2008. **71**(14): p. 1057-64.

181. Bruce-Keller, A.J., J.N. Keller, and C.D. Morrison, *Obesity and vulnerability of the CNS.* Biochim Biophys Acta, 2009. **1792**(5): p. 395-400.

182. Simon, G.E., et al., *Association between obesity and psychiatric disorders in the US adult population.* Arch Gen Psychiatry, 2006. **63**(7): p. 824-30.

183. Steiner, J., et al., *S100B serum levels are closely correlated with body mass index: an important caveat in neuropsychiatric research.* Psychoneuroendocrinology, 2010. **35**(2): p. 321-4.

184. Fujiya, A., et al., *The role of S100B in the interaction between adipocytes and macrophages.* Obesity (Silver Spring), 2013.

185. Kosteli, A., et al., *Weight loss and lipolysis promote a dynamic immune response in murine adipose tissue.* J Clin Invest, 2010. **120**(10): p. 3466-79.

186. Ebke, L.A., et al., *Tight association between macrophages and adipocytes in obesity: Implications for adipocyte preparation.* Obesity (Silver Spring), 2013.

187. Michetti, F., et al., *Immunochemical and immunocytochemical study of S-100 protein in rat adipocytes.* Brain Res, 1983. **262**(2): p. 352-6.

188. Hofmann, M.A., et al., *RAGE mediates a novel proinflammatory axis: a central cell surface receptor for S100/calgranulin polypeptides.* Cell, 1999. **97**(7): p. 889-901.

189. Goncalves, C.A., M.C. Leite, and M.C. Guerra, *Adipocytes as an Important Source of Serum S100B and Possible Roles of This Protein in Adipose Tissue.* Cardiovasc Psychiatry Neurol, 2010. **2010**: p. 790431.

190. Gaens, K.H., C.D. Stehouwer, and C.G. Schalkwijk, *Advanced glycation endproducts and its receptor for advanced glycation endproducts in obesity.* Curr Opin Lipidol, 2013. **24**(1): p. 4-11.

191. Gross, S., et al., *Body mass index and creatinine clearance are associated with steady-state serum concentrations of the cell damage marker S100B in renal transplant recipients.* Med Sci Monit, 2010. **16**(7): p. CR318-24.

192. O'Connell, K., J. Thakore, and K.K. Dev, *Levels of S100B are raised in female patients with schizophrenia.* BMC Psychiatry, 2013. **13**: p. 146.

193. Steiner, J., et al., *S100B Serum Levels in Schizophrenia Are Presumably Related to Visceral Obesity and Insulin Resistance.* Cardiovasc Psychiatry Neurol, 2010. **2010**: p. 480707.

194. Pham, N., et al., *Extracranial sources of S100B do not affect serum levels.* PLoS One, 2010. **5**(9).

195. Kislinger, T., et al., *Receptor for advanced glycation end products mediates inflammation and enhanced expression of tissue factor in vasculature of diabetic apolipoprotein E-null mice.* Arterioscler Thromb Vasc Biol, 2001. **21**(6): p. 905-10.

196. Wendt, T., et al., *RAGE modulates vascular inflammation and atherosclerosis in a murine model of type 2 diabetes.* Atherosclerosis, 2006. **185**(1): p. 70-7.

197. Flyvbjerg, A., et al., *Long-term renal effects of a neutralizing RAGE antibody in obese type 2 diabetic mice.* Diabetes, 2004. **53**(1): p. 166-72.

198. Williams, K.W. and J.K. Elmquist, *From neuroanatomy to behavior: central integration of peripheral signals regulating feeding behavior.* Nat Neurosci, 2012. **15**(10): p. 1350-5.

199. Zeltser, L.M., R.J. Seeley, and M.H. Tschop, *Synaptic plasticity in neuronal circuits regulating energy balance.* Nat Neurosci, 2012. **15**(10): p. 1336-42.

200. Chowen, J.A., J. Argente, and T.L. Horvath, *Uncovering novel roles of nonneuronal cells in body weight homeostasis and obesity.* Endocrinology, 2013. **154**(9): p. 3001-7.

201. Buckman, L.B., et al., *Regional astrogliosis in the mouse hypothalamus in response to obesity.* J Comp Neurol, 2013. **521**(6): p. 1322-33.

202. Butler, A.A., et al., *Melanocortin-4 receptor is required for acute homeostatic responses to increased dietary fat.* Nat Neurosci, 2001. **4**(6): p. 605-11.

203. Srisai, D., et al., *Characterization of the hyperphagic response to dietary fat in the MC4R knockout mouse.* Endocrinology, 2011. **152**(3): p. 890-902.

204. Bae, M.K., et al., *Aspirin-induced blockade of NF-kappaB activity restrains up-regulation of glial fibrillary acidic protein in human astroglial cells.* Biochim Biophys Acta, 2006. **1763**(3): p. 282-9.

205. Yeo, S., et al., *Transgenic analysis of GFAP promoter elements.* Glia, 2013. **61**(9): p. 1488-99.

206. Nemeth, J., et al., *S100A8 and S100A9 are novel nuclear factor kappa B target genes during malignant progression of murine and human liver carcinogenesis.* Hepatology, 2009. **50**(4): p. 1251-62.

207. Carlsson, H., et al., *Psoriasin (S100A7) and calgranulin-B (S100A9) induction is dependent on reactive oxygen species and is downregulated by Bcl-2 and antioxidants.* Cancer Biol Ther, 2005. **4**(9): p. 998-1005.

208. Berthoud, H.R., *Vagal and hormonal gut-brain communication: from satiation to satisfaction.* Neurogastroenterol Motil, 2008. **20 Suppl 1**: p. 64-72.

209. Gard, A.L., F.P. White, and G.R. Dutton, *Extra-neural glial fibrillary acidic protein (GFAP) immunoreactivity in perisinusoidal stellate cells of rat liver.* J Neuroimmunol, 1985. **8**(4-6): p. 359-75.

210. Apte, M.V., et al., *Periacinar stellate shaped cells in rat pancreas: identification, isolation, and culture.* Gut, 1998. **43**(1): p. 128-33.

211. Jessen, K.R. and R. Mirsky, *Glial cells in the enteric nervous system contain glial fibrillary acidic protein.* Nature, 1980. **286**(5774): p. 736-7.

212. Benani, A., et al., *Food intake adaptation to dietary fat involves PSA-dependent rewiring of the arcuate melanocortin system in mice.* J Neurosci, 2012. **32**(35): p. 11970-9.

213. Tasker, J.G., et al., *Glial regulation of neuronal function: from synapse to systems physiology.* J Neuroendocrinol, 2012. **24**(4): p. 566-76.

214. Gupta, S., et al., *Saturated long-chain fatty acids activate inflammatory signaling in astrocytes.* J Neurochem, 2012. **120**(6): p. 1060-71.

215. Xanthos, D.N. and J. Sandkuhler, *Neurogenic neuroinflammation: inflammatory CNS reactions in response to neuronal activity.* Nat Rev Neurosci, 2014. **15**(1): p. 43-53.

216. Benediktsson, A.M., et al., *Neuronal activity regulates glutamate transporter dynamics in developing astrocytes.* Glia, 2012. **60**(2): p. 175-88.

217. Duan, S., et al., *Glutamate induces rapid upregulation of astrocyte glutamate transport and cell-surface expression of GLAST.* J Neurosci, 1999. **19**(23): p. 10193-200.

218. Fellin, T., et al., *Bidirectional astrocyte-neuron communication: the many roles of glutamate and ATP.* Novartis Found Symp, 2006. **276**: p. 208-17; discussion 217-21, 233-7, 275-81.

219. Horvath, T.L., *Synaptic plasticity in energy balance regulation.* Obesity (Silver Spring), 2006. **14 Suppl 5**: p. 228S-233S.

220. Pinto, S., et al., *Rapid rewiring of arcuate nucleus feeding circuits by leptin.* Science, 2004. **304**(5667): p. 110-5.

221. Garcia-Segura, L.M., et al., *Gonadal hormone regulation of glial fibrillary acidic protein immunoreactivity and glial ultrastructure in the rat neuroendocrine hypothalamus.* Glia, 1994. **10**(1): p. 59-69.

222. Hatton, G.I., *Function-related plasticity in hypothalamus.* Annu Rev Neurosci, 1997. **20**: p. 375-97.

223. Kokoeva, M.V., H. Yin, and J.S. Flier, *Neurogenesis in the hypothalamus of adult mice: potential role in energy balance.* Science, 2005. **310**(5748): p. 679-83.

224. Sousa-Ferreira, L., et al., *Proliferative hypothalamic neurospheres express NPY, AGRP, POMC, CART and Orexin-A and differentiate to functional neurons.* PLoS One. **6**(5): p. e19745.

225. Markakis, E.A., et al., *Novel neuronal phenotypes from neural progenitor cells.* J Neurosci, 2004. **24**(12): p. 2886-97.

226. Lee, D.A., et al., *Tanycytes of the hypothalamic median eminence form a diet-responsive neurogenic niche.* Nat Neurosci. **15**(5): p. 700-2.

227. Pierce, A.A. and A.W. Xu, *De novo neurogenesis in adult hypothalamus as a compensatory mechanism to regulate energy balance.* J Neurosci. **30**(2): p. 723-30.

228. McNay, D.E., et al., *Remodeling of the arcuate nucleus energy-balance circuit is inhibited in obese mice.* J Clin Invest. **122**(1): p. 142-52.

229. Barkho, B.Z., et al., *Identification of astrocyte-expressed factors that modulate neural stem/progenitor cell differentiation.* Stem Cells Dev, 2006. **15**(3): p. 407-21.

230. Cacci, E., et al., *In vitro neuronal and glial differentiation from embryonic or adult neural precursor cells are differently affected by chronic or acute activation of microglia.* Glia, 2008. **56**(4): p. 412-25.

231. Liu, Y.P., H.I. Lin, and S.F. Tzeng, *Tumor necrosis factor-alpha and interleukin-18 modulate neuronal cell fate in embryonic neural progenitor culture.* Brain Res, 2005. **1054**(2): p. 152-8.

232. Barger, S.W., et al., *Glutamate release from activated microglia requires the oxidative burst and lipid peroxidation.* J Neurochem, 2007. **101**(5): p. 1205-13.

233. Bal-Price, A., Z. Moneer, and G.C. Brown, *Nitric oxide induces rapid, calcium-dependent release of vesicular glutamate and ATP from cultured rat astrocytes.* Glia, 2002. **40**(3): p. 312-23.

234. Korn, T., T. Magnus, and S. Jung, *Autoantigen specific T cells inhibit glutamate uptake in astrocytes by decreasing expression of astrocytic glutamate transporter GLAST: a mechanism mediated by tumor necrosis factor-alpha.* FASEB J, 2005. **19**(13): p. 1878-80.

235. Wang, Z., et al., *Reduced expression of glutamate transporter EAAT2 and impaired glutamate transport in human primary astrocytes exposed to HIV-1 or gp120.* Virology, 2003. **312**(1): p. 60-73.

236. Wake, H., et al., *Resting microglia directly monitor the functional state of synapses in vivo and determine the fate of ischemic terminals.* J Neurosci, 2009. **29**(13): p. 3974-80.

237. Greenwood, C.E. and G. Winocur, *Learning and memory impairment in rats fed a high saturated fat diet.* Behav Neural Biol, 1990. **53**(1): p. 74-87.

238. Greenwood, C.E. and G. Winocur, *Cognitive impairment in rats fed high-fat diets: a specific effect of saturated fatty-acid intake.* Behav Neurosci, 1996. **110**(3): p. 451-9.

239. Pistell, P.J., et al., *Cognitive impairment following high fat diet consumption is associated with brain inflammation.* J Neuroimmunol. **219**(1-2): p. 25-32.

240. Posey, K.A., et al., *Hypothalamic proinflammatory lipid accumulation, inflammation, and insulin resistance in rats fed a high-fat diet.* Am J Physiol Endocrinol Metab, 2009. **296**(5): p. E1003-12.

241. Borg, M.L., et al., *Consumption of a high-fat diet, but not regular endurance exercise training, regulates hypothalamic lipid accumulation in mice.* J Physiol. **590**(Pt 17): p. 4377-89.

242. Gupta, S., et al., *Saturated long-chain fatty acids activate inflammatory signaling in astrocytes.* J Neurochem. **120**(6): p. 1060-71.

243. Rasouli, N. and P.A. Kern, *Adipocytokines and the metabolic complications of obesity.* J Clin Endocrinol Metab, 2008. **93**(11 Suppl 1): p. S64-73.

244. Jung, T.W., et al., *Adiponectin protects human neuroblastoma SH-SY5Y cells against acetaldehyde-induced cytotoxicity.* Biochem Pharmacol, 2006. **72**(5): p. 616-23.

245. Chen, B., et al., *Adiponectin protects against cerebral ischemia-reperfusion injury through anti-inflammatory action.* Brain Res, 2009. **1273**: p. 129-37.

246. Ouchi, N. and K. Walsh, *Adiponectin as an anti-inflammatory factor.* Clin Chim Acta, 2007. **380**(1-2): p. 24-30.

247. John Thundyil, D.P., Christopher G Sobey and Thiruma V Arumugam, *Adiponectin receptor signaling in the brain.* British Journal of Pharmacology, 2011. **165**: p. 313-327

.

248. Tang, C.H., et al., *Leptin-induced IL-6 production is mediated by leptin receptor, insulin receptor substrate-1, phosphatidylinositol 3-kinase, Akt, NF-kappaB, and p300 pathway in microglia.* J Immunol, 2007. **179**(2): p. 1292-302.

249. Pinteaux, E., et al., *Leptin induces interleukin-1beta release from rat microglial cells through a caspase 1 independent mechanism.* J Neurochem, 2007. **102**(3): p. 826-33.

250. de La Serre, C.B., et al., *Propensity to high-fat diet-induced obesity in rats is associated with changes in the gut microbiota and gut inflammation.* Am J Physiol Gastrointest Liver Physiol. **299**(2): p. G440-8.

251. Stangl, D. and S. Thuret, *Impact of diet on adult hippocampal neurogenesis.* Genes Nutr, 2009. **4**(4): p. 271-82.

252. Baumgarner, K.M., et al., *Diet-induced obesity attenuates cytokine production following an immune challenge.* Behav Brain Res. **267C**: p. 33-41.

253. Navarro, V.M. and M. Tena-Sempere, *Neuroendocrine control by kisspeptins: role in metabolic regulation of fertility.* Nat Rev Endocrinol. **8**(1): p. 40-53.

254. Practice, C.o.O., *Obesity in Pregnancy*, in *Committee Opinion*. 2013 The American College of Obstetricians and Gynecologists.

255. Du Plessis, S.S., et al., *The effect of obesity on sperm disorders and male infertility.* Nat Rev Urol. **7**(3): p. 153-61.